NASA SP-3015

CHARTS FOR EQUILIBRIUM

FLOW PROPERTIES OF

CARBON DIOXIDE IN

HYPERVELOCITY NOZZLES

JORGENSEN AND REDMOND

NATIONAL AERONAUTICS AND SPACE ADMINISTRATION

CHARTS FOR EQUILIBRIUM

FLOW PROPERTIES OF

CARBON DIOXIDE IN

HYPERVELOCITY NOZZLES

By Leland H. Jorgensen and Robert J. Redmond

Ames Research Center, Moffett Field, California

SUMMARY

2O479

For initial stagnation pressures from 1 to 1,000 atm and stagnation enthalpies from 400 to 20,000 Btu/lb, nozzle-flow properties for equilibrium carbon dioxide have been computed and plotted on charts. Properties charted as a function of Mach number are as follows: temperature, pressure, density, speed, area ratio, dynamic pressure, stagnation-point pressure coefficient, Reynolds number, isentropic exponent, and molecular weight ratio. Temperatures, pressures, and densities across normal shock waves are also charted, and weight-flow rate is plotted as a function of stagnation enthalpy.

INTRODUCTION

Recently there has been much interest in the problems associated with flight to and within the atmospheres of Mars and Venus and return to Earth. Since the atmospheres of these planets are believed to be mostly carbon dioxide and nitrogen (e.g., ref. 1), experiments in hypervelocity tunnels with these gases and with air may yield important comparative information. Although some recent estimates indicate that the carbon dioxide content in the Venusian atmosphere may be only 20 mole percent (ref. 2) or even as low as 6 percent or less (ref. 3), other estimates have indicated an atmosphere of almost all carbon dioxide (e.g., refs. 4 and 5). There is also considerable uncertainty concerning the Martian atmosphere. Hence, until the chemical compositions of the atmospheres of these planets are better established, preliminary tests with both carbon dioxide and nitrogen alone and in several combinations are being considered. In order to define the conditions for tests in hypervelocity nozzles with these gases, various flow properties must be determined. In the present investigation equilibrium flow properties for carbon dioxide in hypervelocity nozzles have been computed.

It is the purpose of this report to present charts of the computed nozzle-flow properties of carbon dioxide similar to those presented for air in reference 6. The charts for carbon dioxide are for a range of stagnation pressures from 1 to 1,000 atm and stagnation enthalpies from 400 to 20,000 Btu/lb. Properties charted as a function of Mach number are as follows: temperature, pressure, density, speed, area ratio, dynamic pressure, stagnation-point pressure coefficient, Reynolds number, isentropic exponent, and molecular weight ratio. Temperatures, pressures, and densities across normal shock waves are also included. Weight-flow rate is plotted as a function of stagnation enthalpy. Because in an actual nozzle the flow will

probably not be close to equilibrium for high stagnation enthalpies and low stagnation pressures, care should be exercised in the application of these charts.

NOTATION AND CONSTANTS

A   nozzle cross-sectional area, ft^2

a   isentropic speed of sound, ft/sec

$C_{p_{stag}}$ $\dfrac{p_{t_2} - p_1}{q_1}$

h   enthalpy (h = 0   for molecular gas at 0° R), Btu/lb

$\dfrac{h}{RT_O}$ enthalpy, dimensionless

L   characteristic length, ft

M   Mach number

m   molecular weight of mixture, lb/mole

m_O molecular weight of undissociated gas, 44.011 lb/mole for CO_2

p   pressure, atm unless specified

q   dynamic pressure $\left(\dfrac{1}{2}\rho u^2\right)$, lb/ft^2

R   universal gas constant: 1.987 cal/mole $^\circ$K; 8.3144 J/mole $^\circ$K; 1.987 Btu/mole $^\circ$R; 1545 $\dfrac{ft\text{-}lb}{mole\text{-}^\circ R}$; or 0.7302 $\dfrac{ft^3\text{-}atm}{mole\text{-}^\circ R}$

Re   Reynolds number, $\dfrac{u\rho L}{\mu}$

RT_O 22.20 Btu/lb for CO_2

S   entropy, Btu/(initial mole)($^\circ$R)

$\dfrac{S}{R}$ entropy, dimensionless

T   temperature, $^\circ$R or $^\circ$K as specified

T_O reference temperature, 492° R = 273° K

u   speed, ft/sec

w   weight-flow rate, lb/sec

Z   molecular weight ratio, m_O/m

2

γ isentropic exponent, $\left(\dfrac{\partial \ln p}{\partial \ln \rho}\right)_s$

μ coefficient of viscosity, $lb\text{-}sec/ft^2$

ρ density, $slugs/ft^3$

ρ_o reference density, 0.00384 $slug/ft^3$ for CO_2

$(\ )^*$ sonic point

Subscripts

c   condensation

o   reference condition

t   reservoir or total condition

1   conditions in front of normal shock wave

2   conditions behind normal shock wave

Conversion From Units In This Report To SI Units[1]

Physical quantity	To convert from report units	Multiply by	To obtain SI units
Area	ft^2	9.290×10^{-2}	m^2
Density	$slugs/ft^3$	5.154×10^2	kg/m^3
Dynamic pressure	lb/ft^2	47.88	N/m^2
Enthalpy	Btu/lb	2.324×10^3	J/kg
Length	ft	0.3048	m
Speed	ft/sec	0.3048	m/s
Temperature	$^\circ R$	$5/9$	$^\circ K$
Viscosity coefficient	$lb\text{-}sec/ft^2$	47.88	$N\text{-}s/m^2$
Weight-flow rate	lb/sec	0.4536	kg/s

THERMODYNAMIC PROPERTIES AND VAPOR PRESSURES

The thermodynamic properties of carbon dioxide which were used for the present study were computed by H. E. Bailey of Ames Research Center. His results (ref. 7) are recorded on magnetic tape for use in nozzle and body flow-field calculations with an IBM 7094/7040 direct couple system. The data cover a temperature range of 100° to $25,000^\circ$ K, a density range of 10^{-7} to 10^3 times earth sea-level density, and a pressure range of about 10^{-7} to 10^5 atm. There is very close agreement between the Bailey data and those of references 8 and 9. The reader should be cautioned, however, that because of

---

[1] The "SI system" (International System of Units, NASA TT F-200).

3

a difference in choice of enthalpy reference datum, the value of $h/RT_O = 173.1$ should be added to the enthalpy results in reference 9 to make them compatible with those of reference 8 and Bailey (ref. 7).

Because it is important to avoid condensation conditions when testing models in a nozzle flow, a graph of vapor pressure as a function of temperature is very useful. For ready reference vapor pressures as a function of temperature for carbon dioxide are compared with those for air, oxygen, and nitrogen in figure 1. The vapor-pressure data for carbon dioxide, oxygen, and nitrogen were obtained from references 8, 10, and 11. The vapor pressures for air were estimated by assuming a perfect liquid or solid solution of oxygen and nitrogen in equilibrium with a 20-percent oxygen, 80-percent nitrogen vapor.

CALCULATION OF NOZZLE-FLOW AND SHOCK PROPERTIES

The nozzle-flow properties as a function of Mach number were desired for use in wind-tunnel testing. For convenience in the computational procedure, however, the flow properties were computed as a function of the ratio of static to stagnation pressure, with the corresponding Mach number being computed. Stagnation conditions p_t and h_t at the reservoir were specified for each case considered. To compute the area ratio, Mach number, and Reynolds number, the density was determined from the thermal equation of state

$$\rho = pm_O/ZRT \tag{1}$$

For ρ in slugs/ft^3, p in atm, and T in ^{O}R,

$$\rho = 1.873\ p/ZT \tag{2}$$

where

$$p = p_t(p/p_t)$$

An isentropic expansion of the gas from the reservoir to downstream stations in the nozzle was assumed, and the molecular weight ratio Z, the temperature T, and the enthalpy $h = (h/RT_O)RT_O$ were determined from the thermodynamic properties. The speed was then computed from the energy relation

$$u = 223.6\sqrt{h_t - h} \tag{3}$$

The area ratio was calculated from the continuity equation

$$A/A^* = \rho^* u^*/\rho u \tag{4}$$

where the weight-flow rate at the throat $(w/A^* = \rho^* u^*)$ was determined as the maximum value of ρu from a plot of ρu vs p/p_t for given stagnation conditions p_t and h_t. (An alternate method which gives nearly identical values of weight-flow rate through the throat is given in ref. 12.) The Mach number

4

was computed from

$$M = \frac{u}{a} = \frac{u}{\sqrt{\gamma Z \frac{R}{m_o} T}} \tag{5}$$

For T in $^\circ R$, the speed of sound a in ft/sec was given by

$$a \equiv \sqrt{\left(\frac{\partial p}{\partial \rho}\right)_s} = 33.61 \sqrt{\gamma ZT} \tag{6}$$

where the isentropic exponent γ was determined from

$$\gamma = \left(\frac{\partial \ln p}{\partial \ln \rho}\right)_s \tag{7}$$

The Reynolds number parameter was calculated from

$$\frac{Re}{Lp_t} = \frac{u\rho}{\mu p_t} \tag{8}$$

The effects of dissociation and ionization on μ were disregarded, and values of μ were computed by (see ref. 13)

$$\mu = 2.28 \times 10^{-8} \ T^{1/2} \left(1 + \frac{202}{T}\right)^{-1} \tag{9}$$

for T in $^\circ R$.

An iterative procedure was used to obtain equilibrium temperature ratios, pressure ratios, and density ratios across a normal shock wave. With the Mach number M_1 in front of the shock specified, the density ratio, ρ_2/ρ_1, was assumed, and the pressure behind the shock was calculated from the expression

$$p_2 = p_1 + (\rho_1 u_1)(u_1)\left(1 - \frac{\rho_1}{\rho_2}\right) \tag{10}$$

which resulted from combining the momentum and continuity equations. For the pressure in atmospheres

$$p_2 = p_1 + \frac{1}{2117} (\rho_1 u_1)(u_1)\left(1 - \frac{\rho_1}{\rho_2}\right) \tag{11}$$

The local enthalpy behind the shock, h_2, was determined by the energy equation

$$h_2 = h_1 + \left(\frac{1}{2} u_1^2\right) - \left(\frac{1}{2} u_2^2\right) \tag{12}$$

5

For h_2 in Btu/lb

$$h_2 = h_1 + \frac{1}{50,060} u_1^2 \left[1 - \left(\frac{\rho_1}{\rho_2} \right)^2 \right] \qquad (13)$$

With p_2 and h_2 known, T_2 and Z_2 were obtained from the thermodynamic properties. The density behind the normal shock, ρ_2, was then computed from equation (1), and ρ_2/ρ_1 was compared to the assumed value. This process was repeated until the assumed and computed values of ρ_2/ρ_1 were in agreement. The stagnation pressure and temperature behind the normal shock were then determined from the thermodynamic properties with an isentropic compression assumed from p_2 to p_{t_2}, corresponding to an enthalpy change from h_2 to $h_{t_2} = h_{t_1}$.

For use in computing forces and moments for entry-type capsules by modified Newtonian theory, the stagnation-point pressure coefficient $C_{p_{stag}}$ was determined by combining equation (10) and the Bernoulli equation for incompressible flow to give

$$C_{p_{stag}} \equiv \frac{p_{t_2} - p_1}{q_1} = 2 - \frac{\rho_1}{\rho_2} \qquad (14)$$

RESULTS

The procedure outlined in the previous section was used to compute nozzle properties for equilibrium flow for various initial stagnation pressures and enthalpies. The initial stagnation pressures for the calculations were 1, 10, 100, and 1,000 atm, and the initial stagnation enthalpies ranged from 400 to 20,000 Btu/lb. All calculations were made on an IBM 7094/7040 system with the thermodynamic properties recorded in tabular form on magnetic tape. The nozzle-flow properties determined were temperature, pressure, density, speed, area ratio, Mach number, dynamic pressure, stagnation-point pressure coefficient, Reynolds number, isentropic exponent, molecular weight ratio, and weight-flow rate. Temperatures, pressures, and densities across normal shock waves were also determined.

Except for weight-flow rate which was plotted as a function of stagnation enthalpy, all properties were plotted as a function of Mach number and are presented on charts which are indexed on page 13. In the calculation of the characteristics with the machine program input values of p_t and $(S/R)_t$ were used. As a result the determined values of h_t varied as much as ± 50 Btu/lb from those desired. The specified values of h_t on each chart have been rounded off to the nearest 100 Btu/lb. For convenience in studies of flows around bodies, the local isentropic exponent γ was plotted as a function of enthalpy (chart 14) as well as Mach number (chart 13). The saturated vapor line for CO_2 in figure 1 (p. 9) was used to obtain the plot of stagnation enthalpy at condensation h_{t_c} vs M (chart 17). The curves on the other charts of this report have not been terminated according to the condensation levels indicated in chart 17, because these saturated levels obviously represent the upper enthalpy limits for condensation. Testing at lower total enthalpies may

6

be permissible for certain applications. The reader should observe that symbols are used on most of the charts only to identify curves, not to indicate the many points computed for each curve.

Note that the plot of $w/p_t A^*$ vs h_t in chart 16 is extremely useful for determining the stagnation enthalpy h_t for a nozzle flow, since measurements of w, p_t, and A^* can be readily obtained. In reference 12 similar plots are given for various gases.

REFERENCES

1. Wegener, P. P.: Flight Regimes in the Atmospheres of Venus and Mars. RM-3388-PR, The Rand Corp., July 1963.

2. Kellogg, William W.; and Sagan, Carl: The Atmospheres of Mars and Venus. Publication 944, Natl. Acad. Sci., Natl. Res. Council, Washington, D.C., 1961.

3. Spinrad, Hyron: Spectroscopic Temperature and Pressure Measurements in the Venus Atmosphere. Publ. Astron. Soc. Pacific, vol. 74, no. 438, June 1962, pp. 187-201.

4. Urey, Harold C.: The Planets. Chapter V of Science in Space. A Report of the Space Sci. Board Natl. Acad. Sci., Natl. Res. Board, Washington, D.C., 1960.

5. Dole, S. H.: The Atmosphere of Venus. P-978, The Rand Corp., Oct. 1956.

6. Jorgensen, Leland H.; and Baum, Gayle M.: Charts for Equilibrium Flow Properties of Air in Hypervelocity Nozzles. NASA TN D-1333, 1962.

7. Bailey, Harry E.: Equilibrium Thermodynamic Properties of Carbon Dioxide. NASA SP-3014, 1965.

8. Hilsenrath, Joseph; Beckett, Charles W.; Benidict, William S.; Fano, Lilla; Hoge, Harold J.; Masi, Joseph F.; Nuttal, Ralph L.; Touloukian, Yerman S.; and Woolley, Harold W.: Tables of Thermal Properties of Gases. NBS Cir. 564, U.S. Department of Commerce, 1955.

9. Raymond, J. L.: Thermodynamic Properties of Carbon Dioxide to 24,000° K With Possible Application to the Atmosphere of Venus. RM-2292, The Rand Corp., Nov. 1958.

10. Hodgman, Charles D., ed.: Handbook of Chemistry and Physics. Forty-third ed., Chemical Rubber Pub. Co., Cleveland, Ohio, 1961.

11. Aoyama, S.; and Kanda, E.: Vapor Tensions of Solid Oxygen and Nitrogen. Tohoku Univ. Sci. Rep., ser. 1, vol. 24, May 1935, pp. 107-115.

12. Jorgensen, Leland H.: The Total Enthalpy of a One-Dimensional Nozzle Flow With Various Gases. NASA TN D-2233, 1964.

13. Hansen, C. Frederick: Approximations for the Thermodynamic and Transport Properties of High-Temperature Air. NASA TR R-50, 1959.
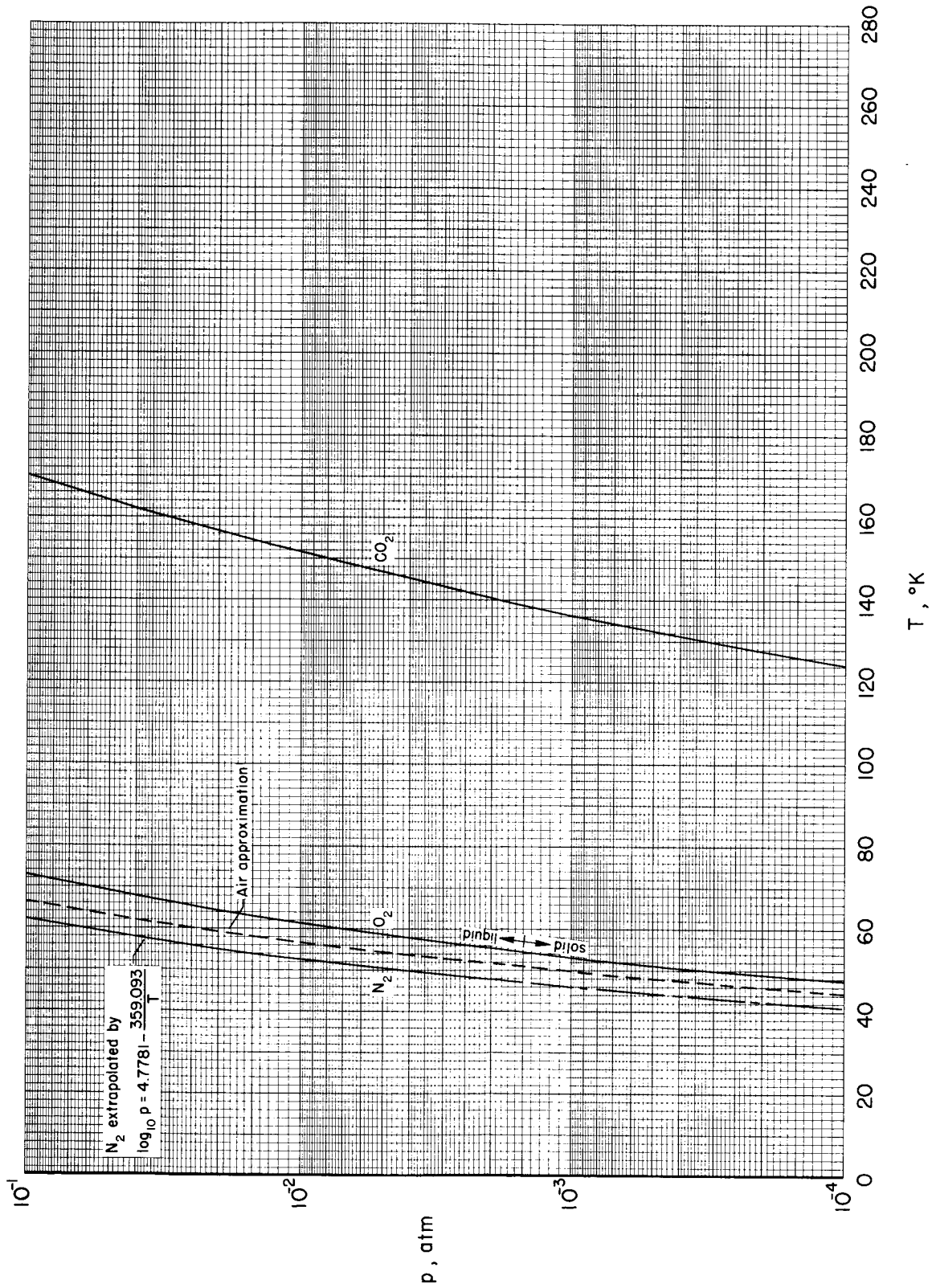
(b) $p = 10^{-4}$ to 10^{-1} atm

Figure 1.- Continued.

10
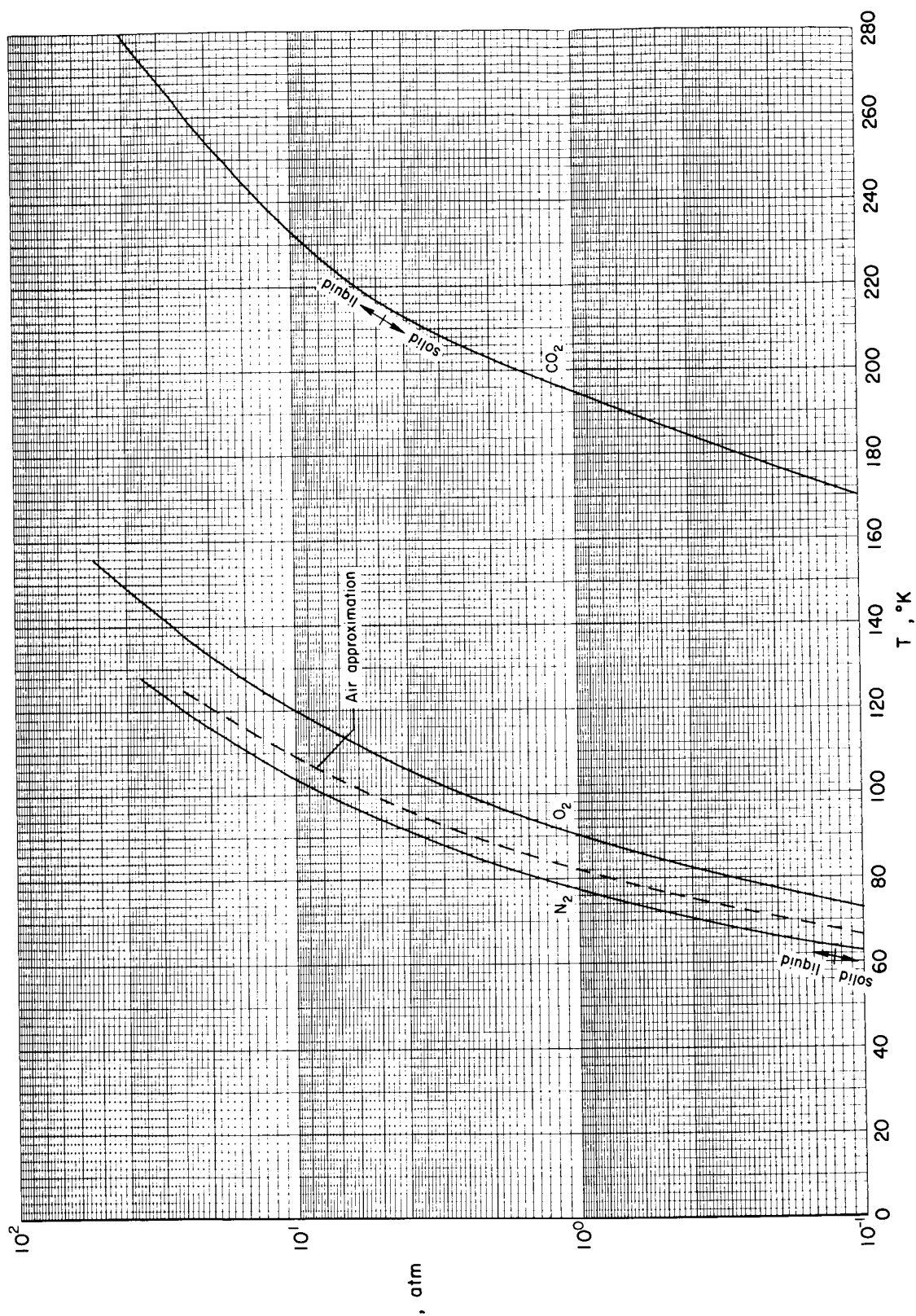
(a) $p \geq 10^{-1}$ atm

Figure 1.- Vapor pressures of carbon dioxide, oxygen, nitrogen, and air.
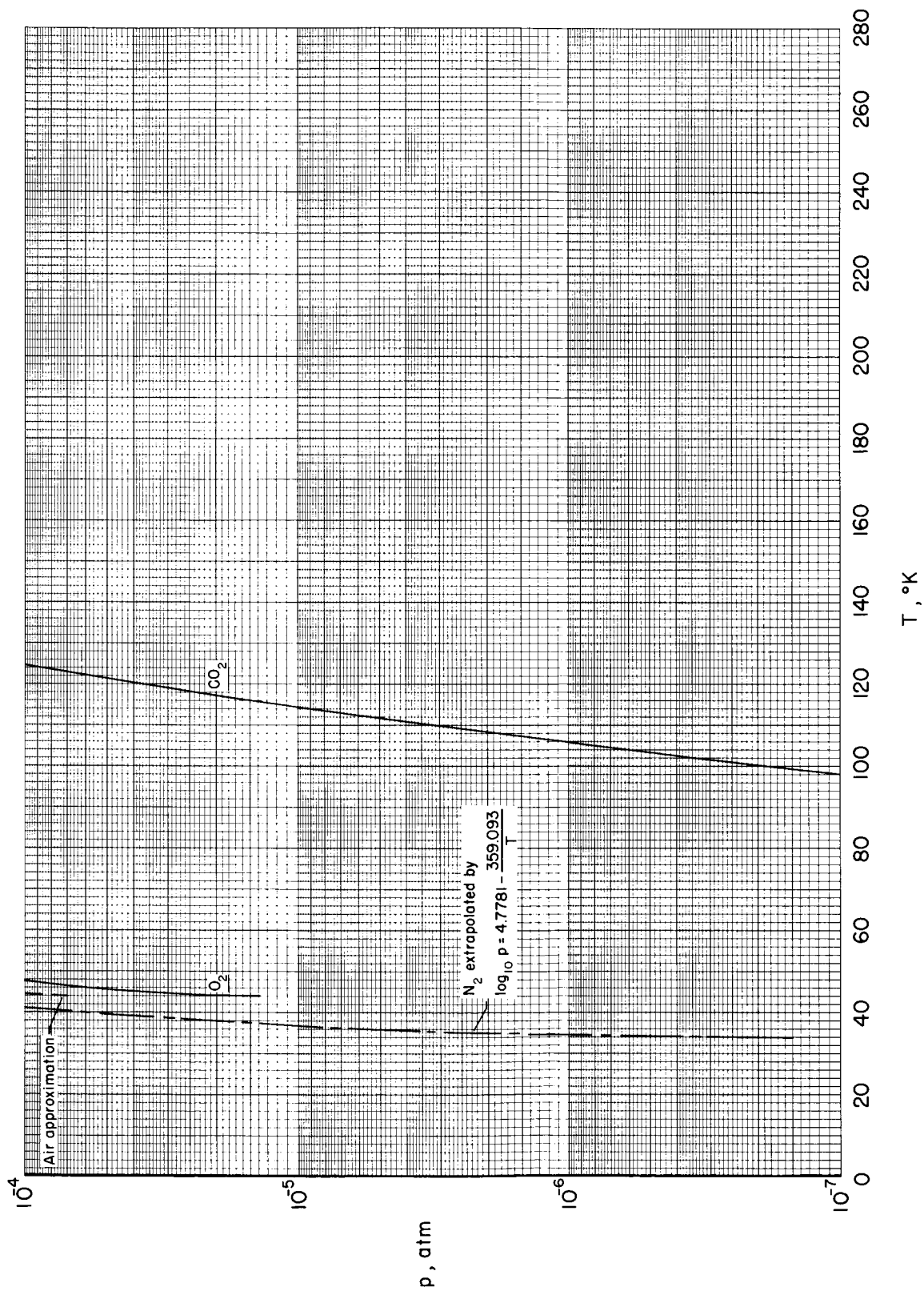
(c) $p \leq 10^{-4}$ atm

Figure 1.- Concluded.

The figure shows a plot of p, atm (vertical axis, from 10^{-7} to 10^4) versus T, °K (horizontal axis, from 0 to 280). Curves are labeled: Air approximation, O_2, CO_2, and N_2 extrapolated by $\log_{10} p = 4.7781 - \dfrac{359.093}{T}$.

INDEX TO CHARTS FOR CO_2-FLOW PROPERTIES

Ordinate		Abscissa	Chart	Page
Temperature	T	M	1	15
	T_{t_2}	M	2	19
Pressure	p/p_t	M	3	23
	p_2/p_1	M	4	27
	p_{t_2}/p_{t_1}	M	5	29
Density	$\rho/\rho_o p_t$	M	6	34
	ρ_2/ρ_1	M	7	42
Speed	u	M	8	46
Area ratio	A/A^*	M	9	50
Dynamic pressure	q/p_t	M	10	54
Stagnation-pressure coefficient	$C_{p_{stag}}$	M	11	58
Reynolds no.	$Re/p_t L$	M	12	62
Isentropic exponent	γ	M	13	66
	γ	h	14	67
Molecular weight ratio	Z	M	15	68
Weight flow	$w/p_t A^*$	h_t	16	70
Stagnation enthalpy for condensation	h_{t_c}	M	17	71
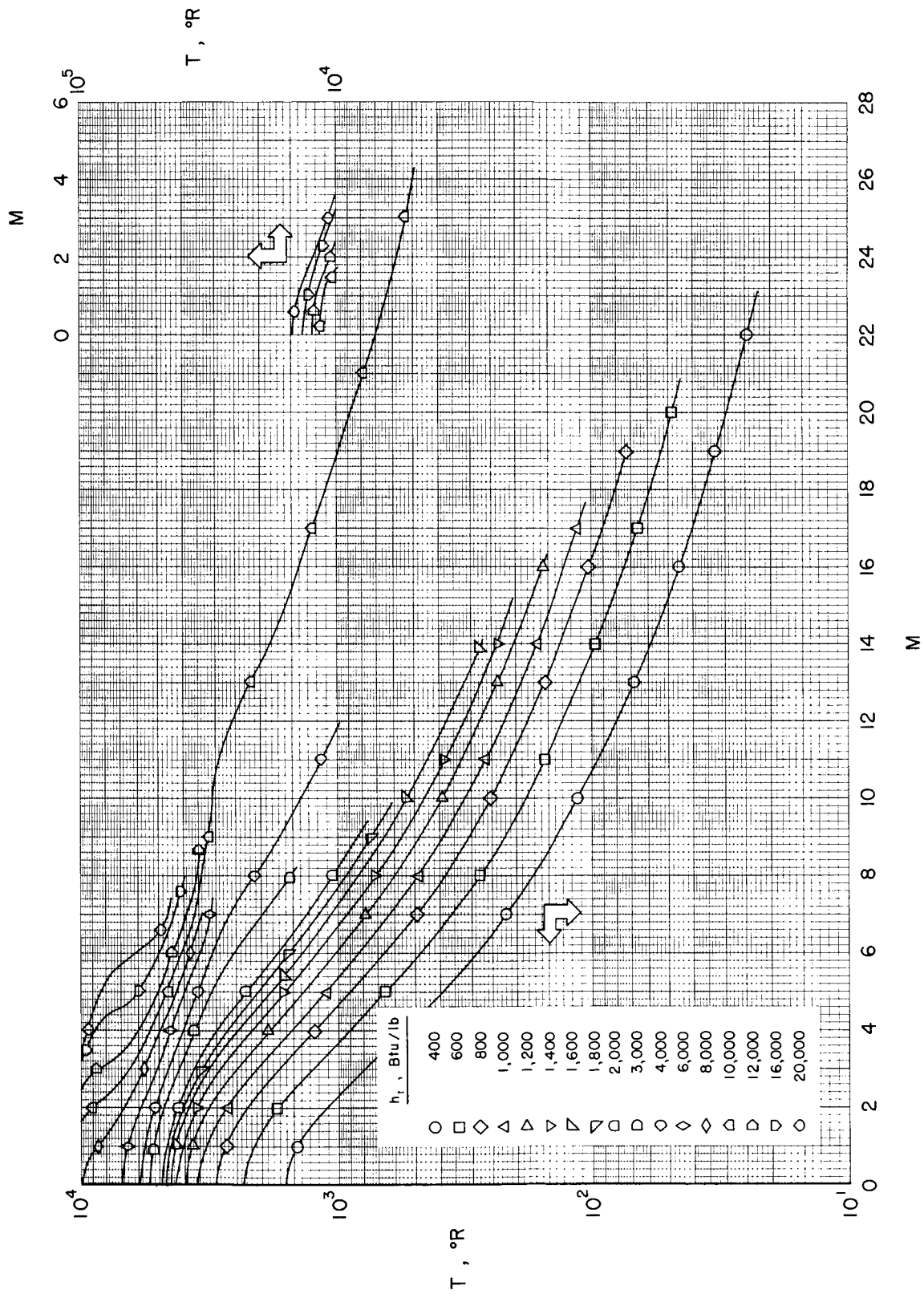
(a) p_t = 1 atm
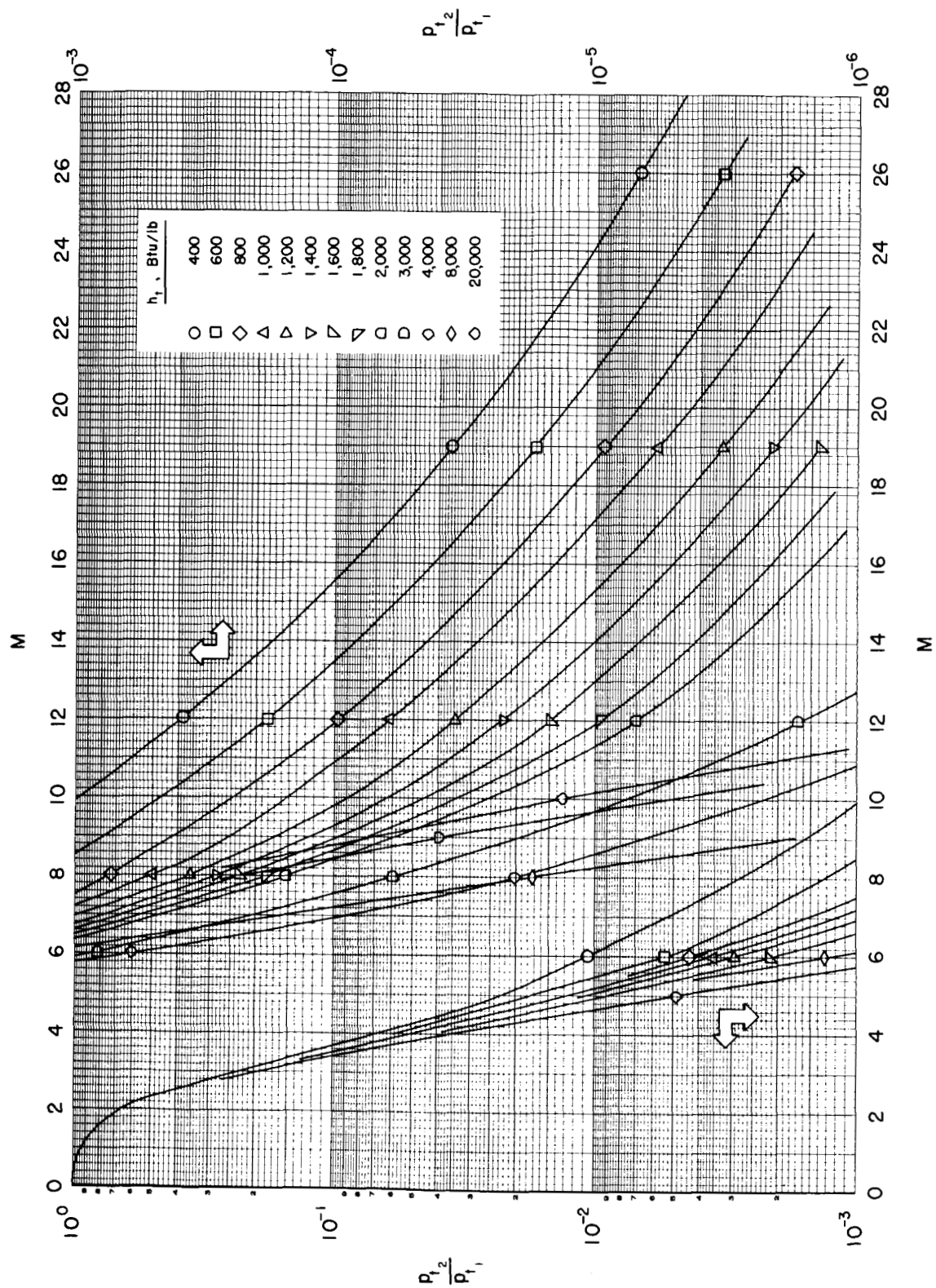
Chart 1.- Variation of temperature with Mach number.
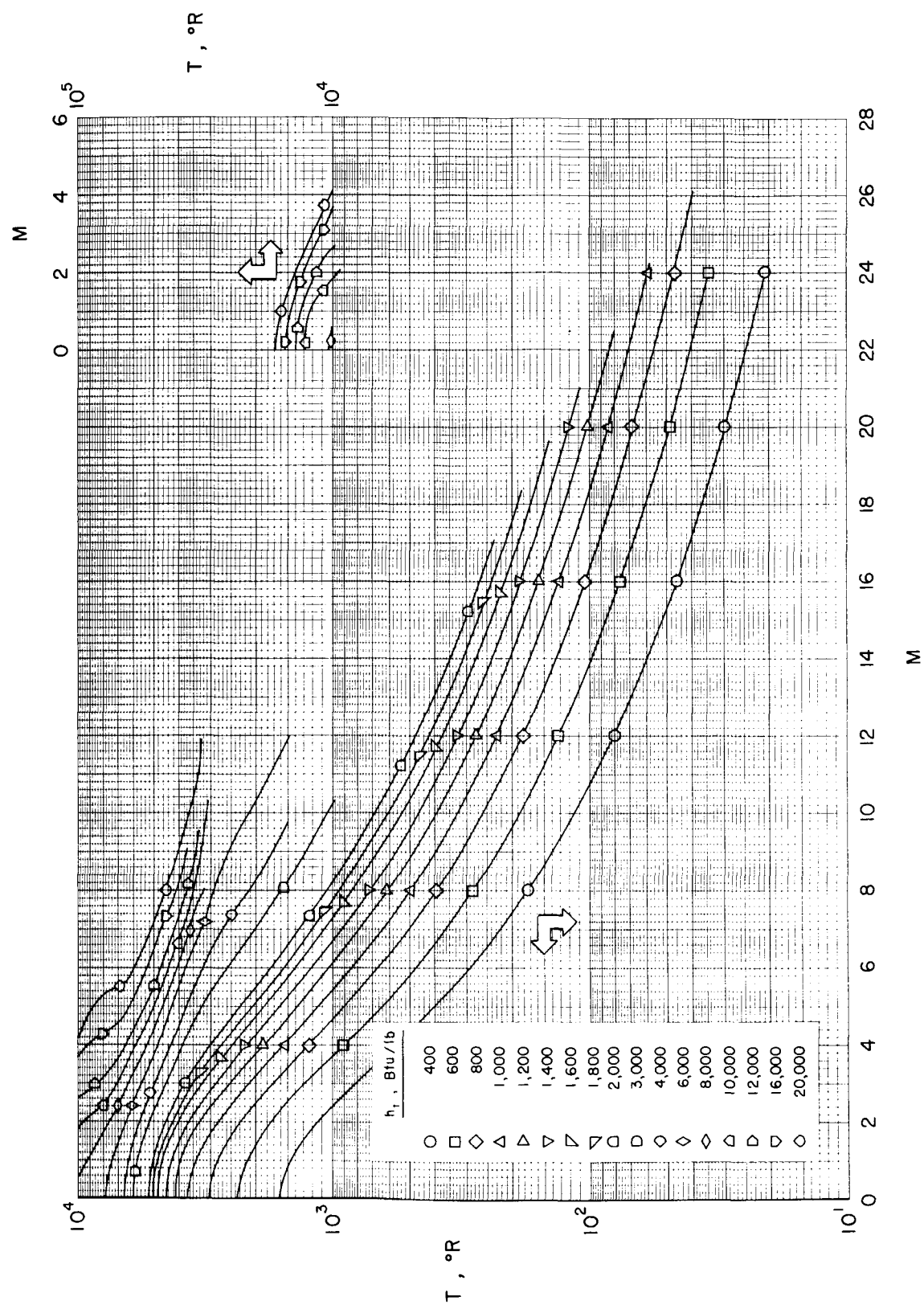
(b) $p_t = 10$ atm

Chart 1.- Continued.
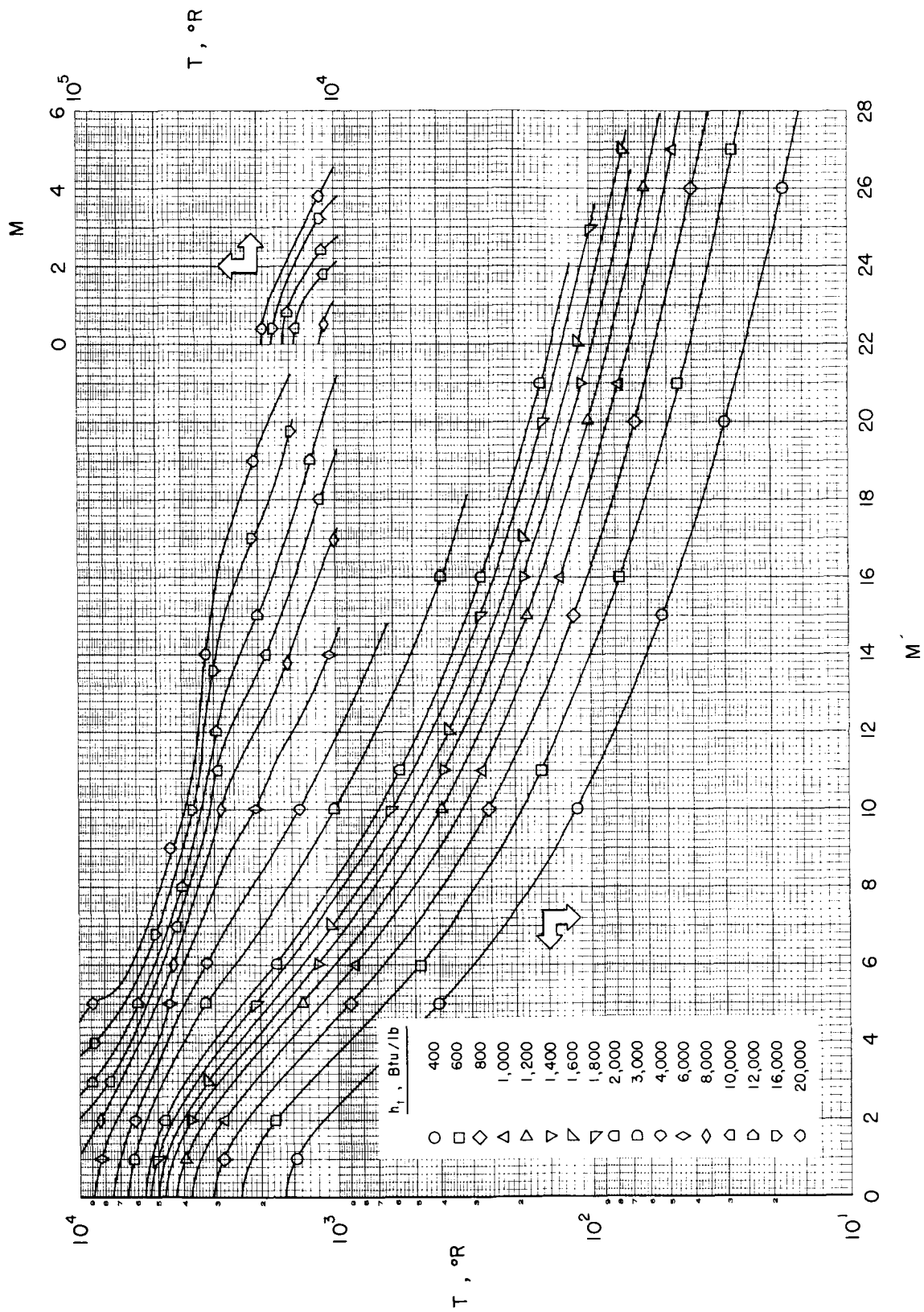
(c) $p_t = 100$ atm

Chart 1.- Continued.
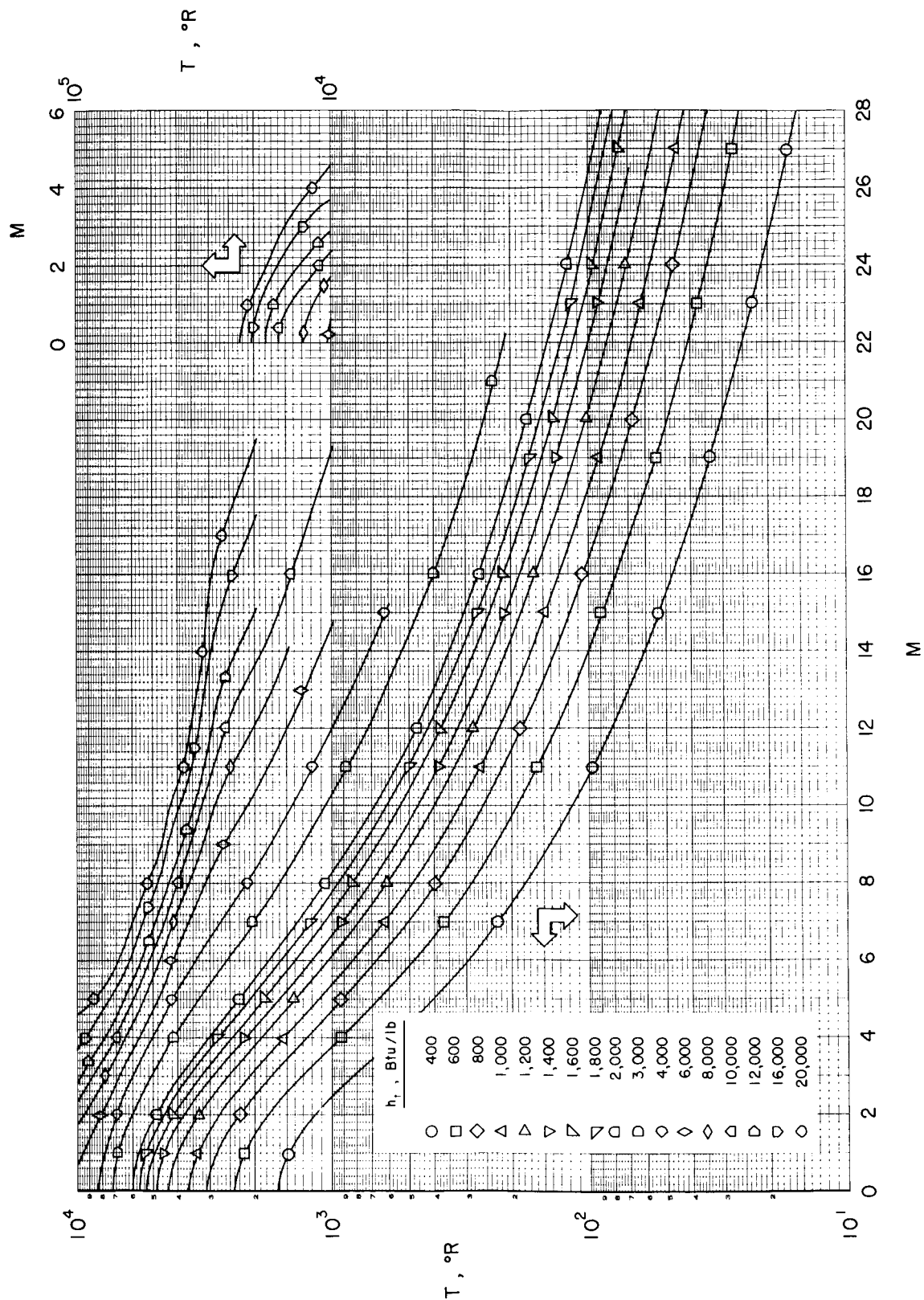
(d) $p_t = 1000$ atm

Chart 1.- Concluded.

18
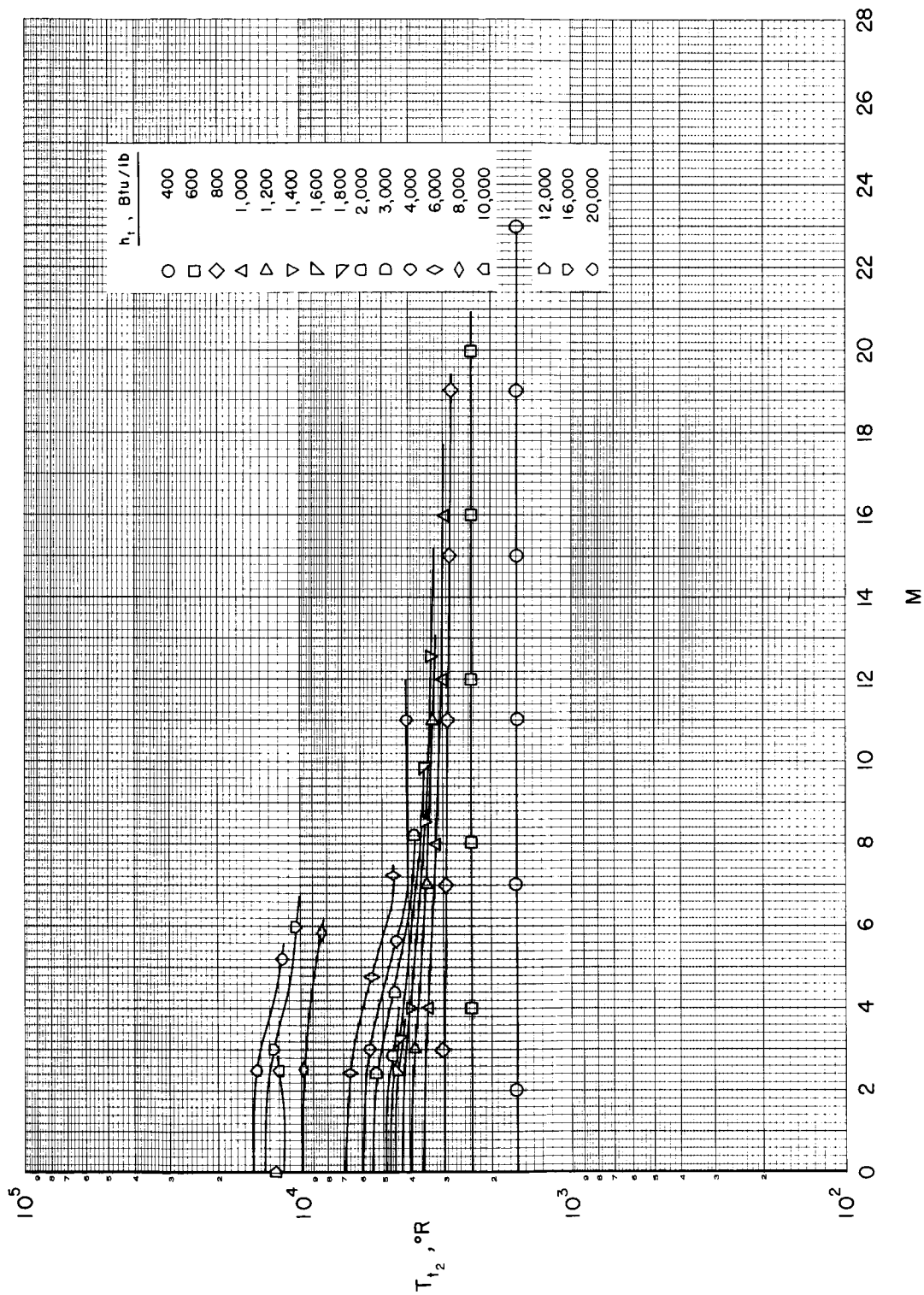
(a) $p_t = 1$ atm

Chart 2.- Variation of total temperature behind a normal shock wave with Mach number.
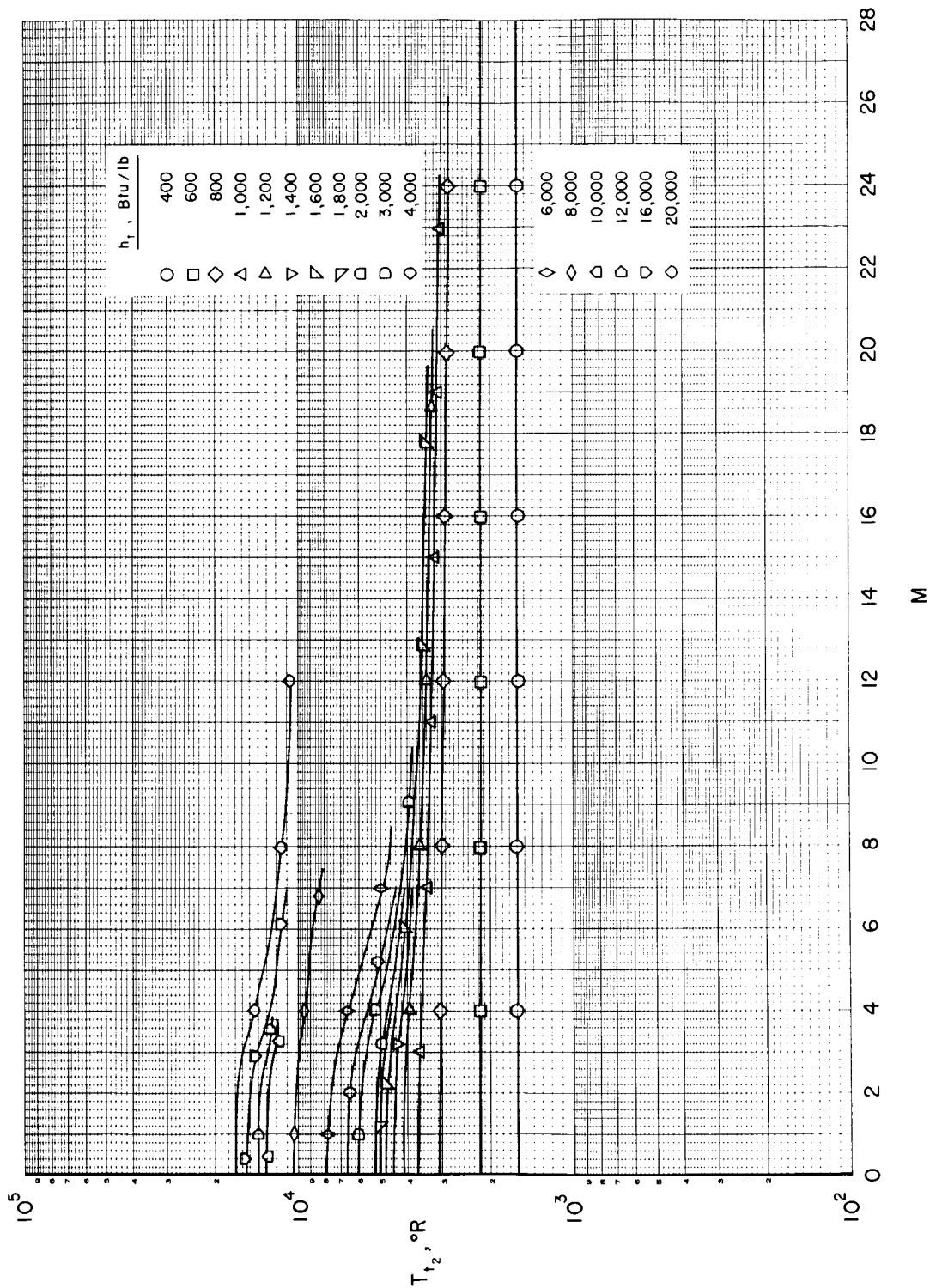
(b) $p_t = 10$ atm

Chart 2.- Continued.
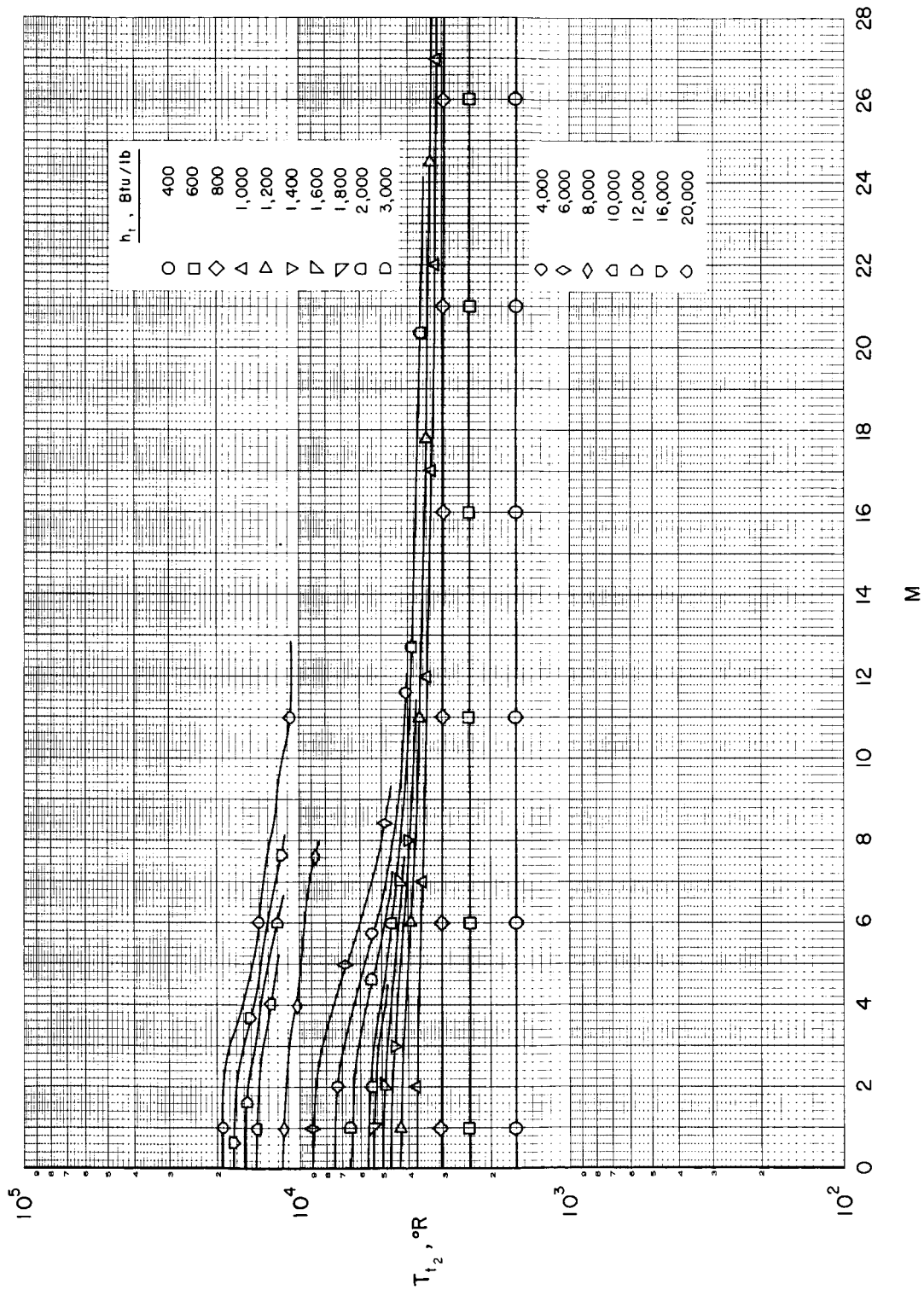
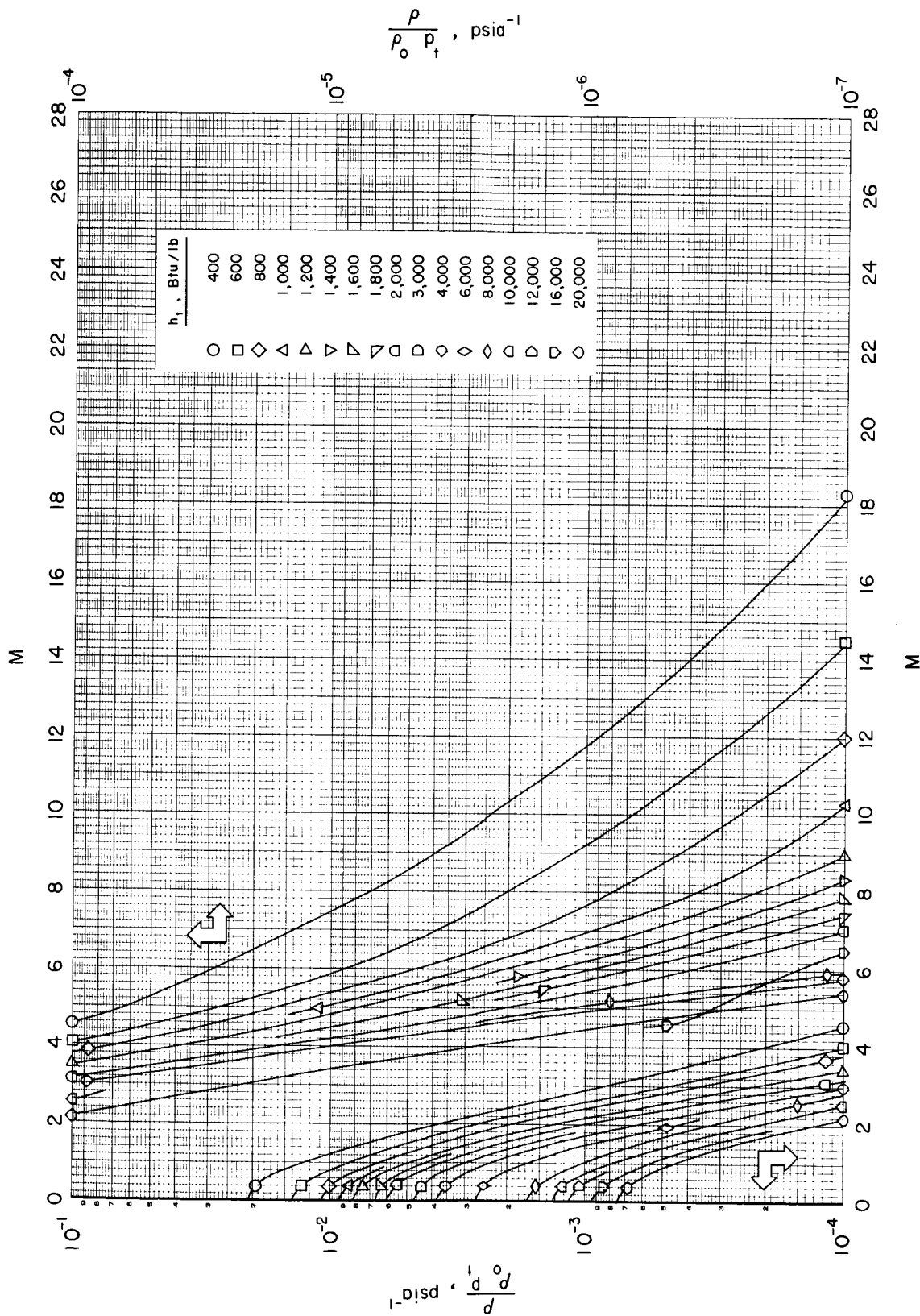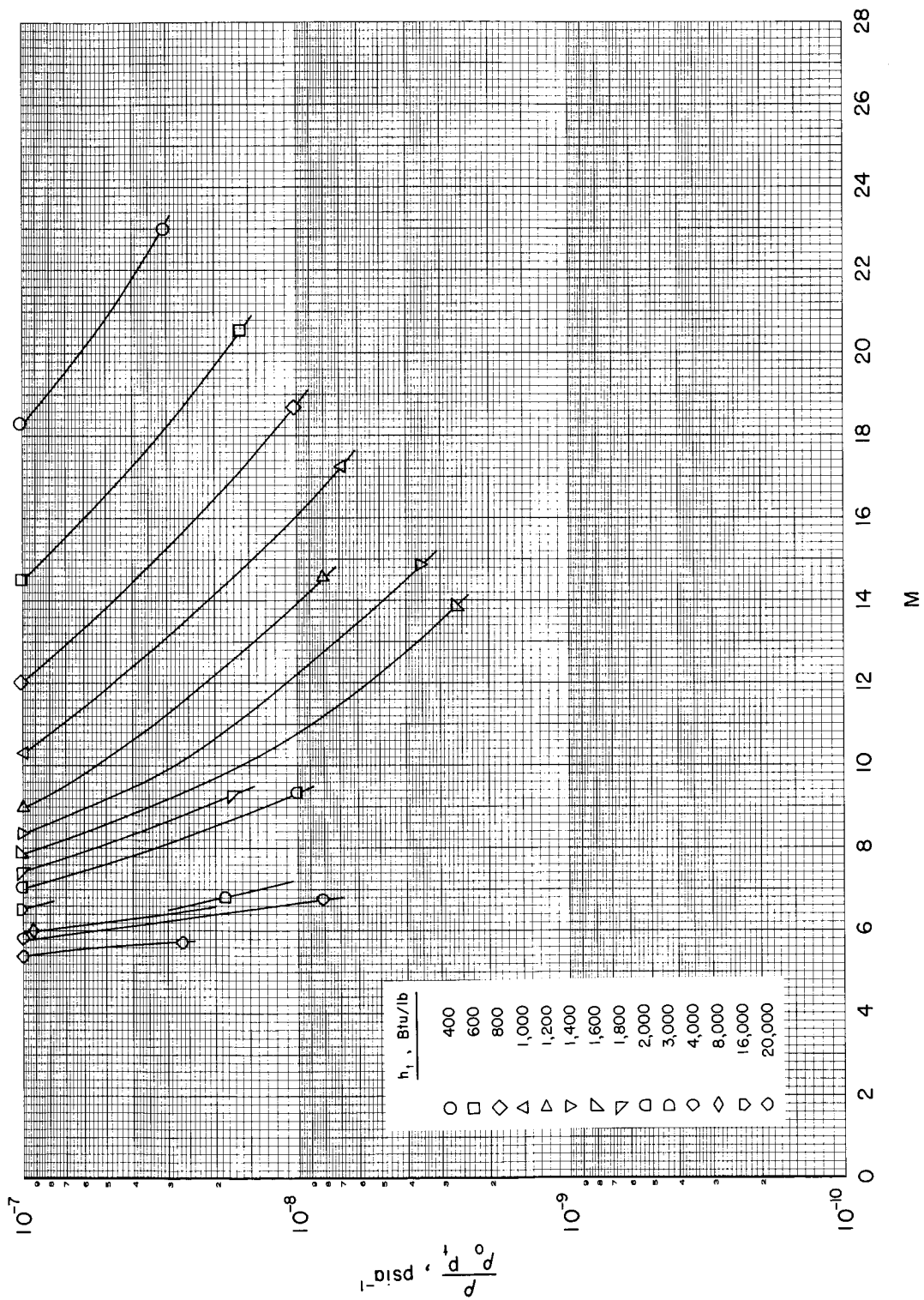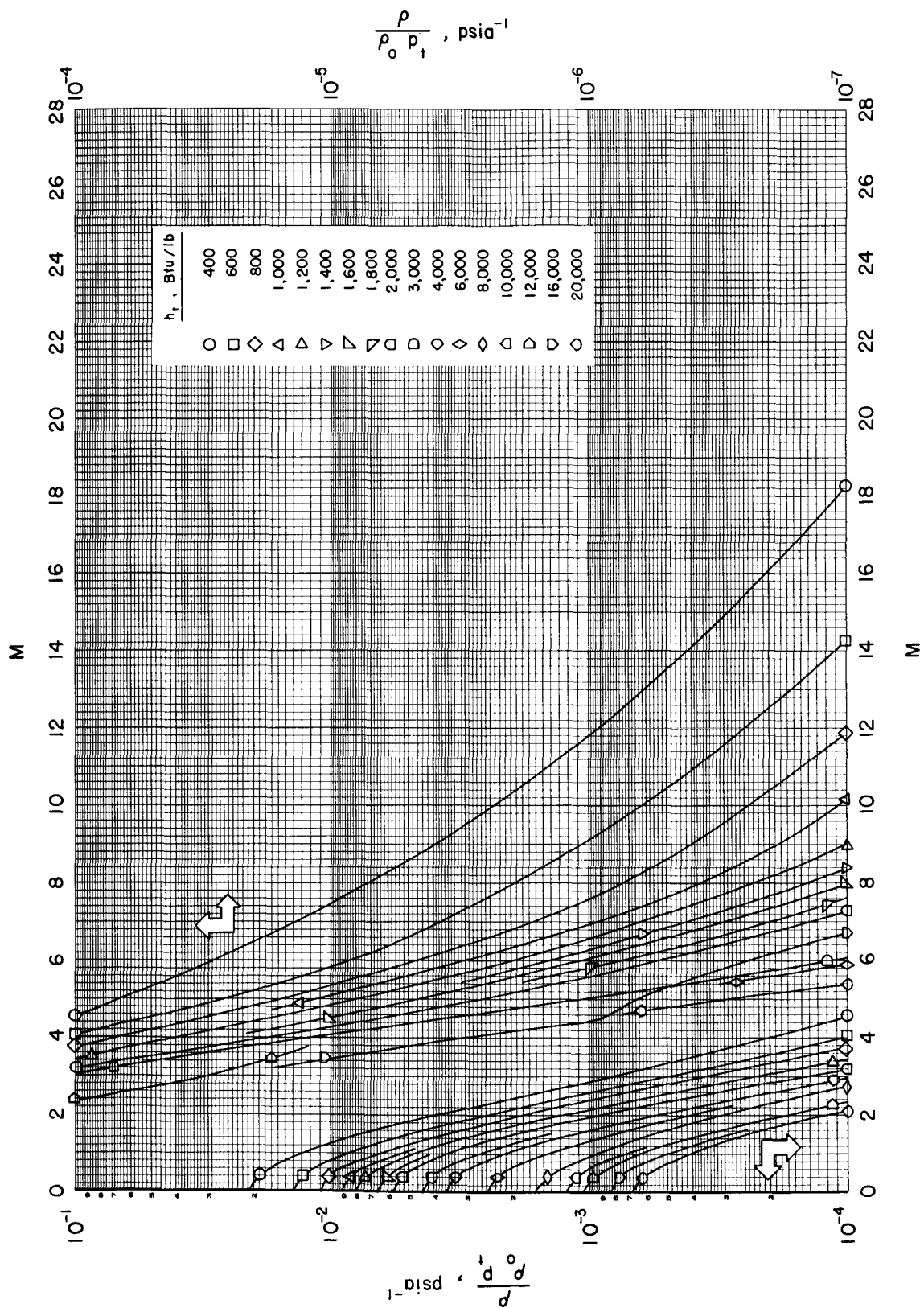(c) $p_t = 100$ atm

Chart 2.- Continued.
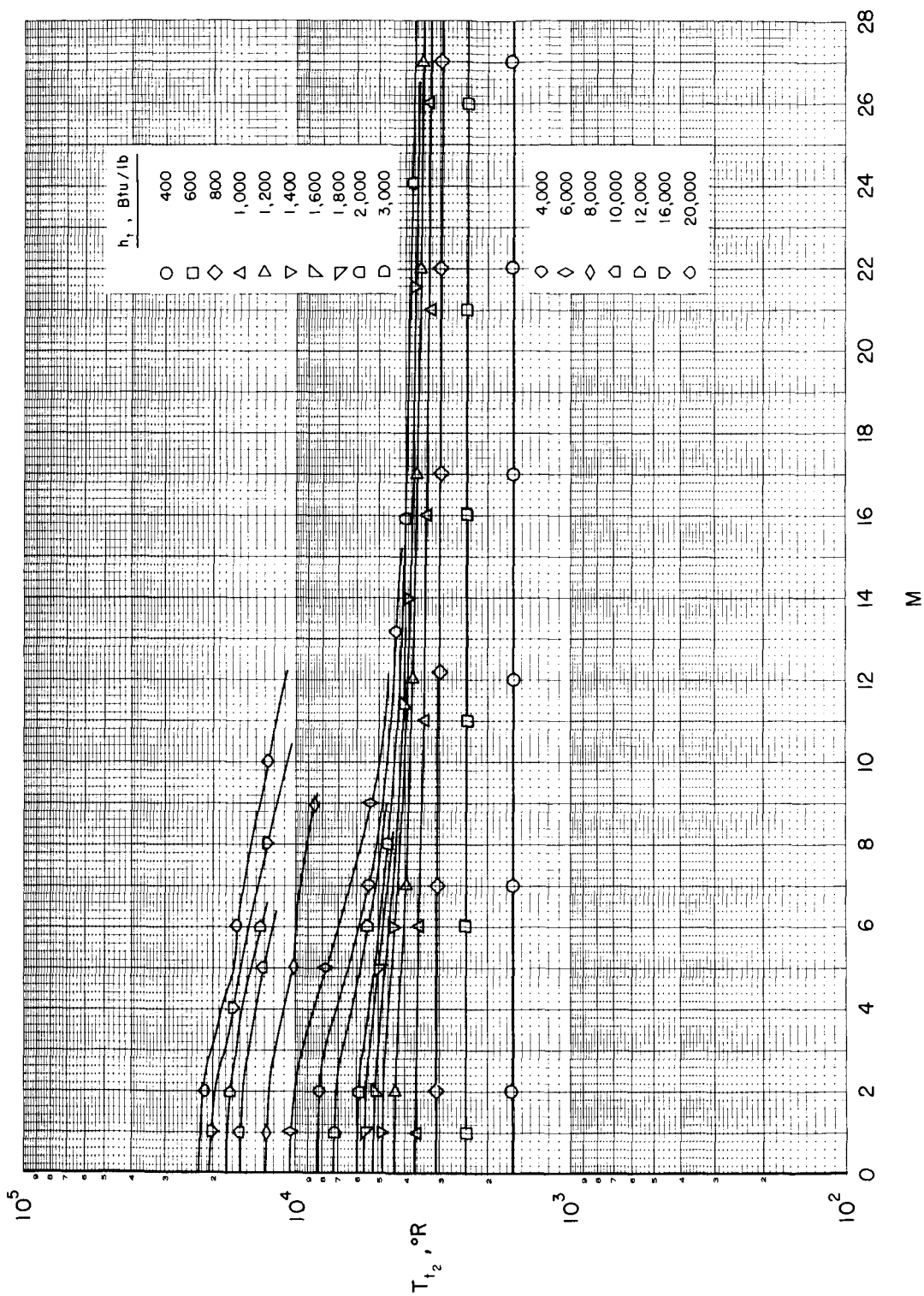
(d) $p_t = 1000$ atm

Chart 2.- Concluded.
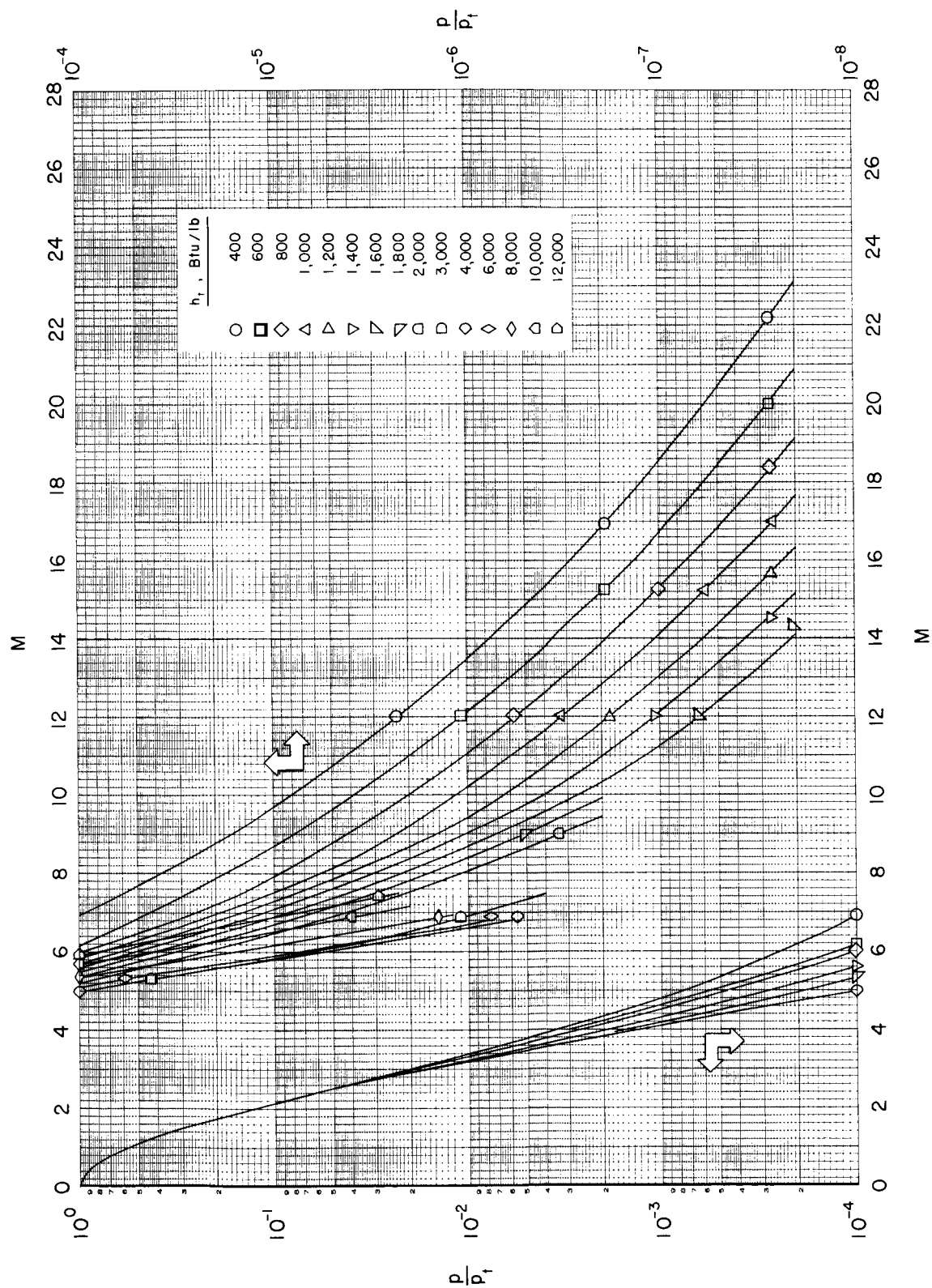
(a) $p_t = 1$ atm

Chart 3.- Variation of the ratio of static to total pressure with Mach number.
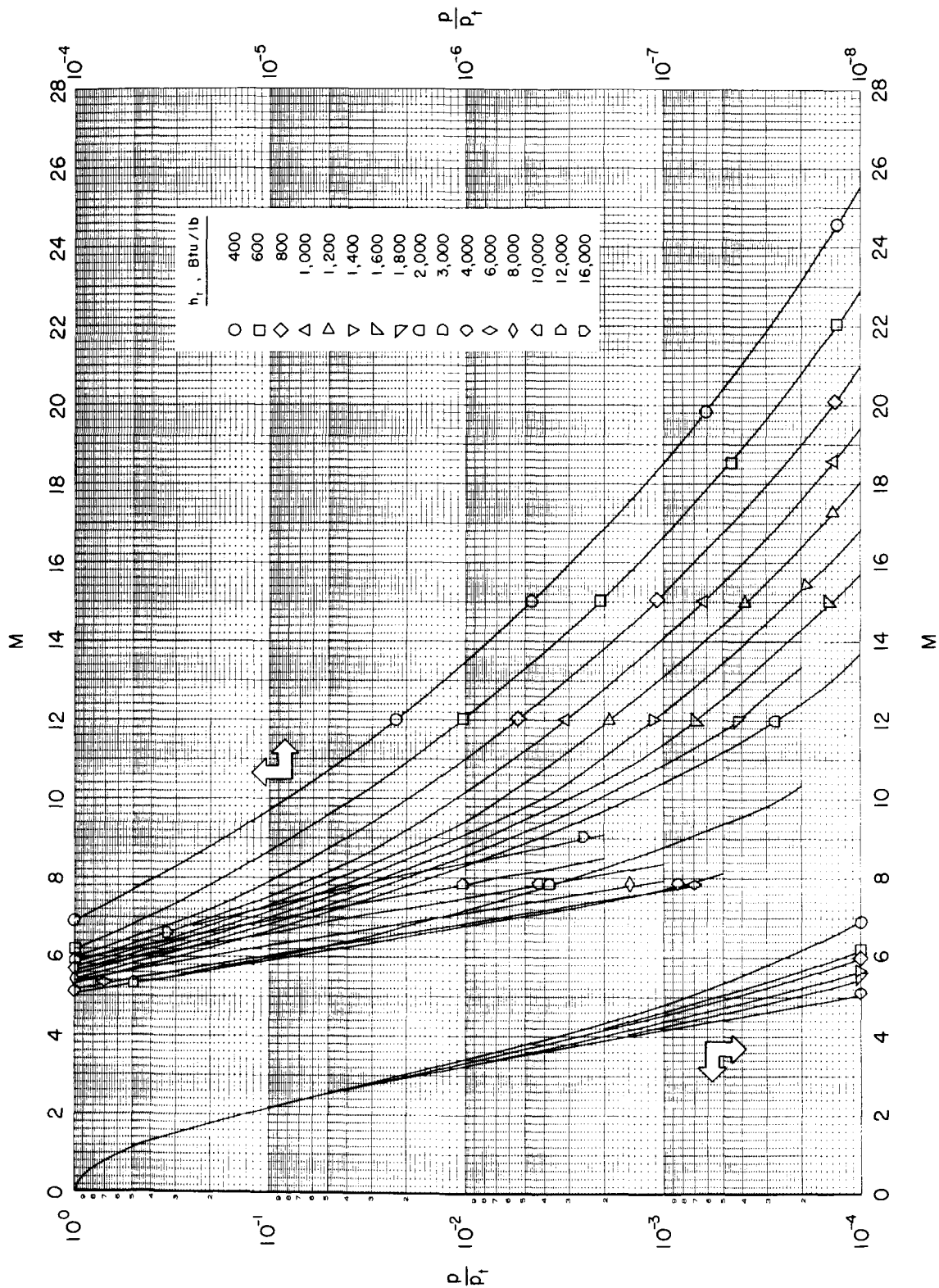
(b) p_t = 10 atm

Chart 3.- Continued.
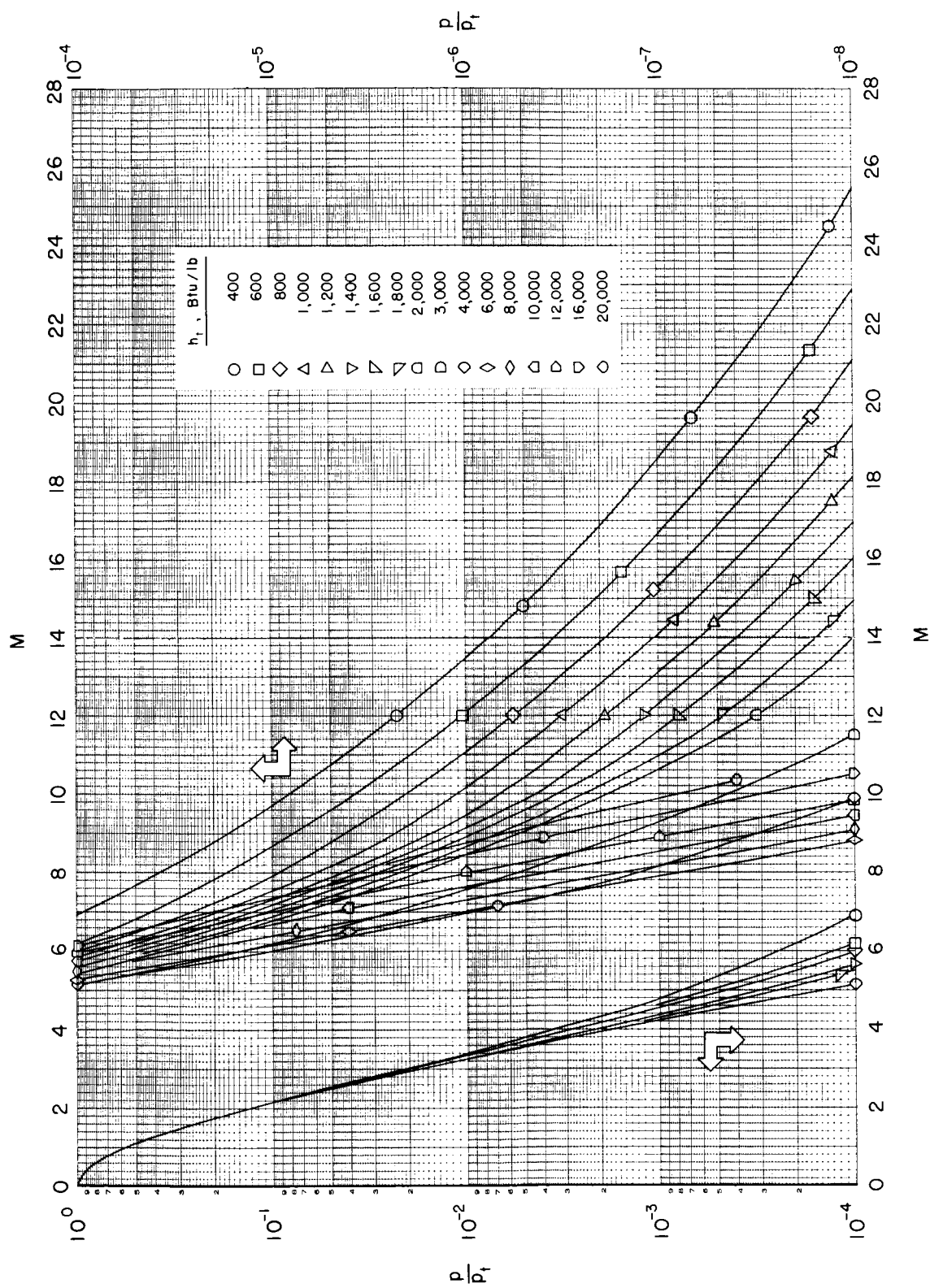
(c) $p_t = 100$ atm

Chart 3.- Continued.
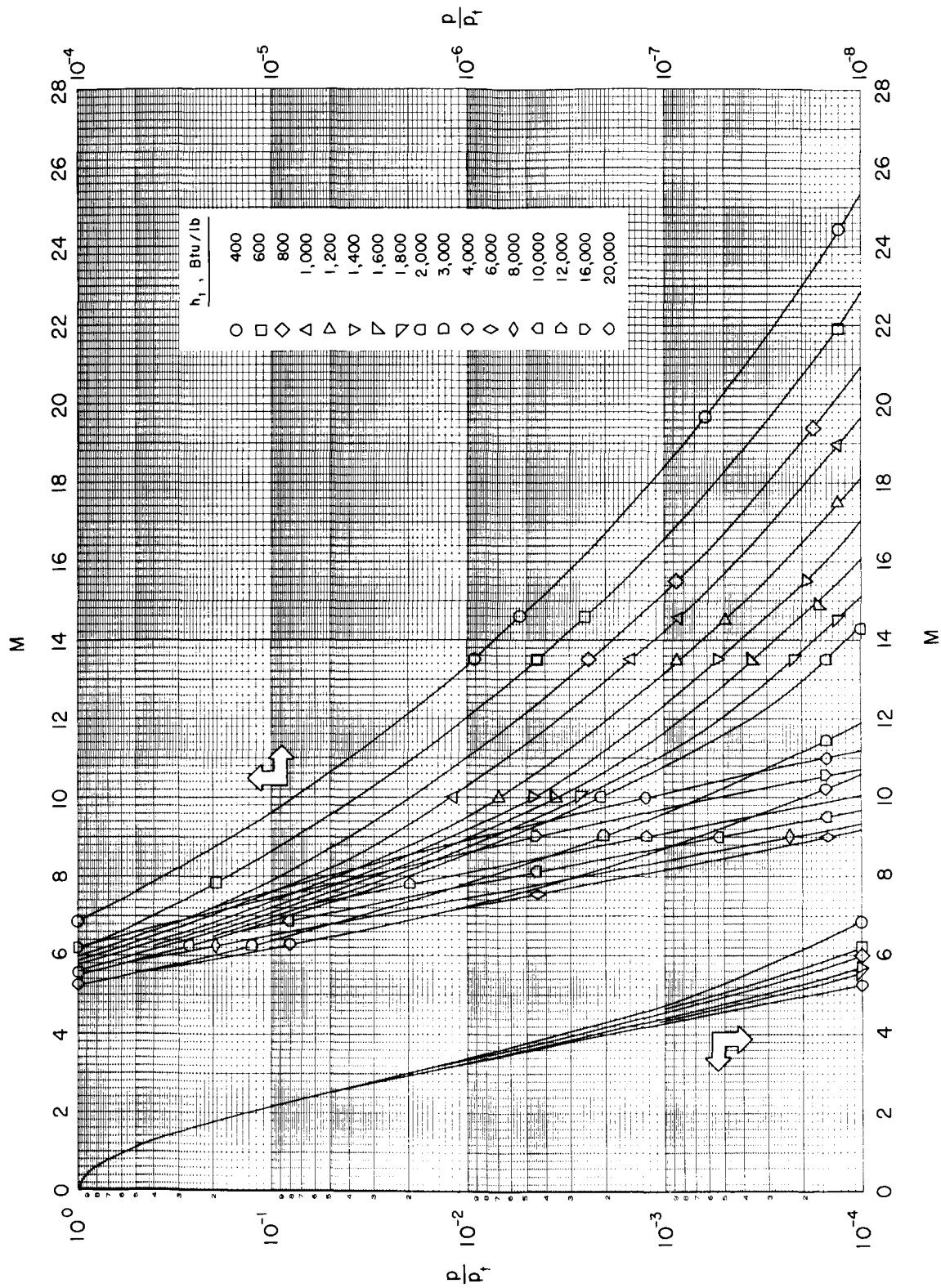
(d) p_t = 1000 atm

Chart 3.- Concluded.
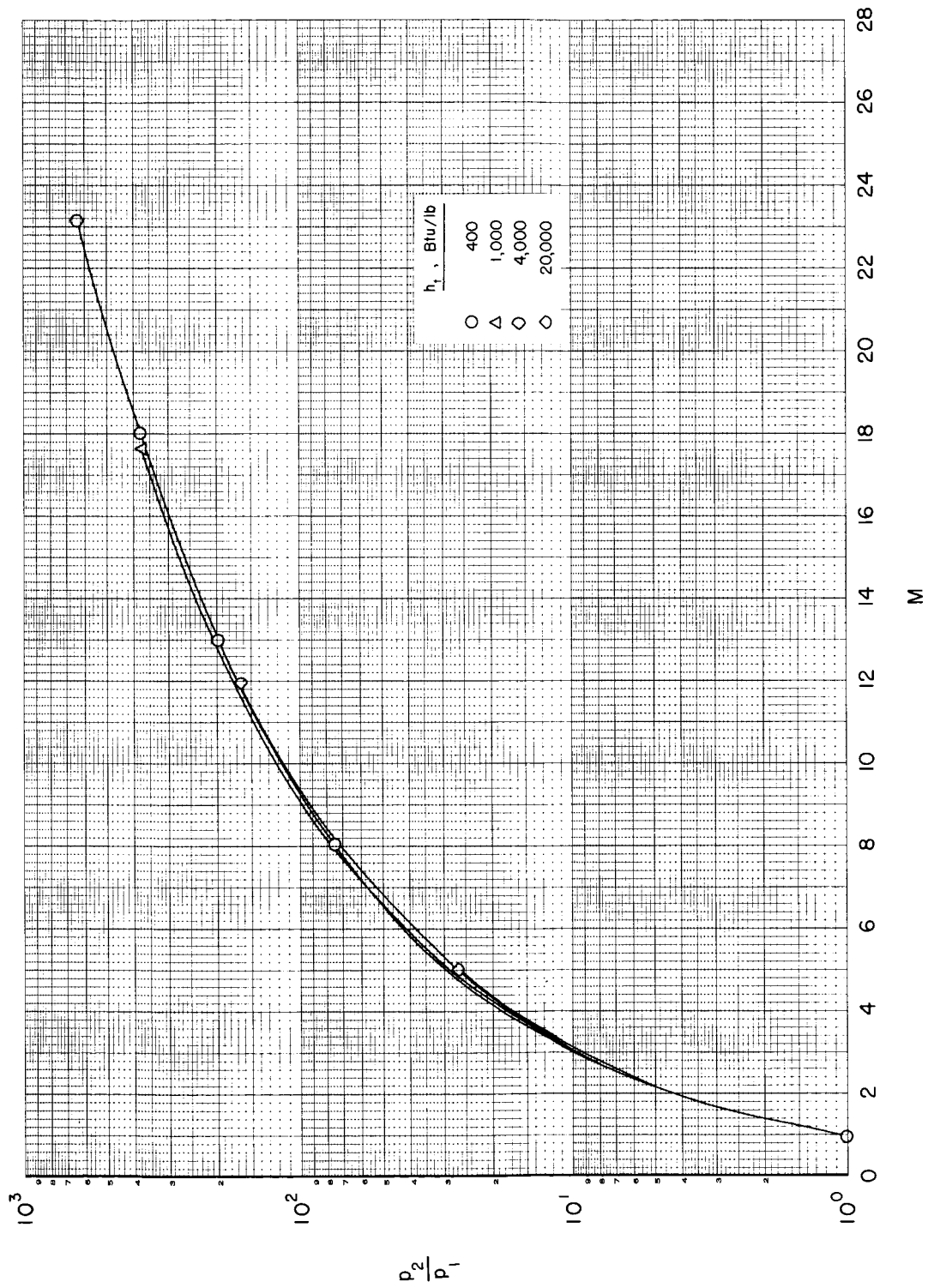
(a) $p_t = 1$ atm

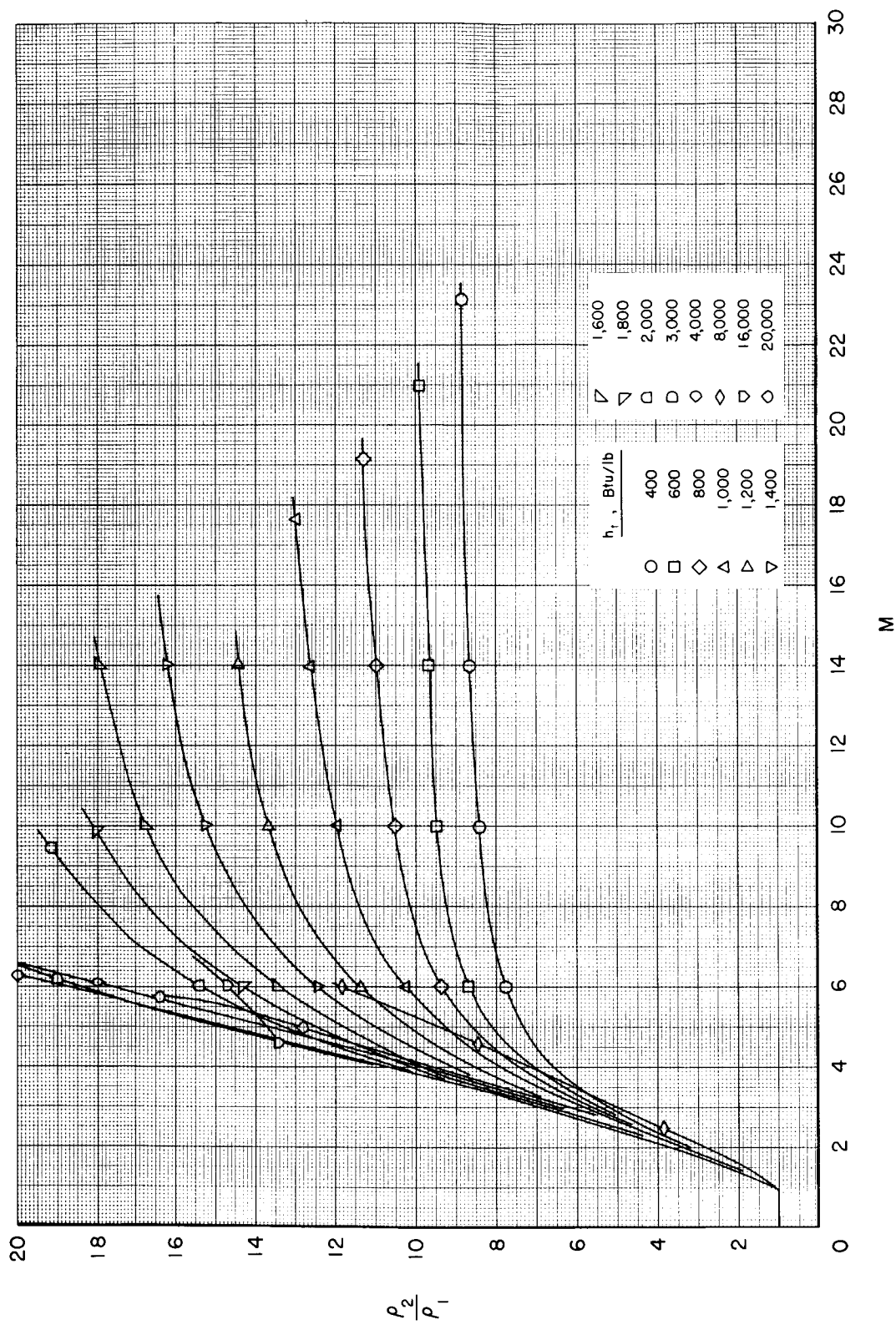Chart 4.- Variation of static pressure ratio across a normal shock wave with Mach number.
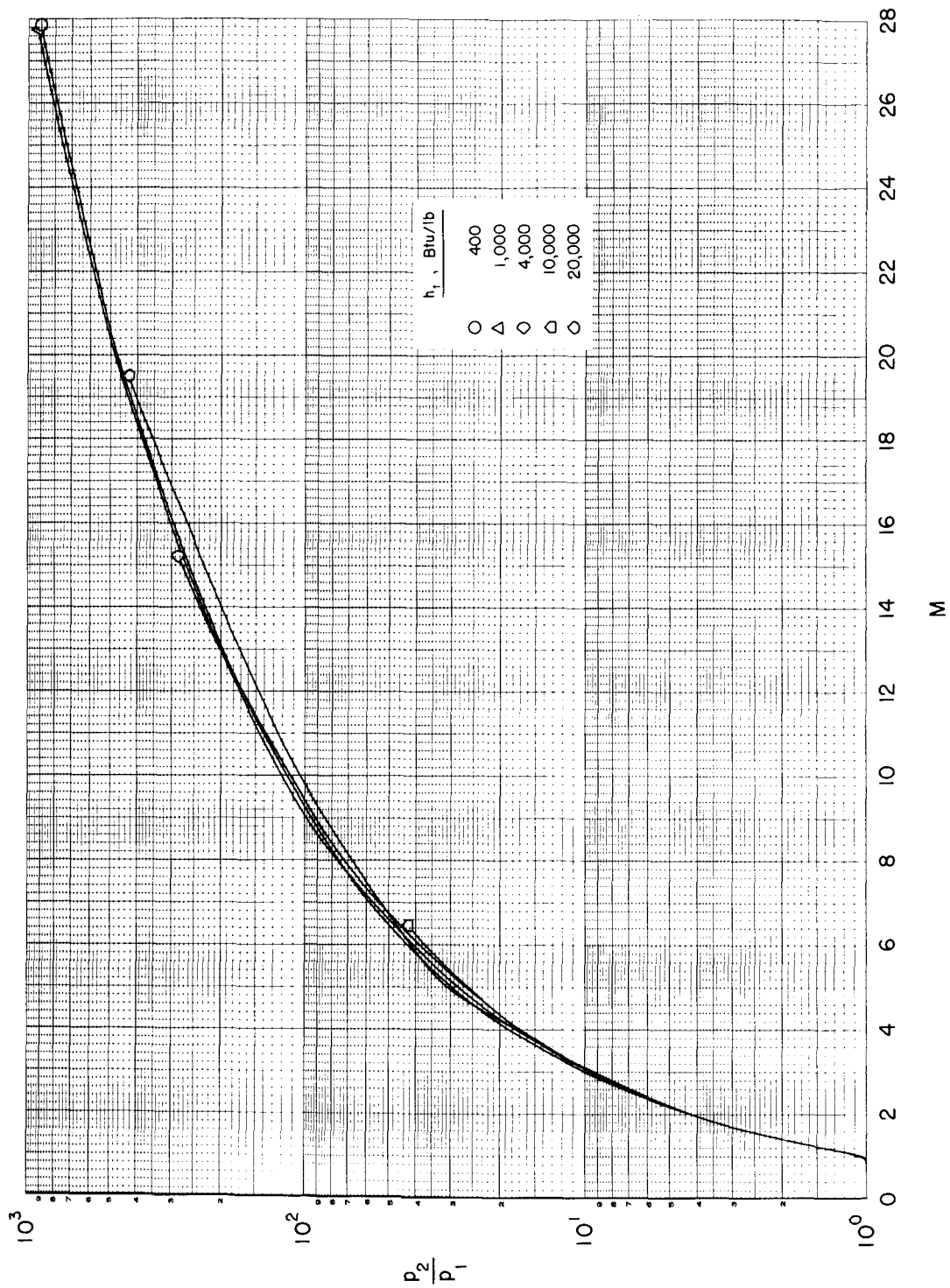
(b) $p_t = 1000$ atm

Chart 4.- Concluded.
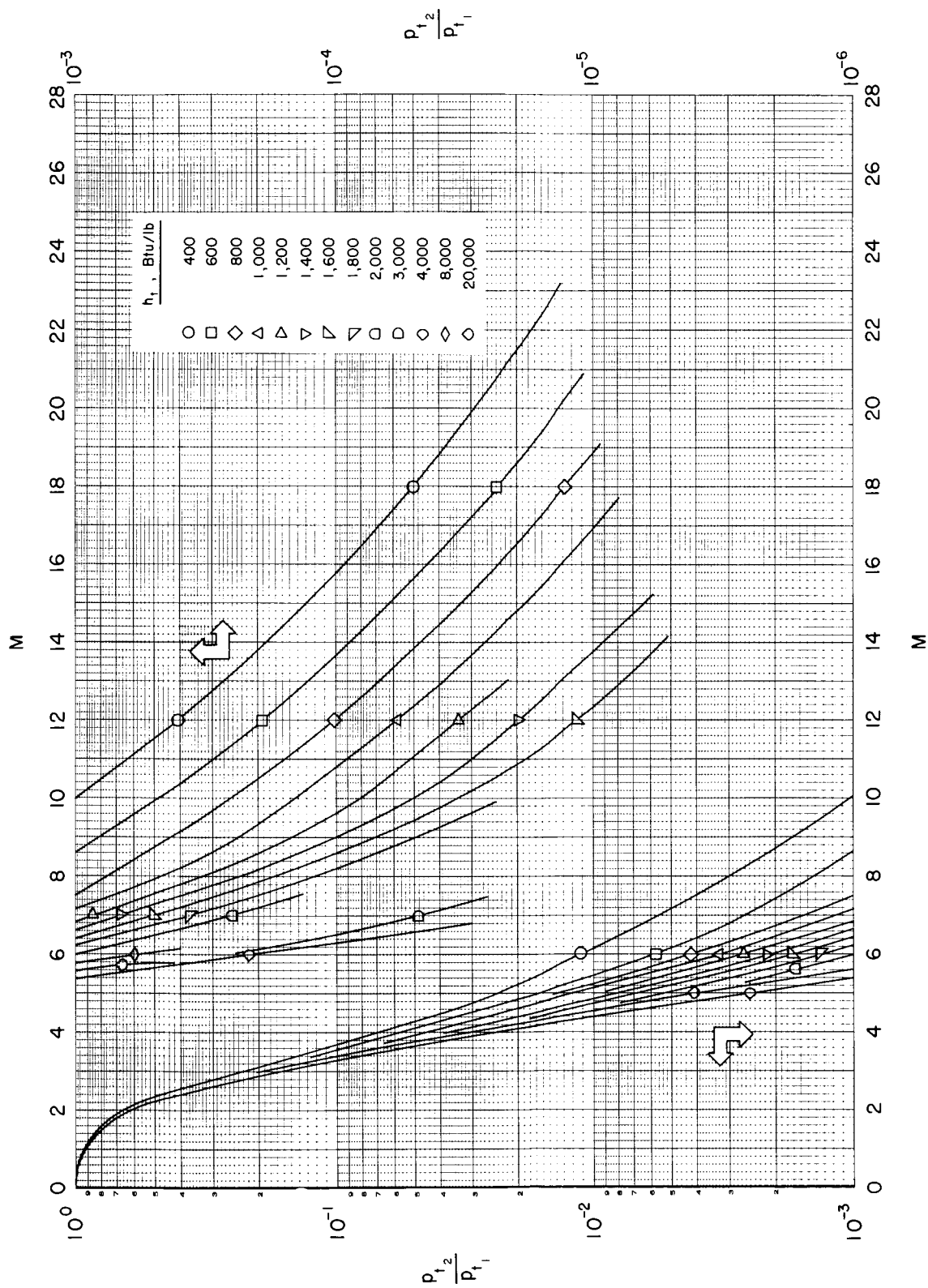
(a) $p_t = 1$ atm

Chart 5.- Variation of total pressure ratio across a normal shock wave with Mach number.
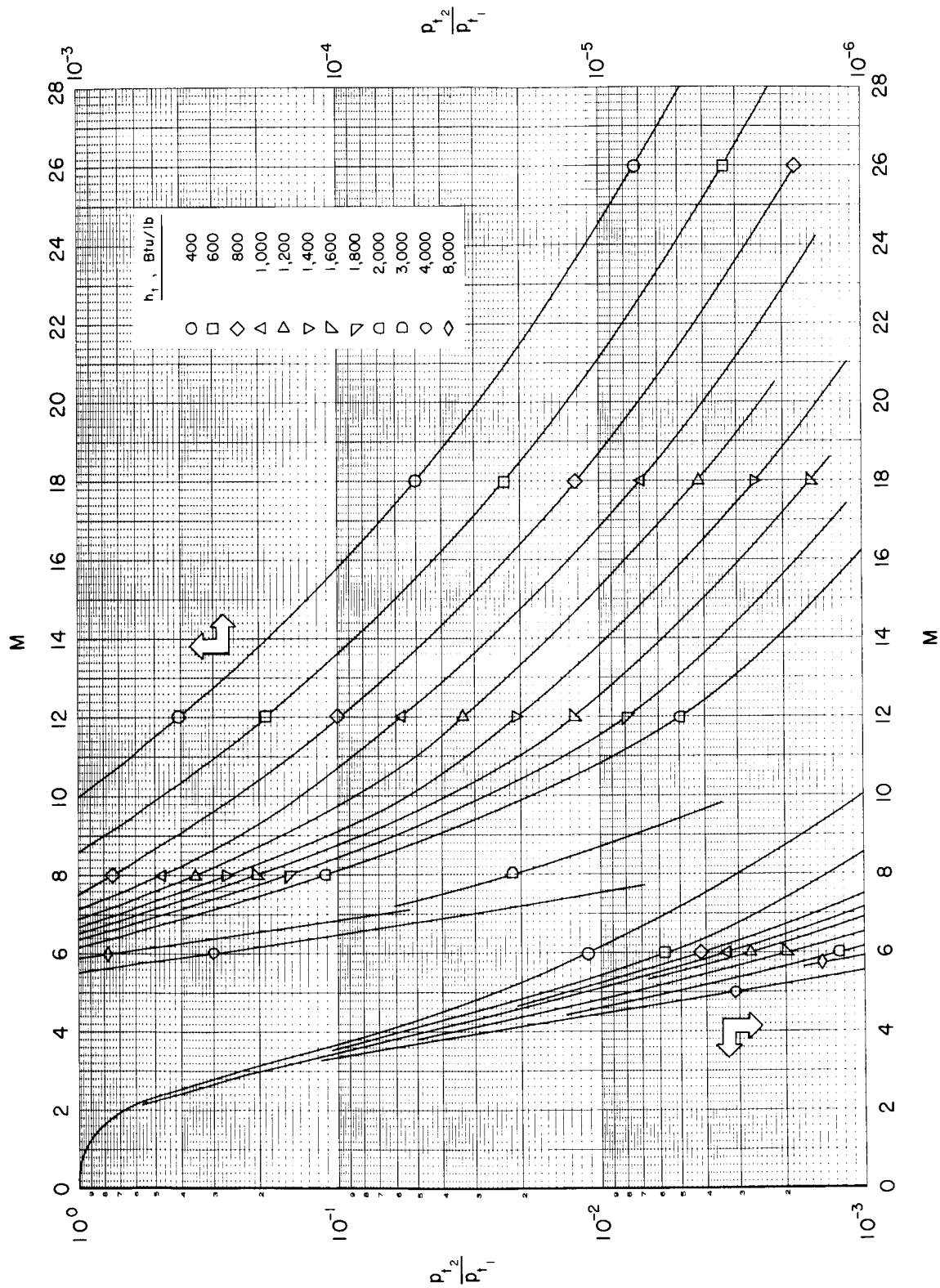
(b) $p_t = 10$ atm

Chart 5.- Continued.
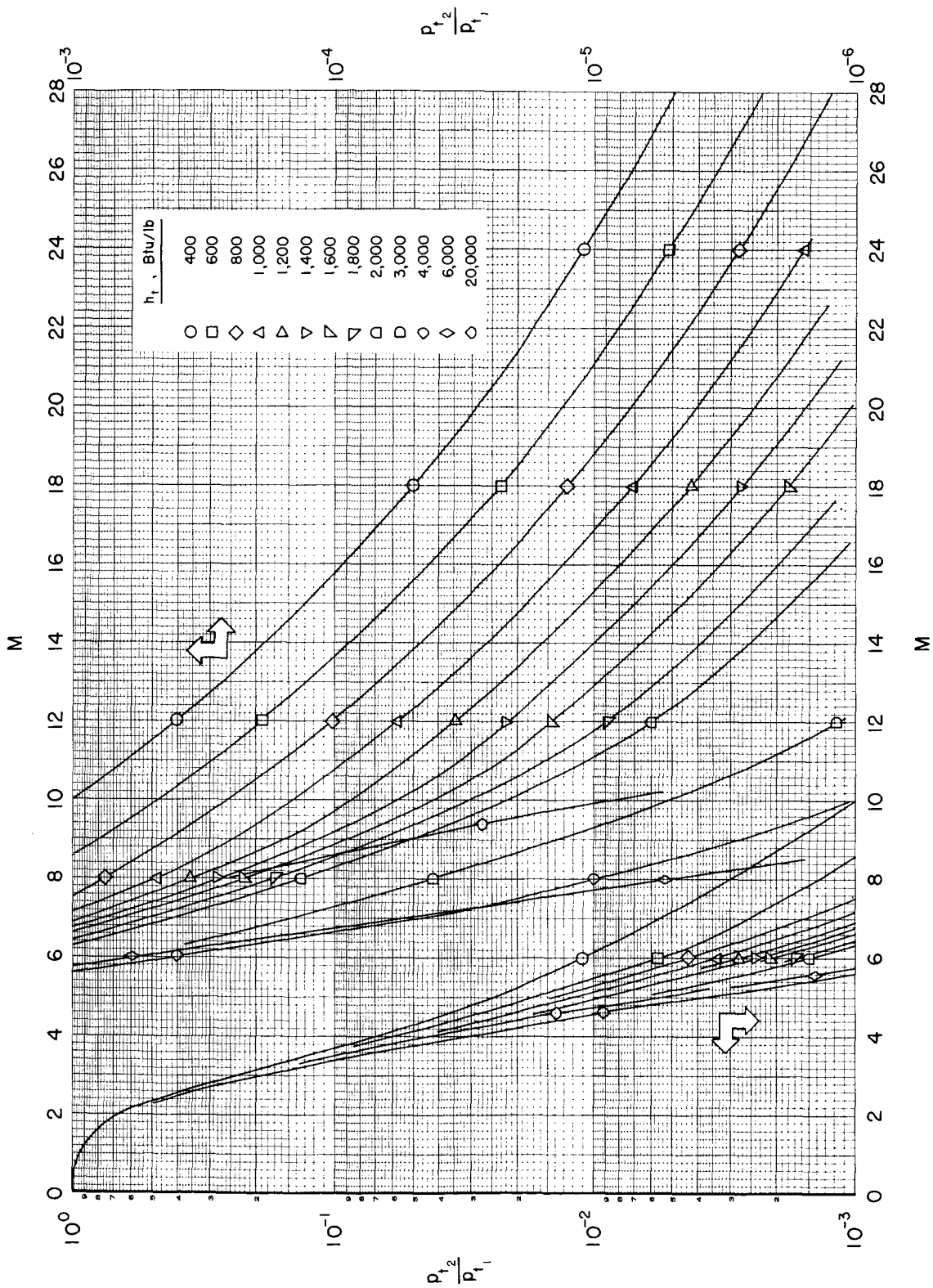
(c) p_t = 100 atm

Chart 5.- Continued.

(d) $p_t = 1000$ atm

Chart 5.- Concluded.

$\dfrac{\rho}{\rho_0 \, p_t}$, psia^{-1}

h_t , Btu/lb	
400	◯
600	☐
800	◇
1,000	◁
1,200	△
1,400	▷
1,600	◹
1,800	◿
2,000	◻
3,000	◇
4,000	◇
6,000	◇
8,000	◻
10,000	△
12,000	▷
16,000	◇
20,000	◇

(a) $p_t = 1$ atm

Chart 6.– Variation of density parameter with Mach number; $\rho_O = 0.00384$ slug/ft^3.

(a) $p_t = 1$ atm – Concluded.

Chart 6.– Continued.

(b) $p_t = 10$ atm

Chart 6.- Continued.
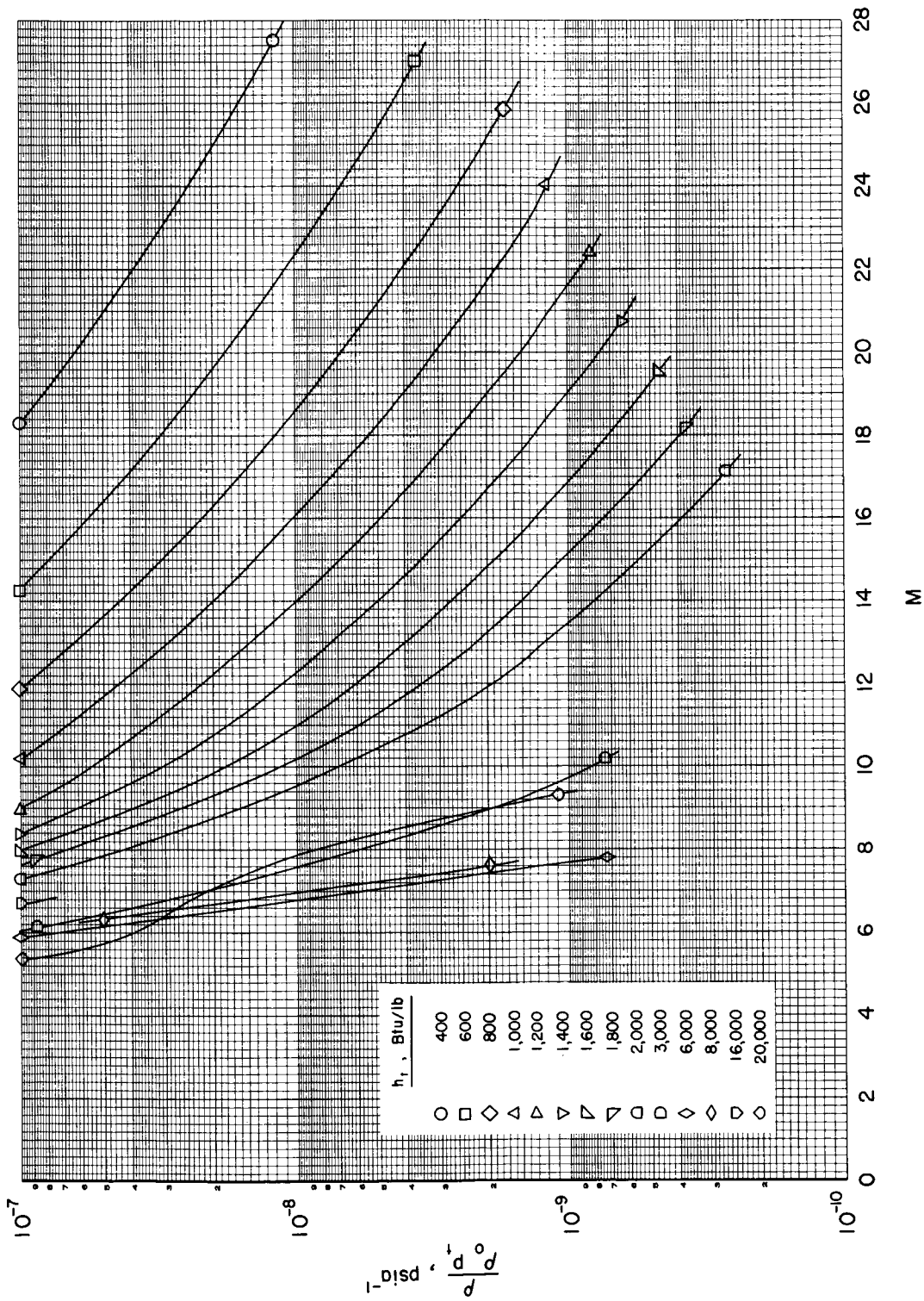
(b) $p_t = 10$ atm – Concluded.

Chart 6.– Continued.
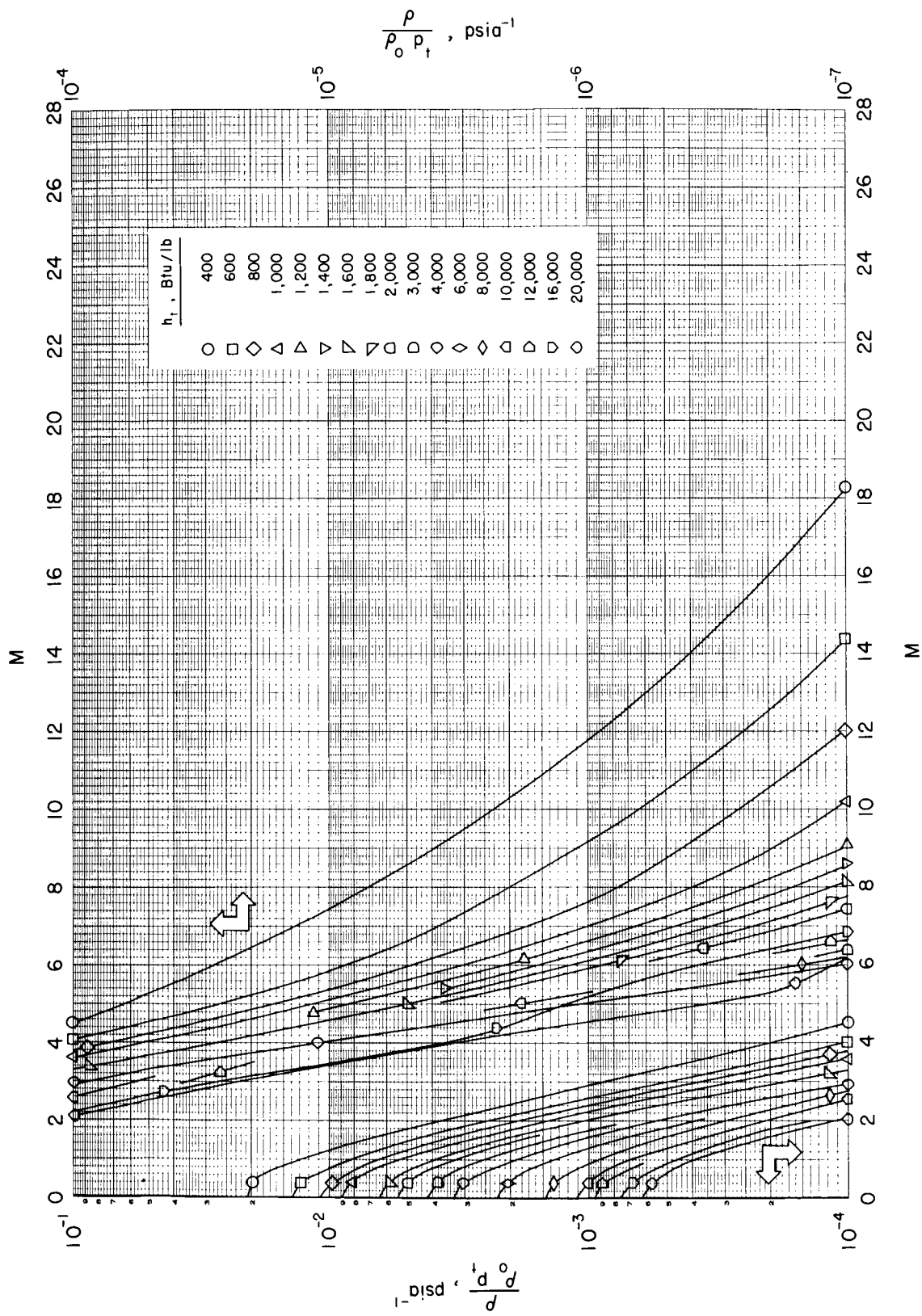
(c) $p_t = 100$ atm

Chart 6.- Continued.

(c) $p_t = 100$ atm - Concluded.

Chart 6.- Continued.

39

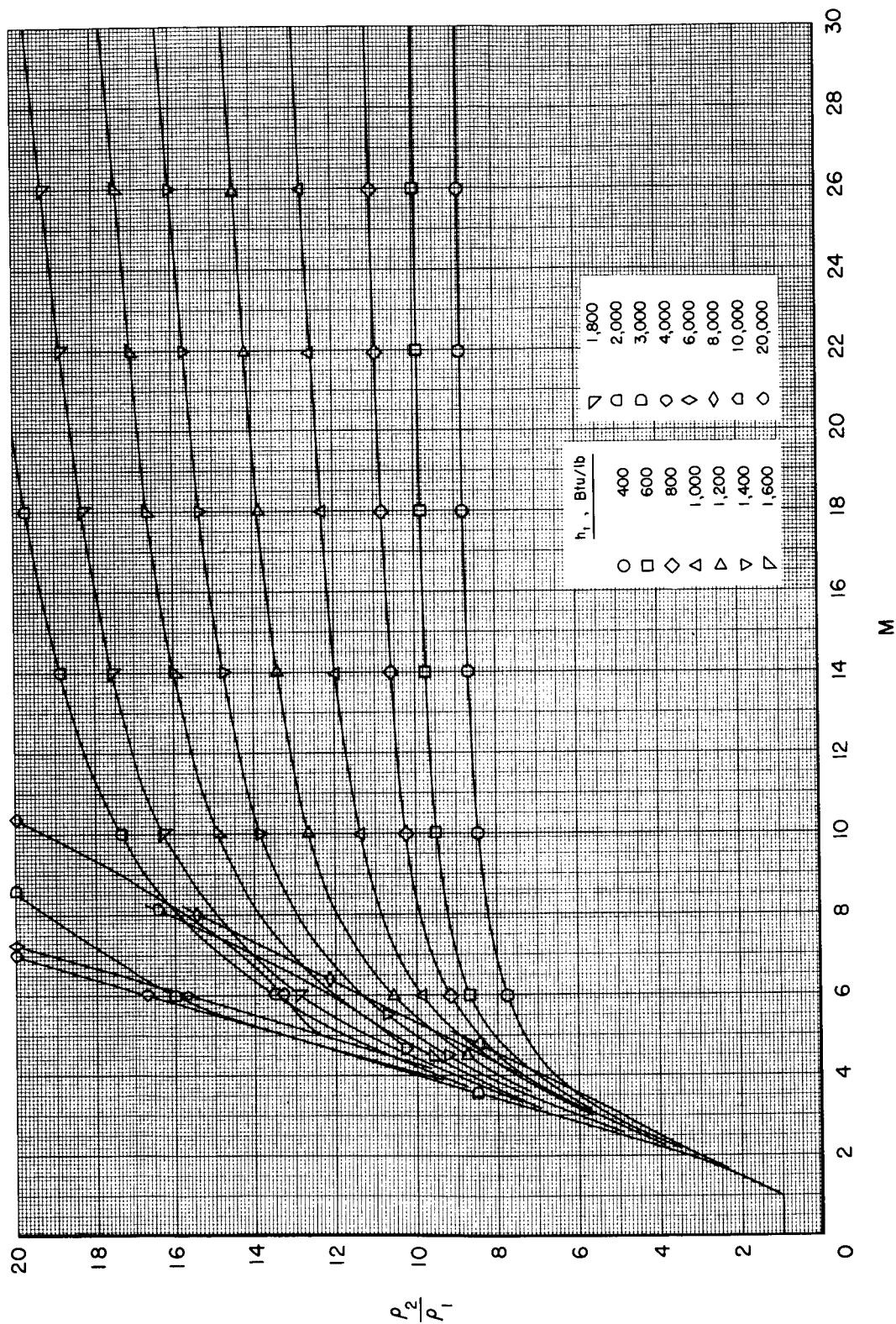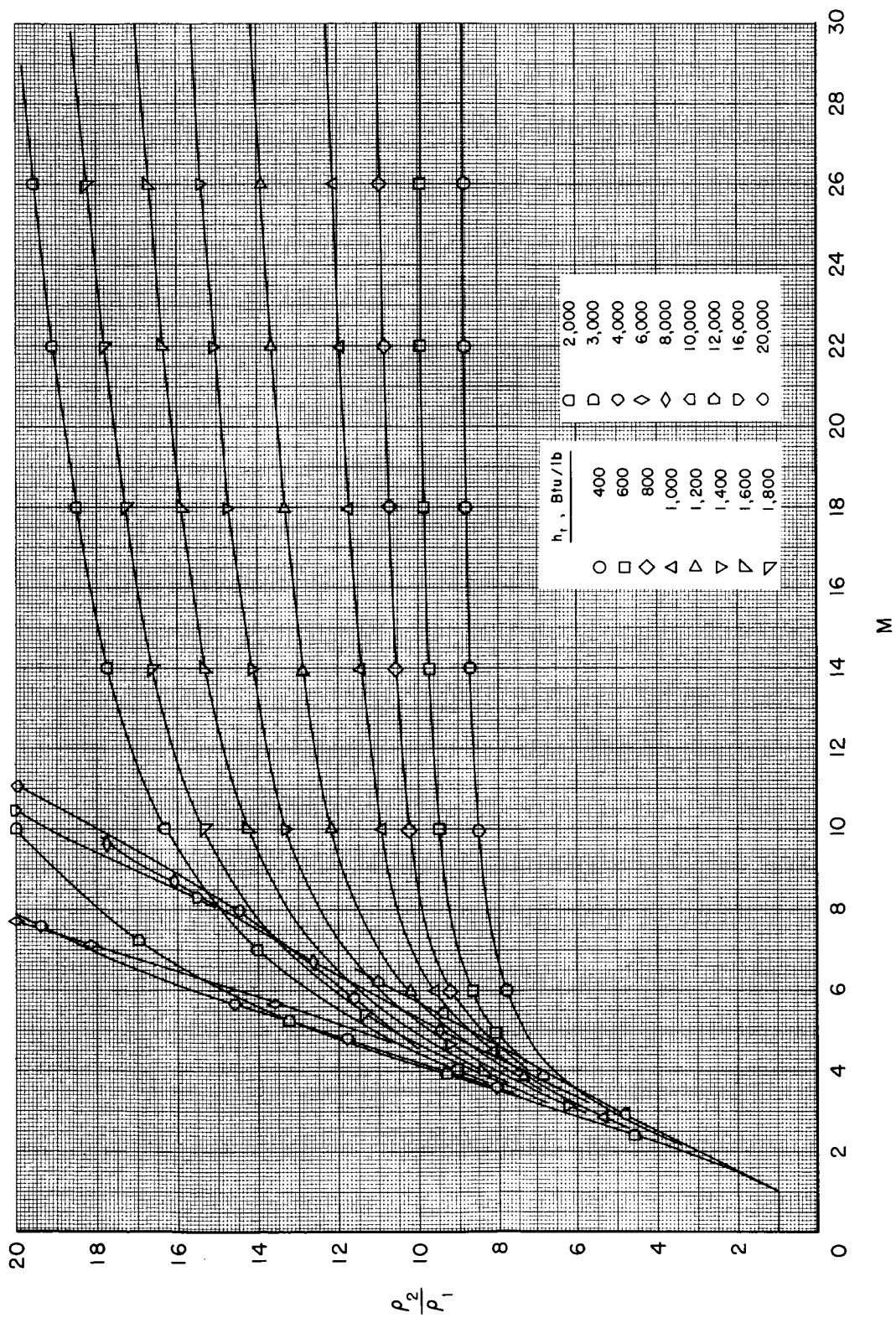$$\frac{\rho}{\rho_0\, p_t} \text{, psia}^{-1}$$

h_t, Btu/lb	
○	400
□	600
◇	800
◁	1,000
△	1,200
▷	1,400
◺	1,600
▽	1,800
◁	2,000
◇	3,000
◇	4,000
◇	6,000
◇	8,000
◁	10,000
△	12,000
◁	16,000
◇	20,000

(d) $p_t = 1000$ atm

Chart 6.– Continued.

M

$\dfrac{p}{p_t}\ \dfrac{p_o}{p}$, psia^{-1}

h_t, Btu/lb	
○	400
□	600
◇	800
◁	1,000
△	1,200
▷	1,400
◺	1,600
▽	1,800
◻	2,000
◻	3,000
◇	4,000
◇	6,000
◇	8,000
◻	10,000
▷	12,000
◇	16,000
	20,000
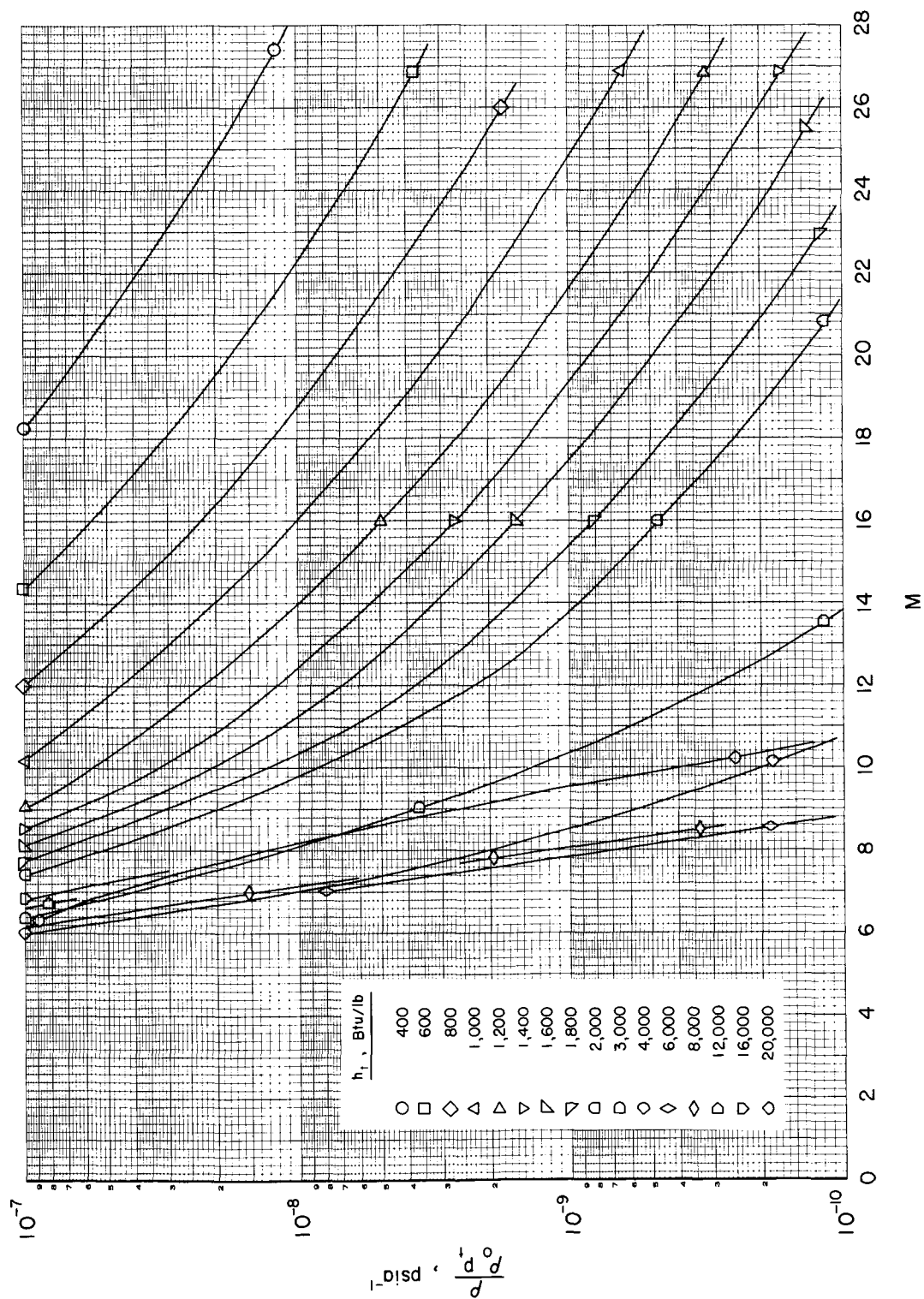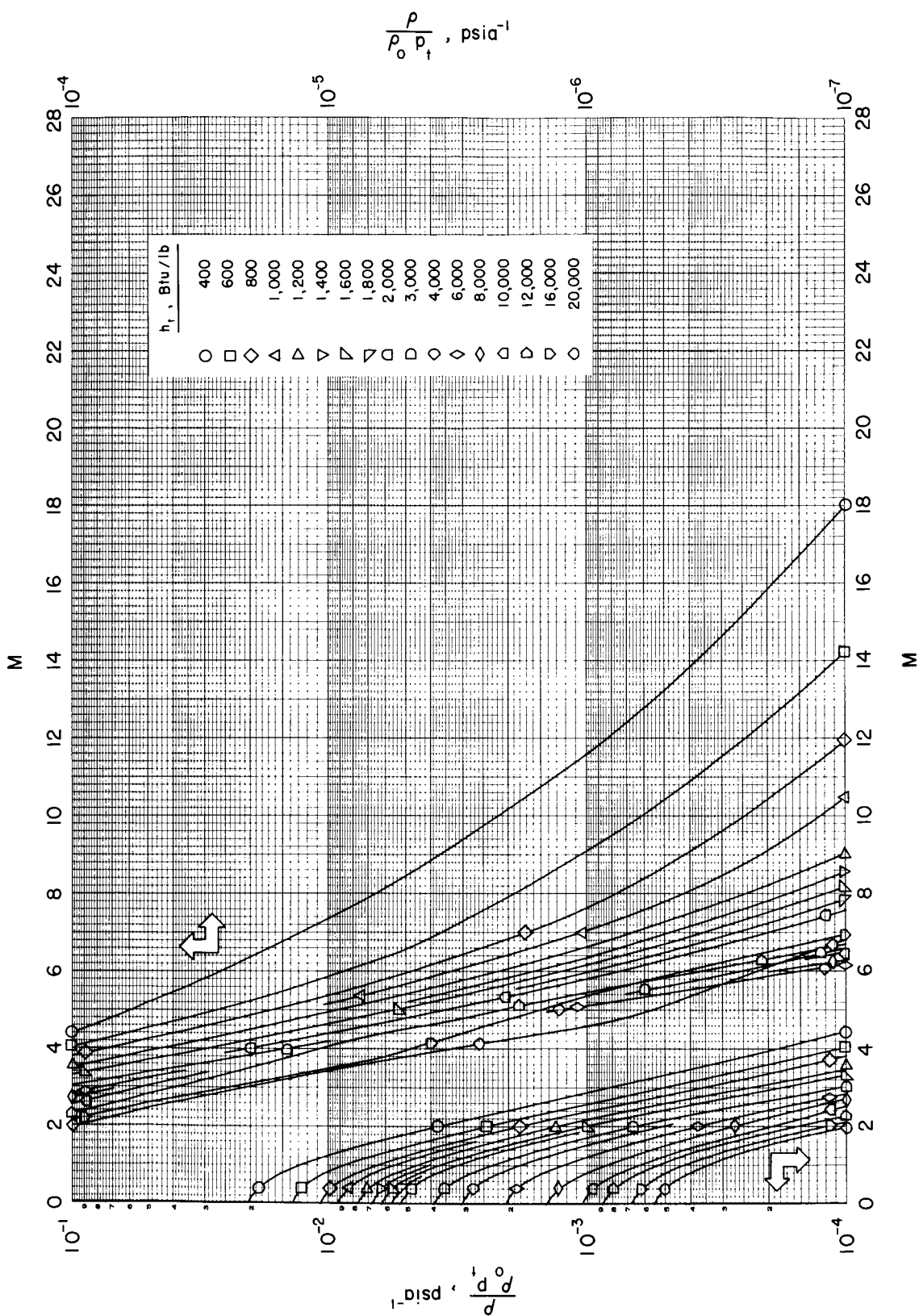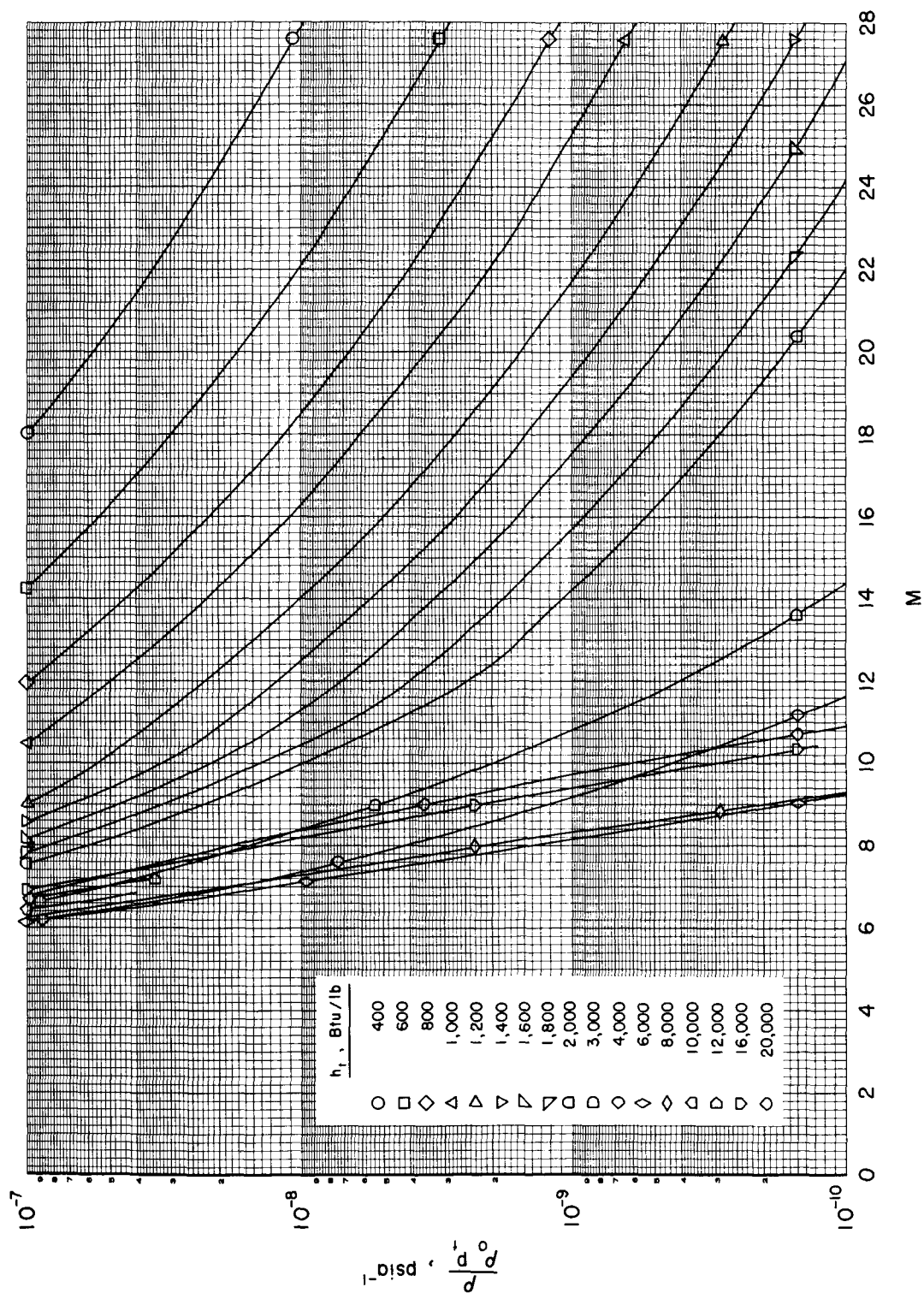
(d) p_t = 1000 atm – Concluded.

Chart 6.– Concluded.

(a) $p_t = 1$ atm

Chart 7.- Variation of density ratio across a normal shock with Mach number.
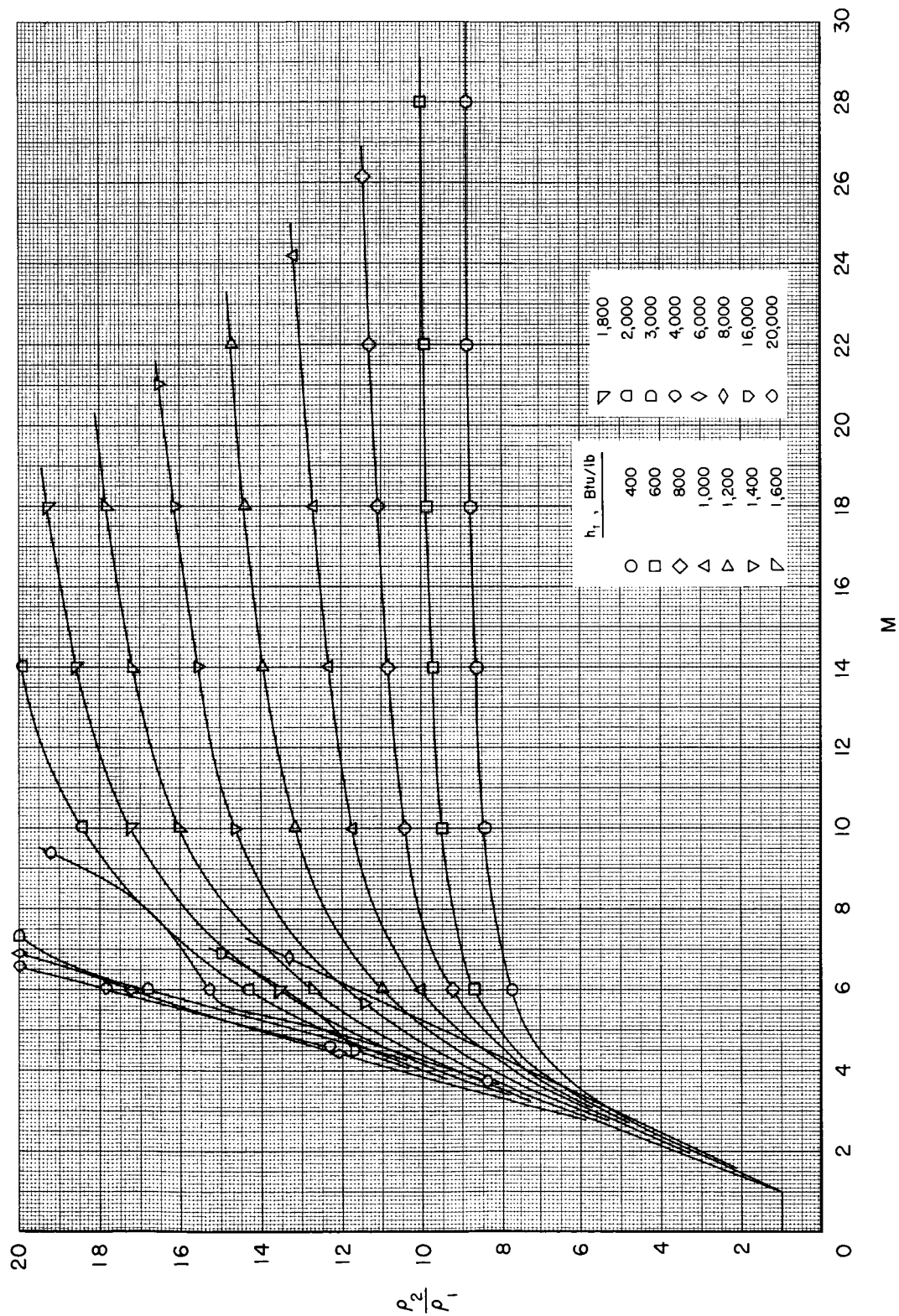
(b) $p_t = 10$ atm

Chart 7.- Continued.

(c) $p_t = 100$ atm

Chart 7.- Continued.

(d) p_t = 1000 atm
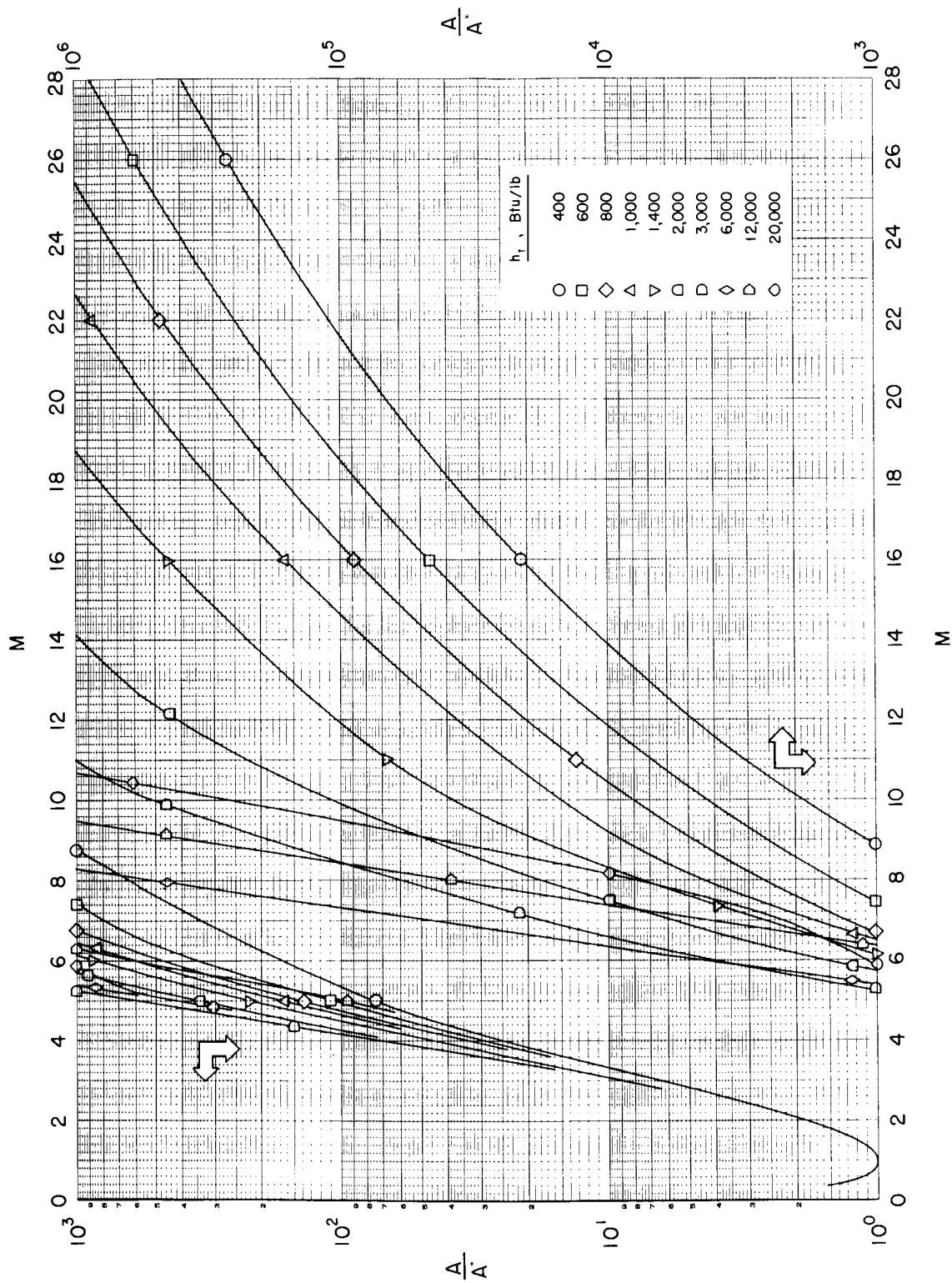
Chart 7.- Concluded.

The figure shows a chart of speed u (ft/sec) versus Mach number M, with the vertical axis u, $\frac{ft}{sec}$ ranging from 0 to 30×10^3 and the horizontal axis M from 0 to 20.

	h_t , Btu/lb
○	400
□	600
◇	800
△	1,000
▷	1,200
▽	1,400
▽	1,600
◁	1,800
◻	2,000
▯	3,000
◇	4,000
◇	6,000
◇	8,000
◻	10,000
▯	12,000
▽	16,000
◇	20,000
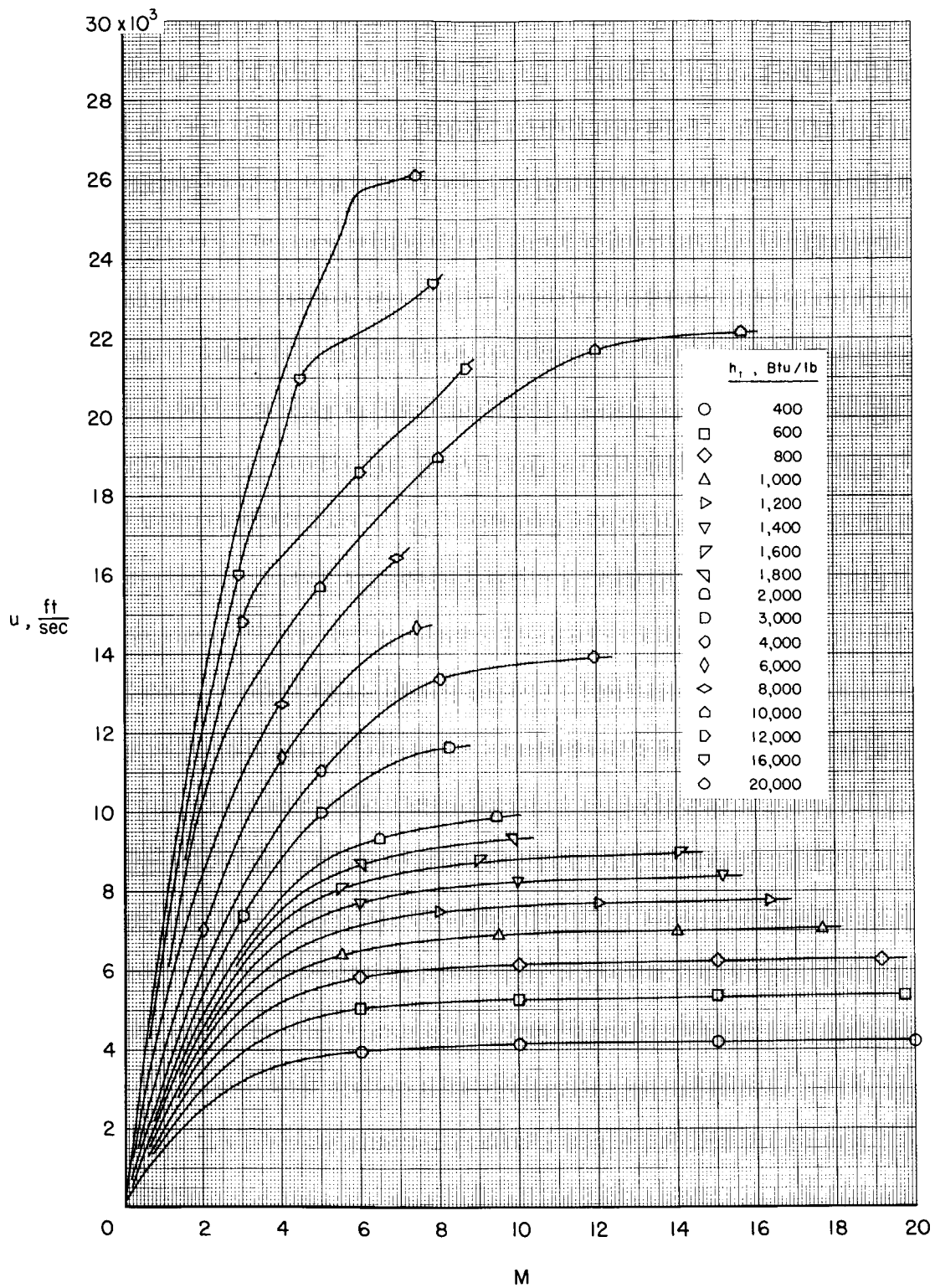
(a) p_t = 1 atm

Chart 8.- Variation of speed with Mach number.
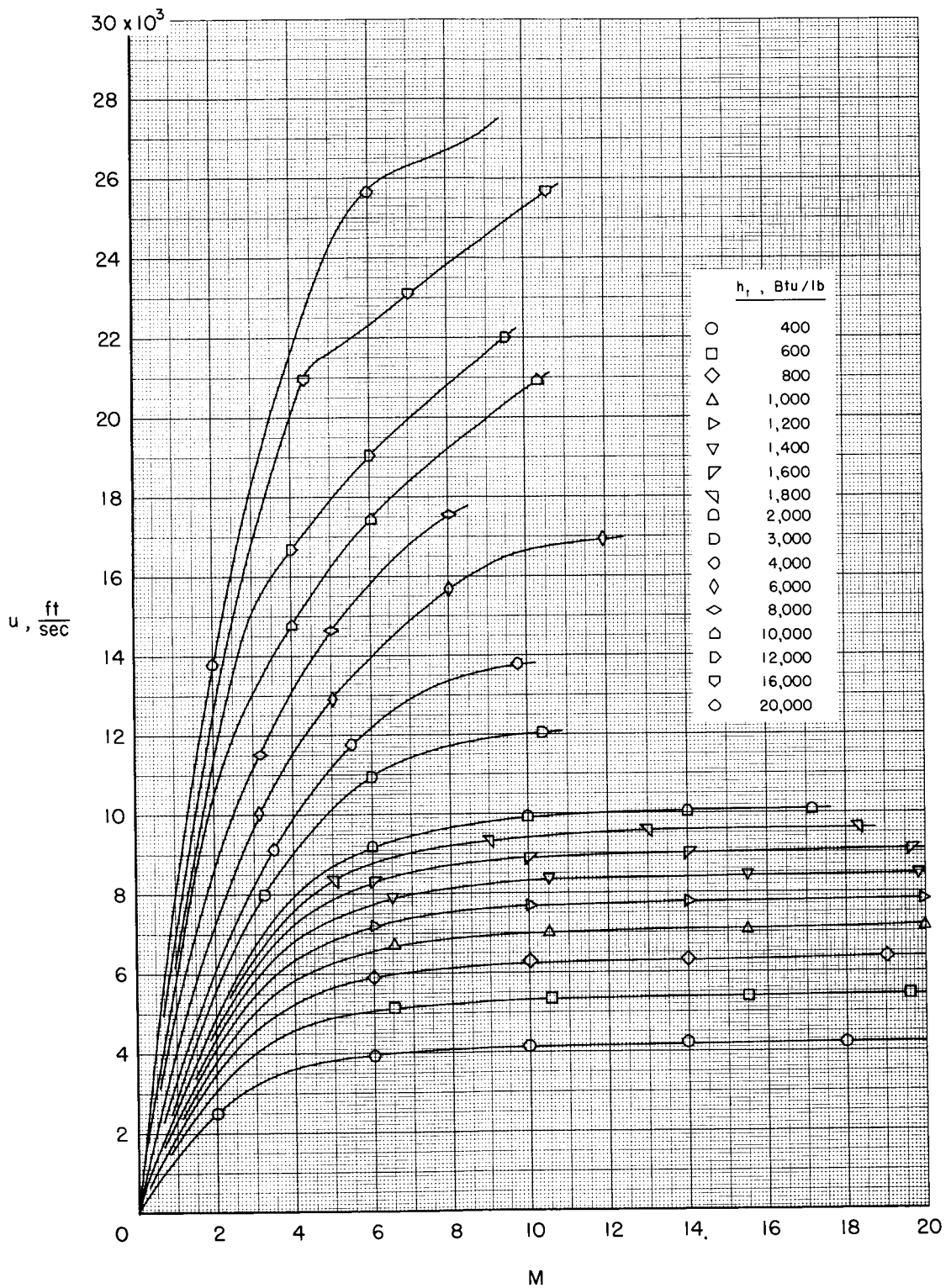
(b) $p_t = 10$ atm

Chart 8.- Continued.
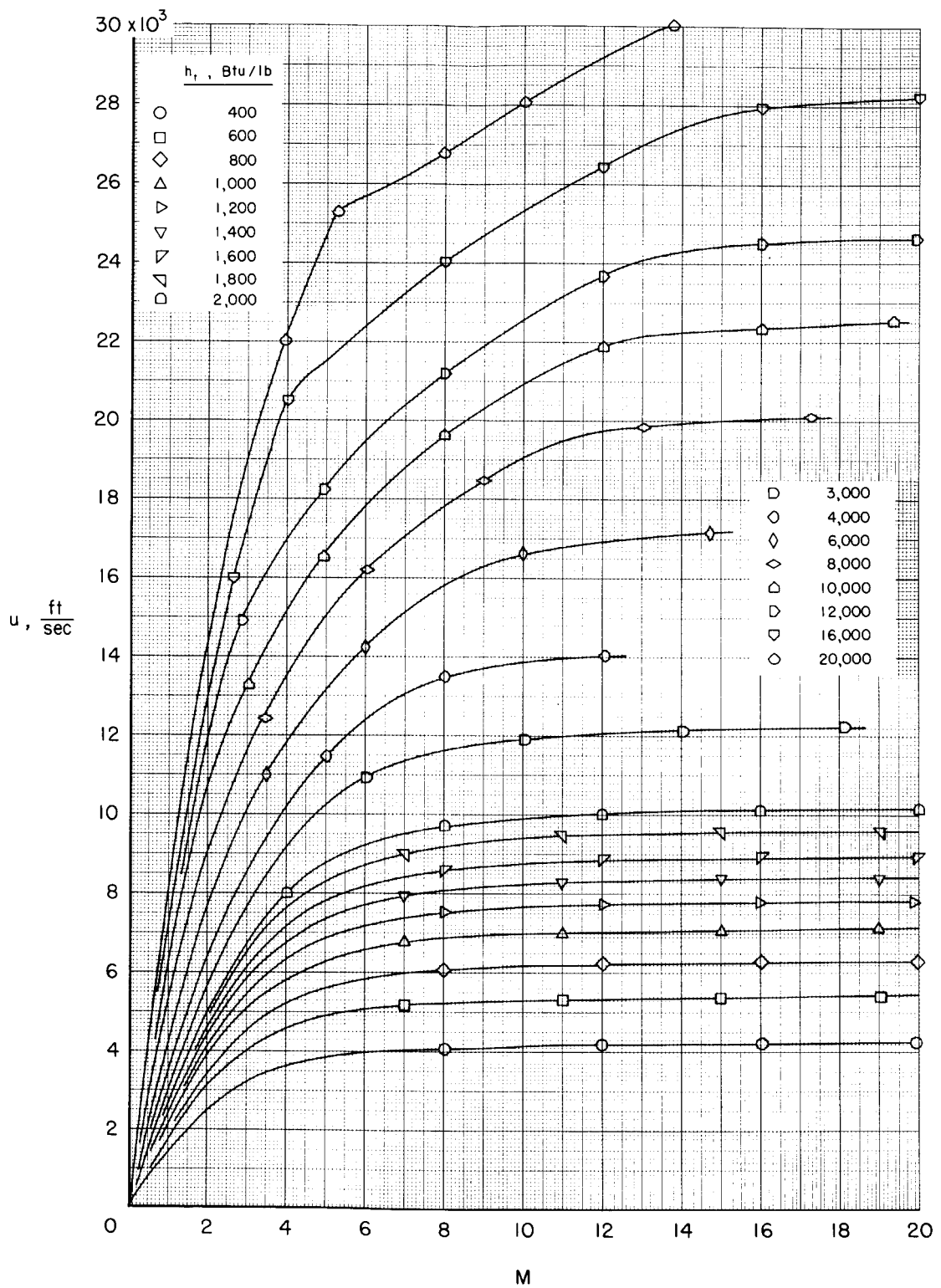
(c) p_t = 100 atm

Chart 8.- Continued.
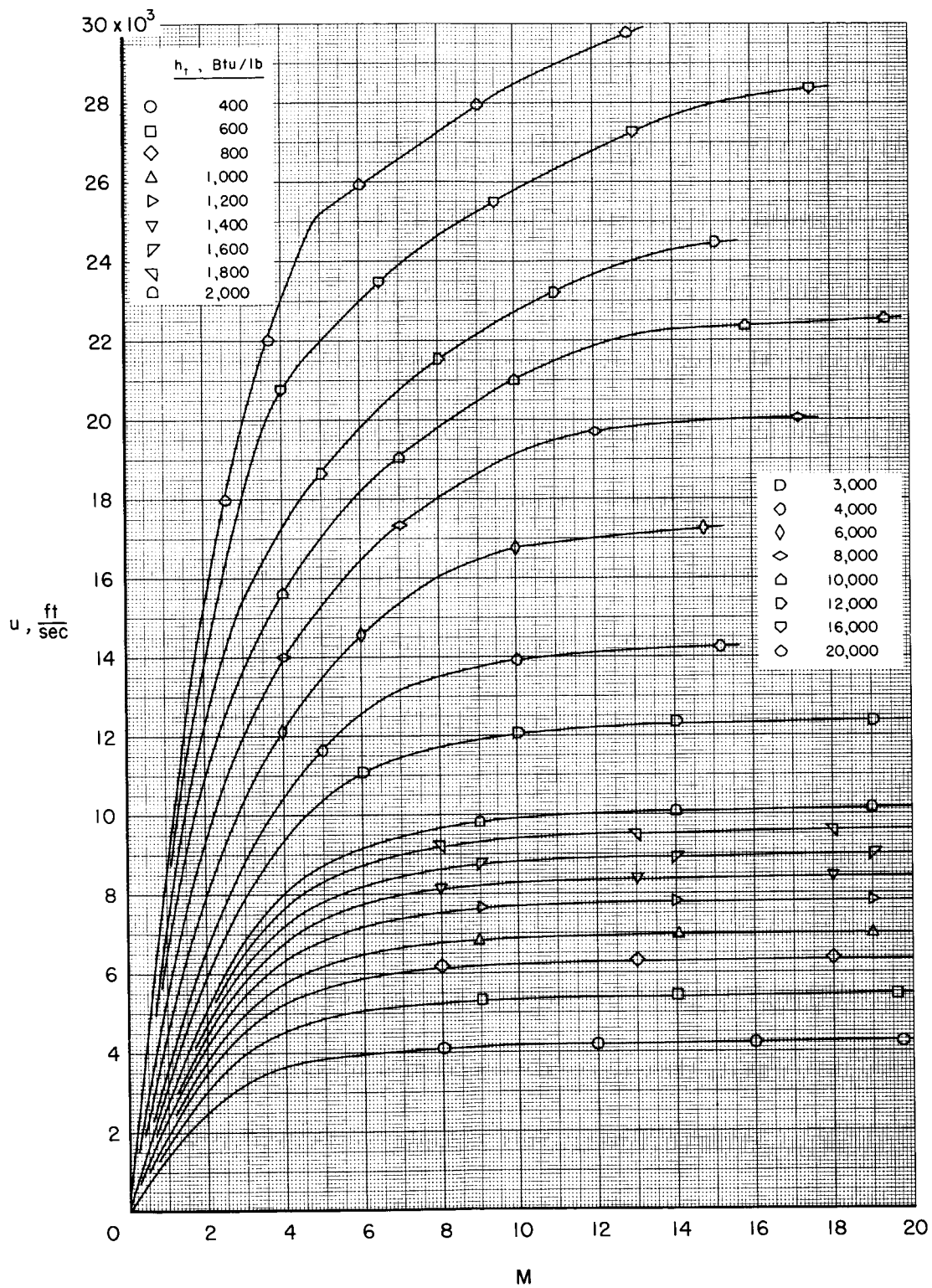
(d) $p_t = 1000$ atm

Chart 8.- Concluded.
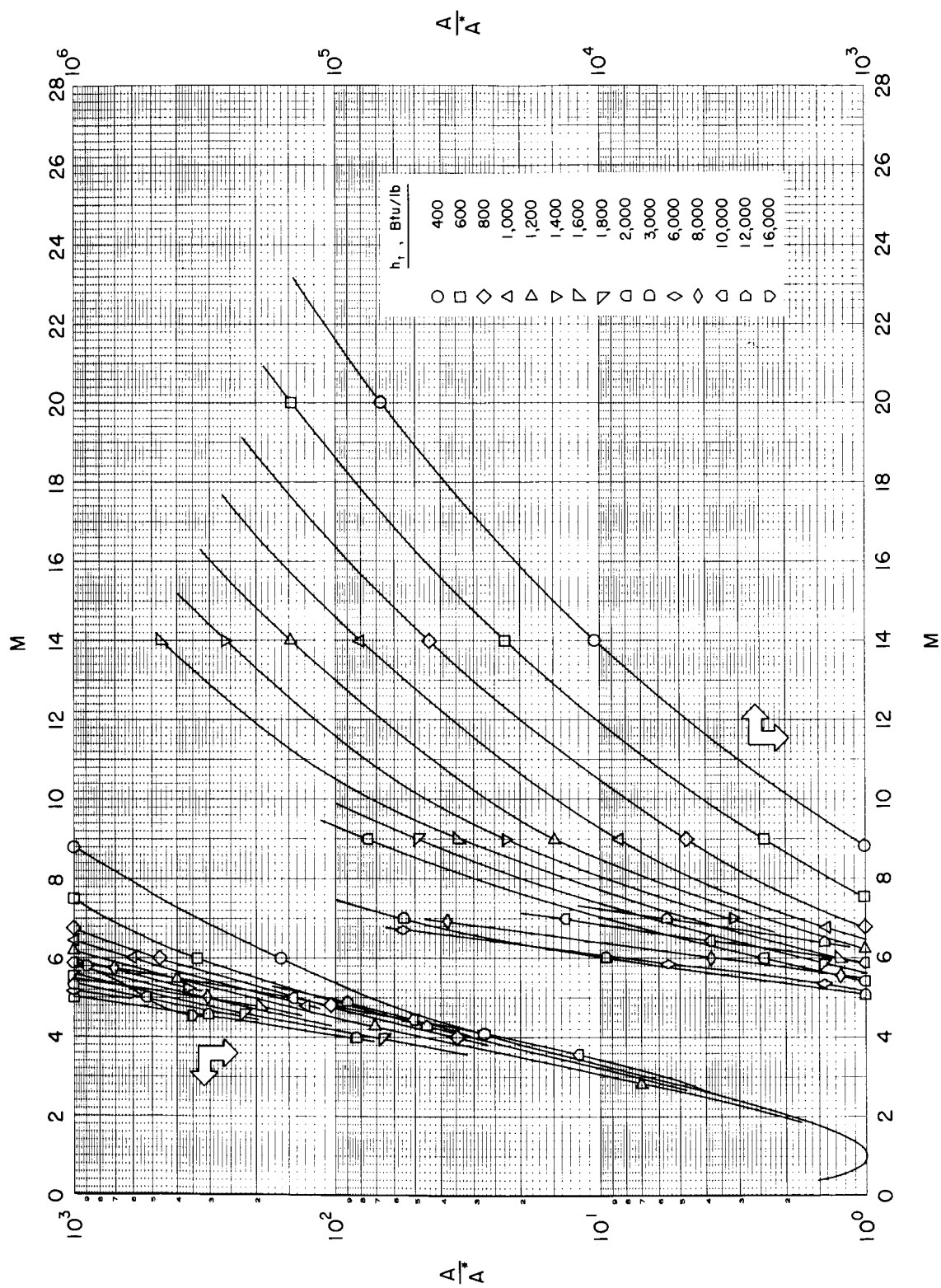
(a) $p_t = 1$ atm

Chart 9.- Variation of area ratio with Mach number.

$\frac{A}{A^*}$
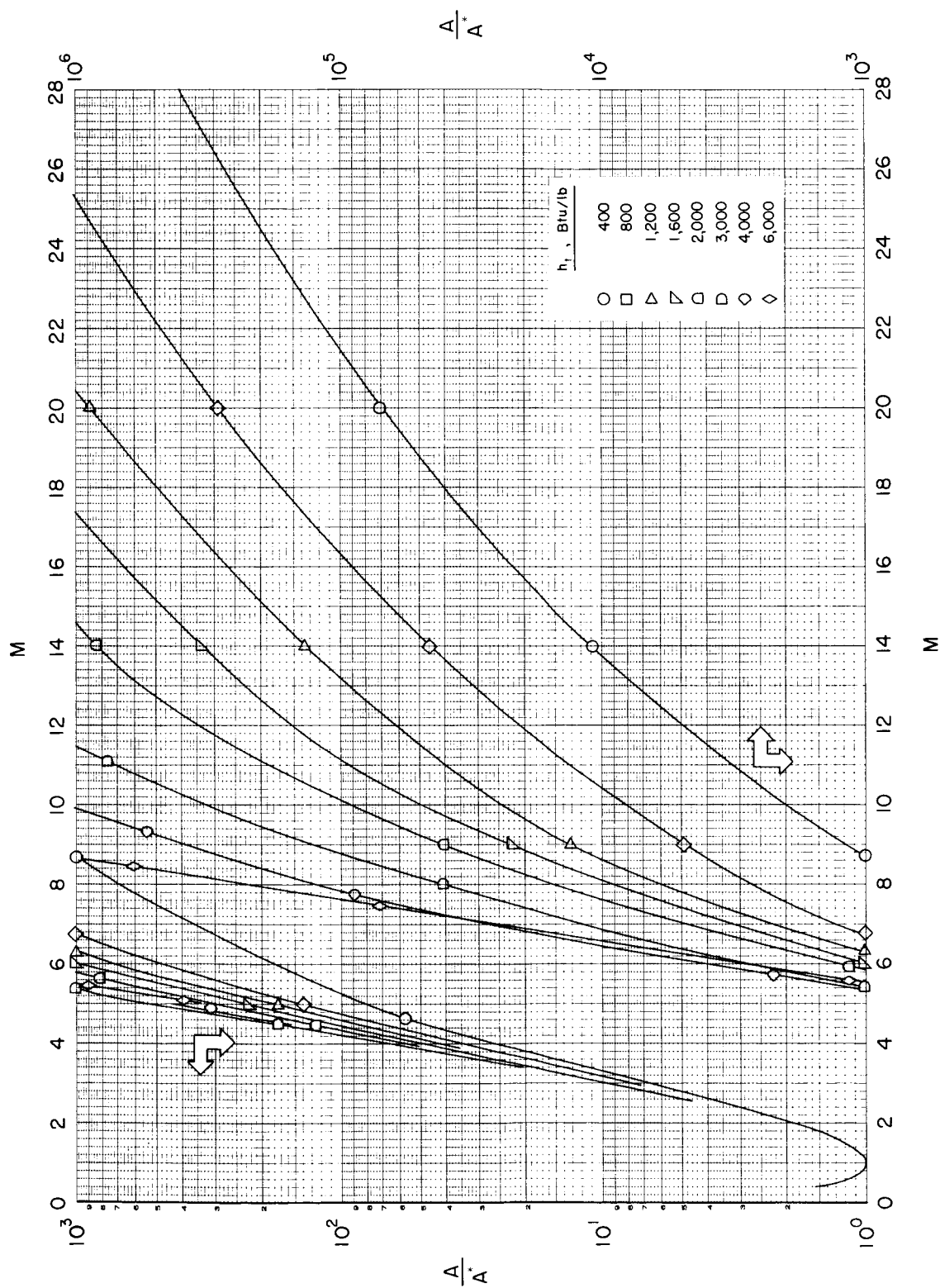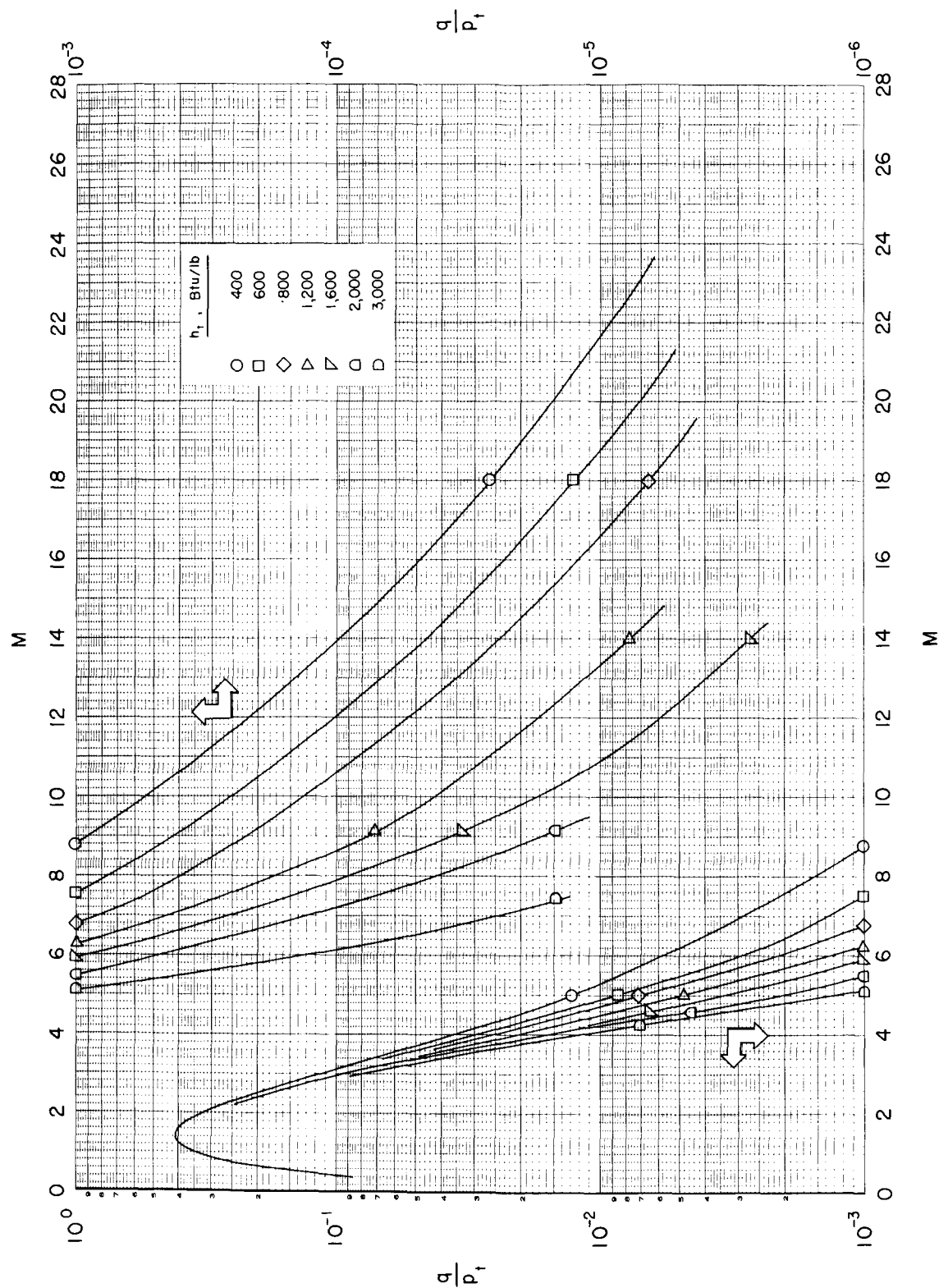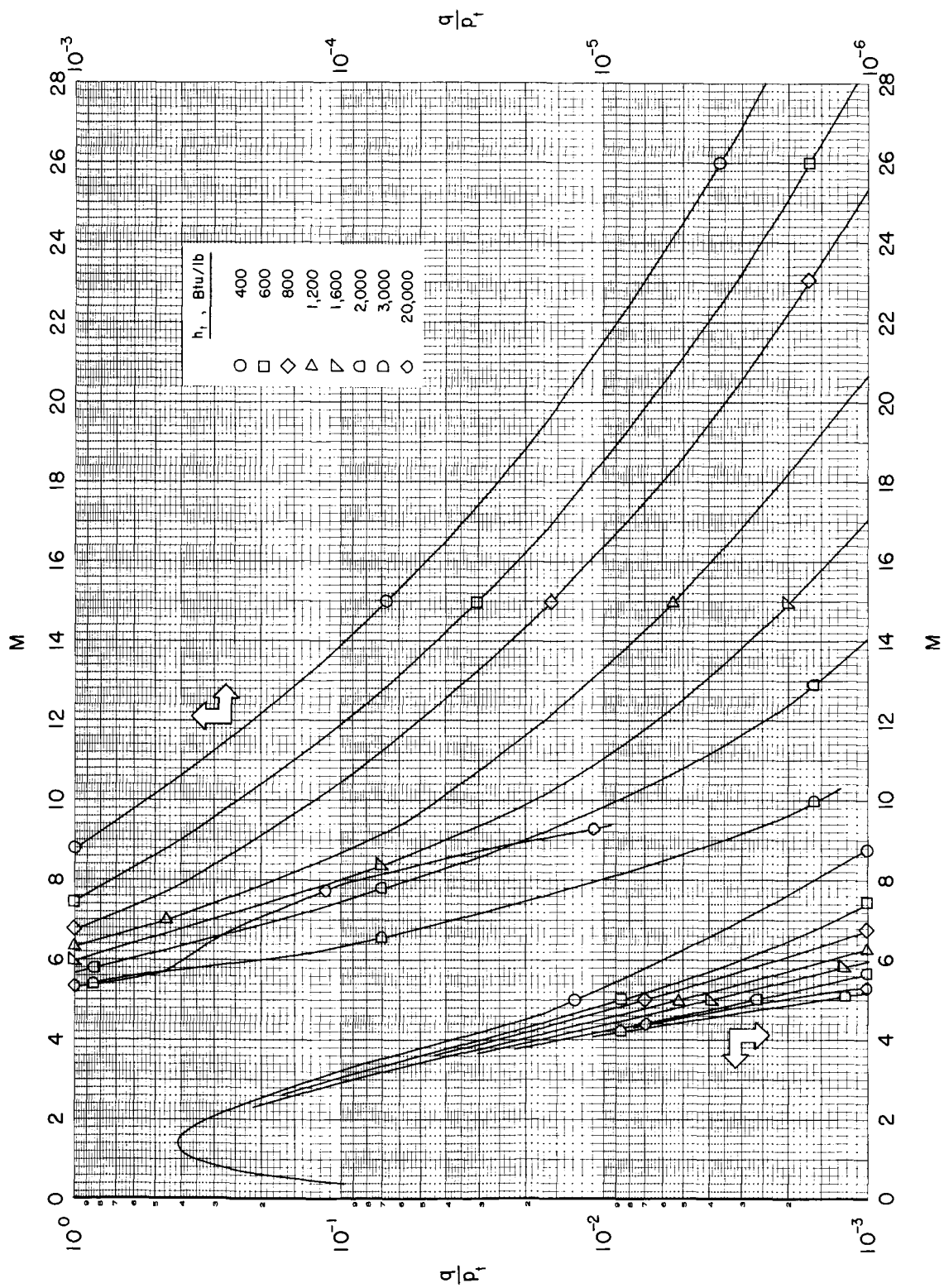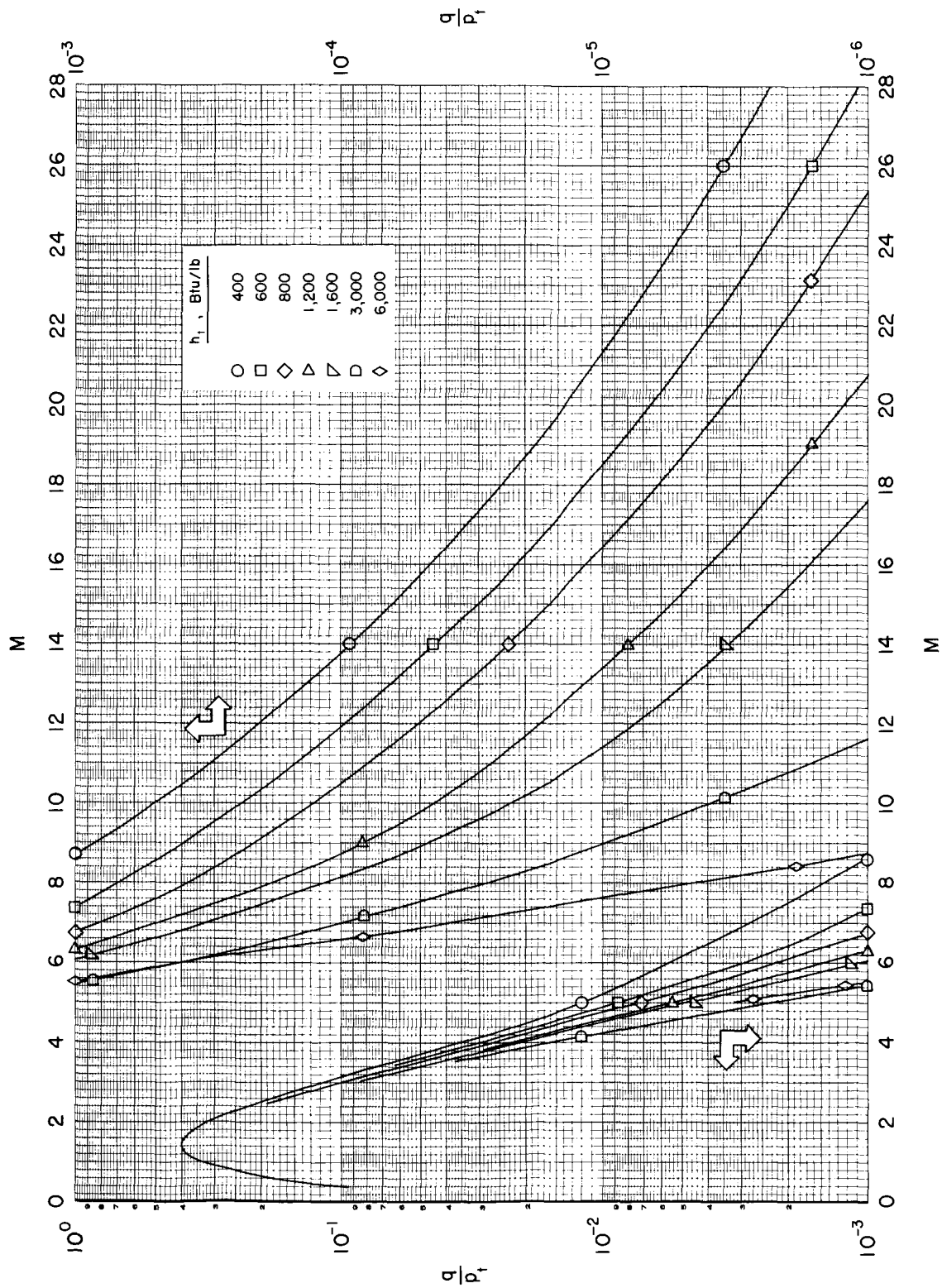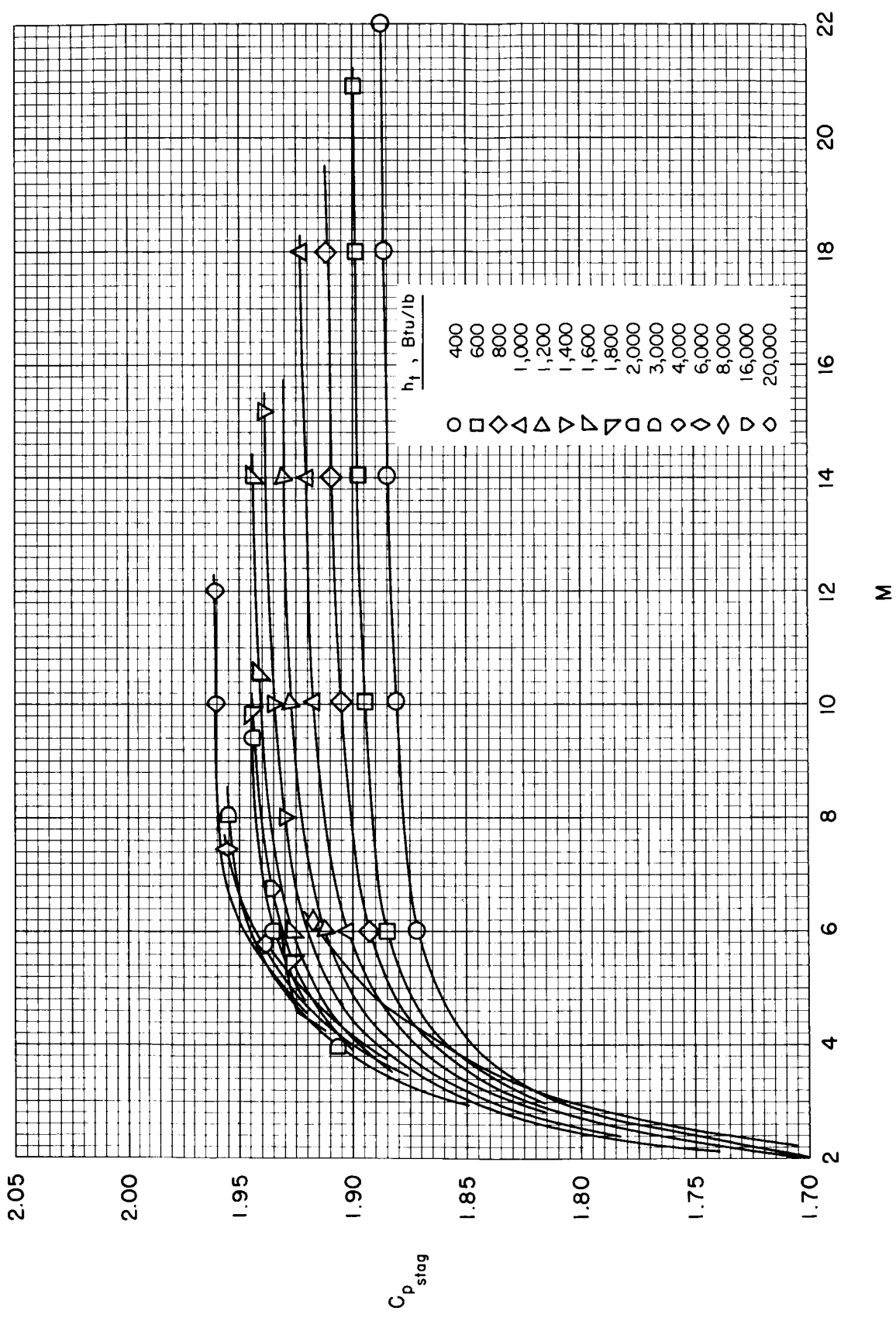
$\frac{A}{A^*}$

M

M

h_t, Btu/lb	
○	400
□	600
◇	800
◁	1,000
△	1,200
▷	1,400
◻	2,000
◇	4,000
△	12,000
▷	16,000
◇	20,000
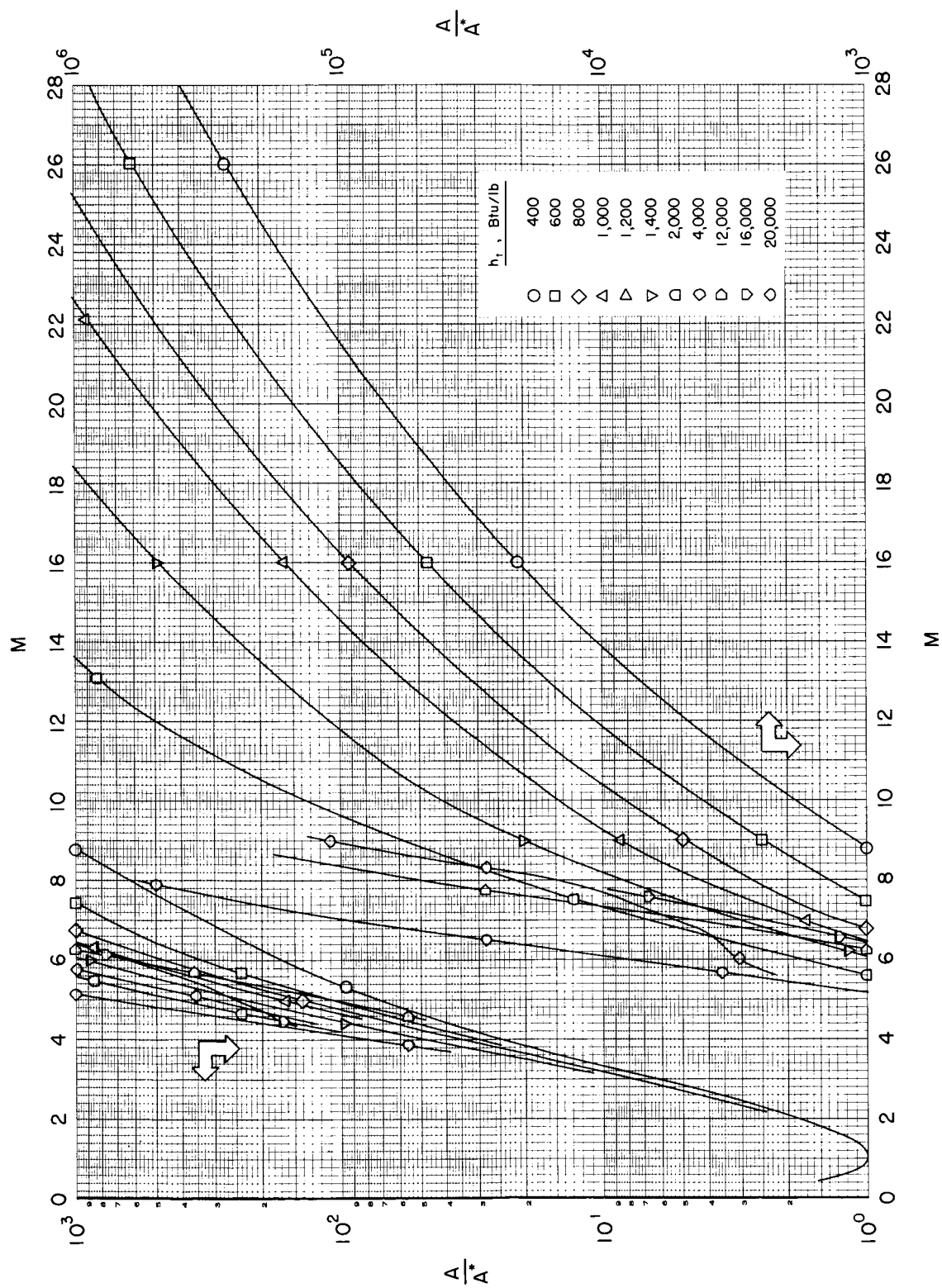
(b) p_t = 10 atm

Chart 9.- Continued.

(c) $p_t = 100$ atm

Chart 9.- Continued.

$\dfrac{A}{A^*}$

h_t, Btu/lb	
○	400
□	800
△	1,200
▽	1,600
◁	2,000
▷	3,000
◇	4,000
◇	6,000

M

M

$\dfrac{A}{A^*}$

(d) $p_t = 1000$ atm

Chart 9.- Concluded.

Chart 10.- Variation of dynamic pressure with Mach number.

(a) $p_t = 1$ atm

(b) $p_t = 10$ atm

Chart 10.- Continued.

(c) $p_t = 100$ atm

Chart 10.- Continued.

(d) $p_t = 1000$ atm

Chart 10.- Concluded.
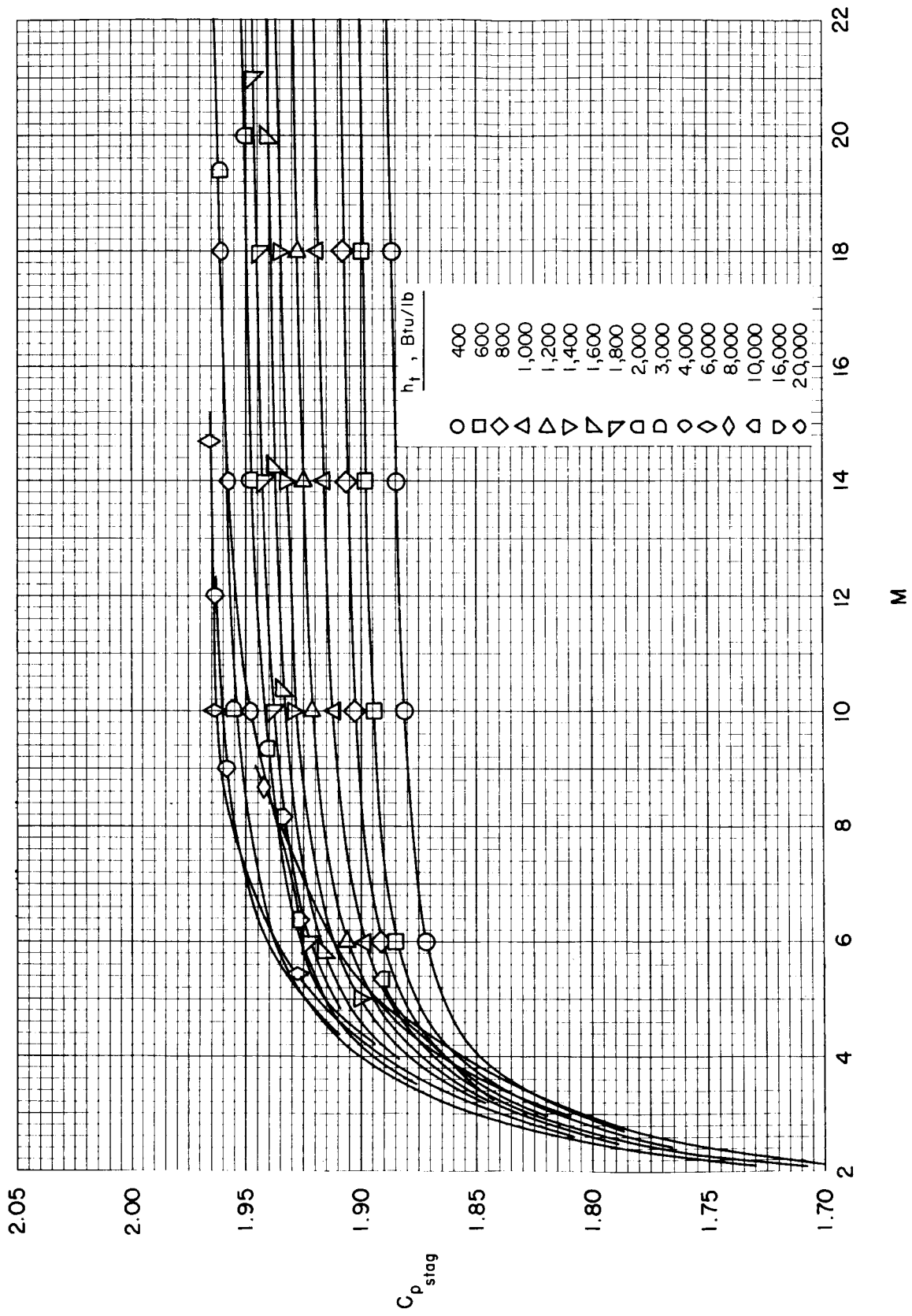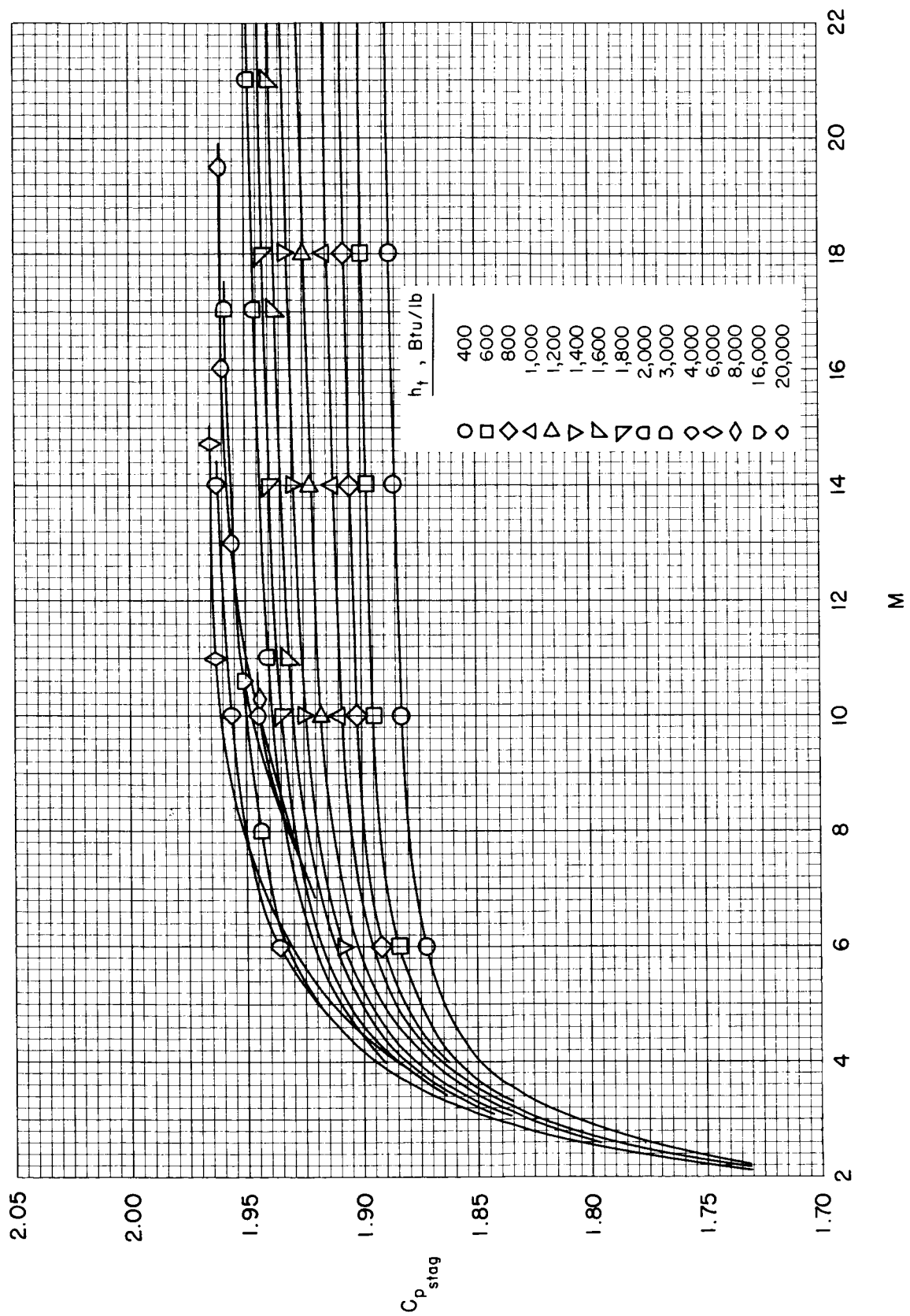
(a) $p_t = 1$ atm

Chart 11.- Variation of stagnation pressure coefficient with Mach number.
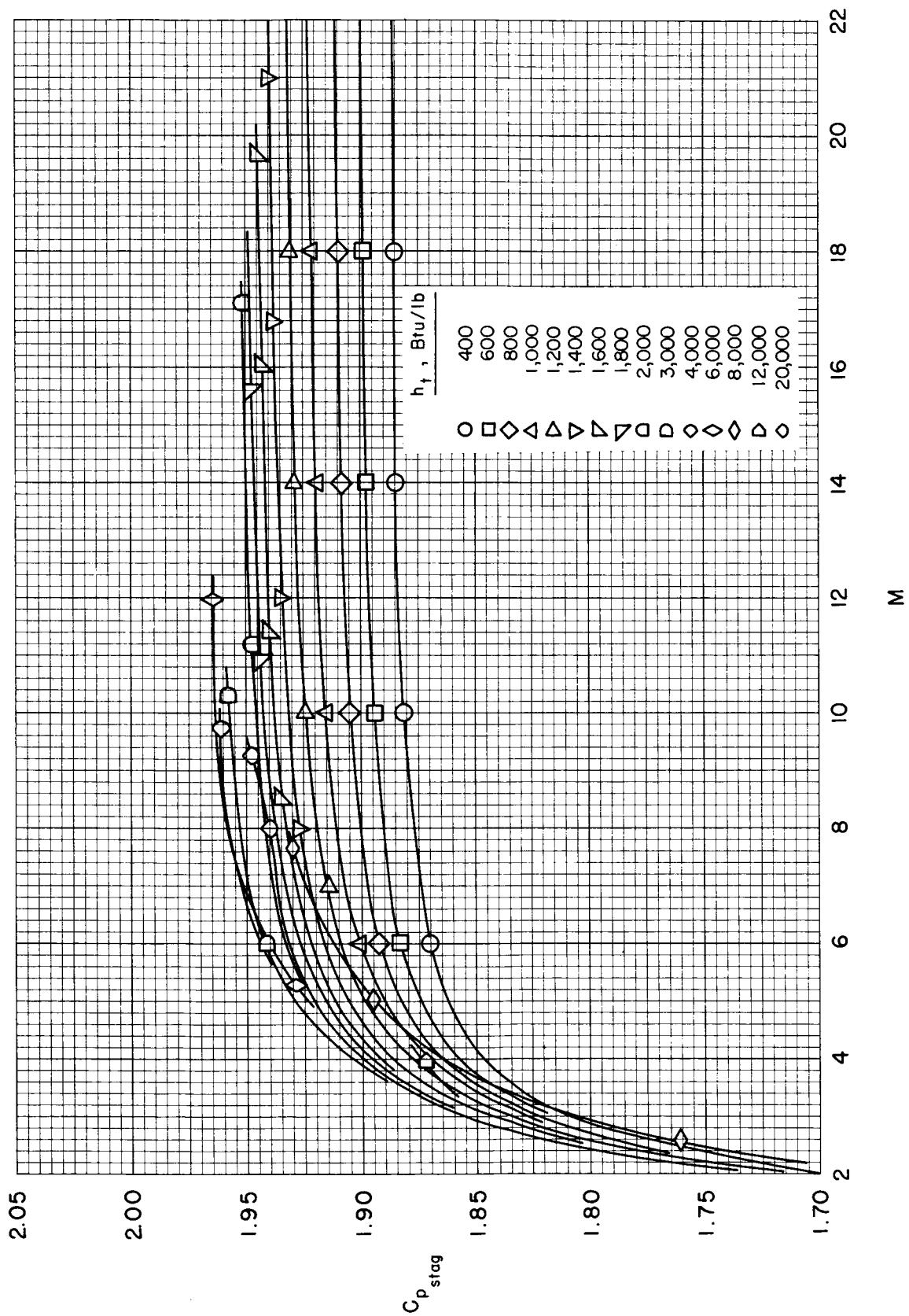
(b) $p_t = 10$ atm

Chart 11.- Continued.

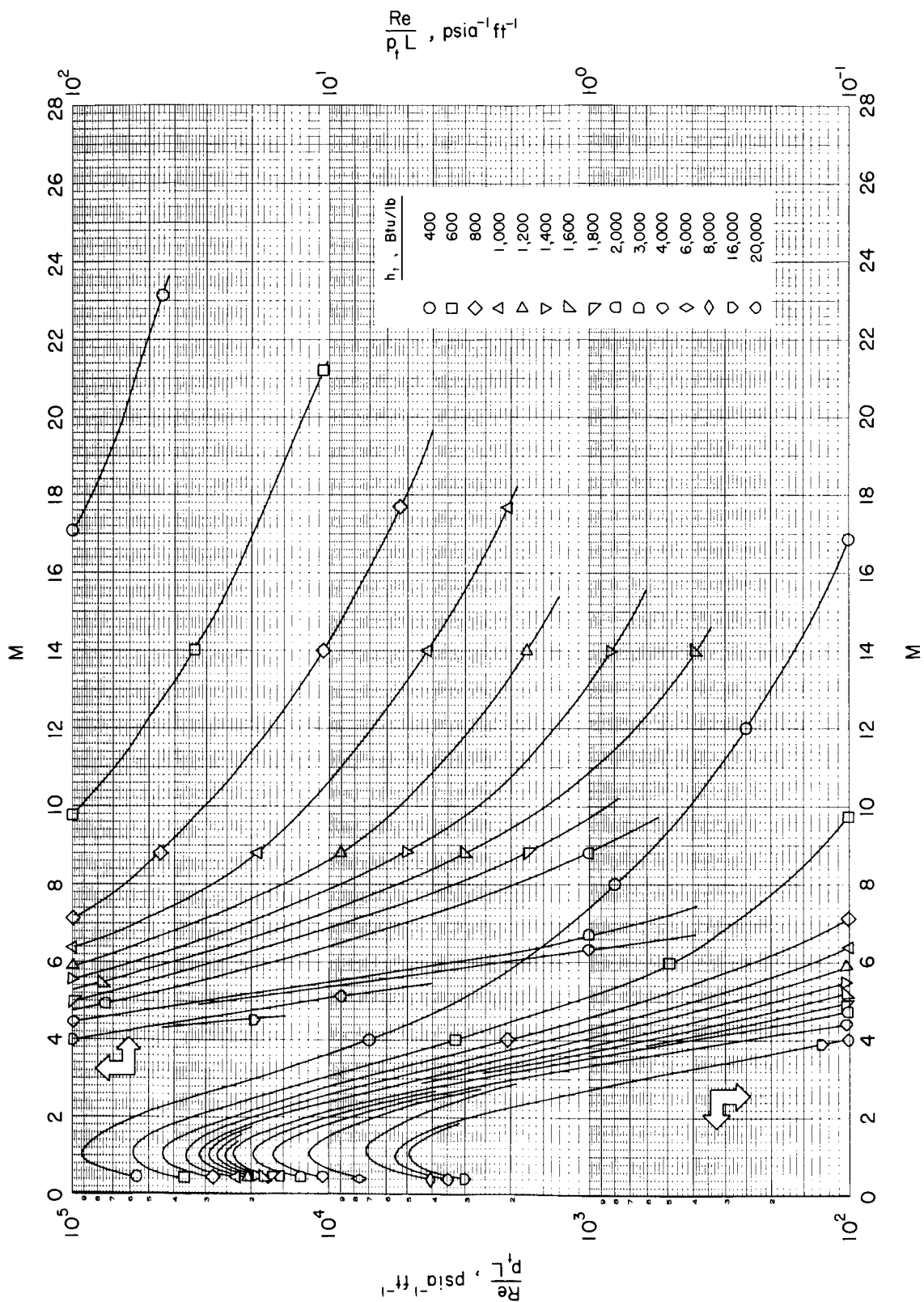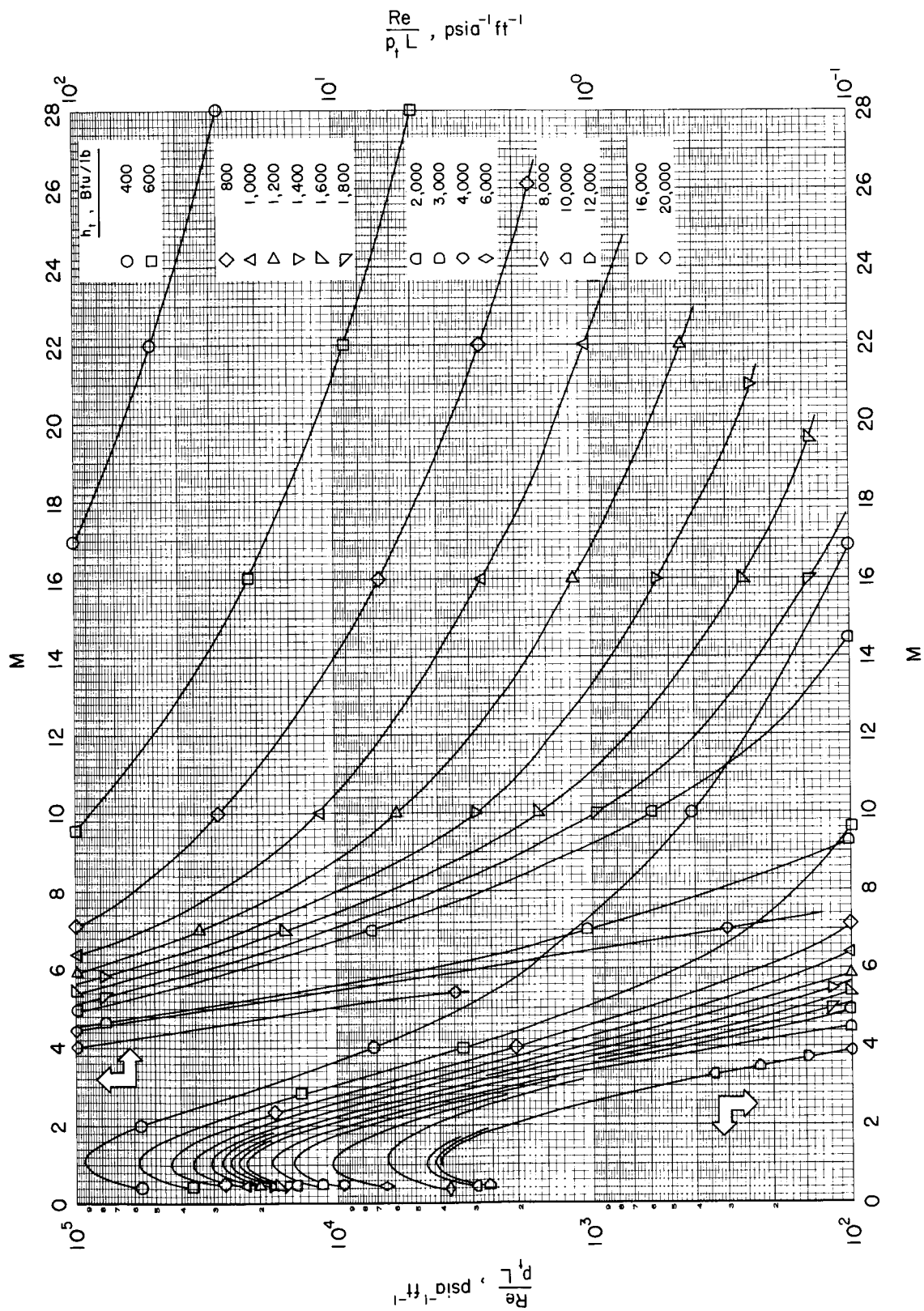(c) $p_t = 100$ atm

Chart 11.- Continued.

60

(d) $p_t = 1000$ atm

Chart 11.- Concluded.

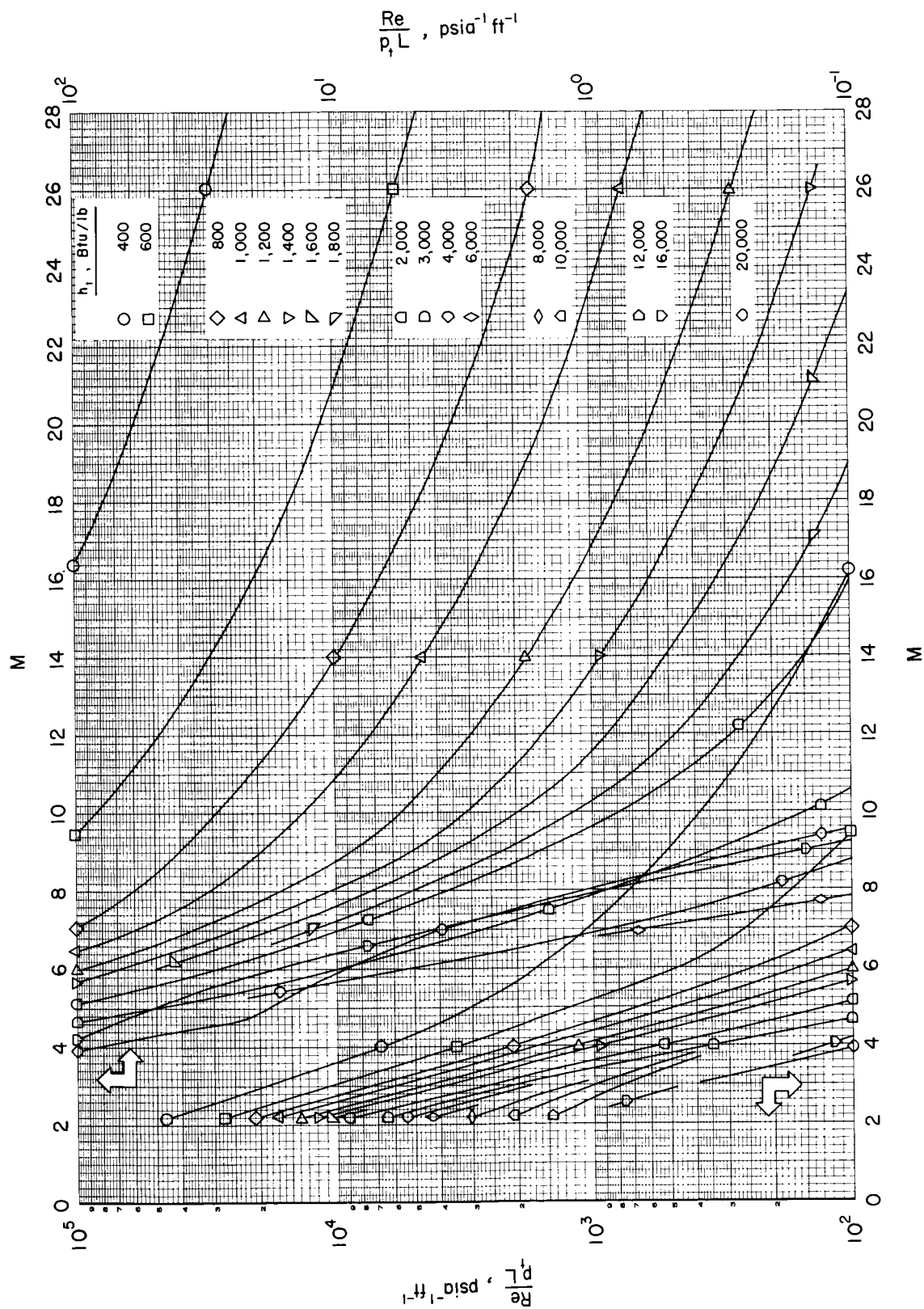$$\frac{Re}{p_t L} \; , \; psia^{-1} ft^{-1}$$

h_t , Btu/lb	
○	400
□	600
◇	800
◁	1,000
△	1,200
▷	1,400
◹	1,600
◺	1,800
◁	2,000
◇	3,000
◇	4,000
◇	6,000
▷	8,000
◇	16,000
	20,000

M

M

$$\frac{Re}{p_t L} \; , \; psia^{-1} ft^{-1}$$

(a) $p_t = 1$ atm

Chart 12.- Variation of Reynolds number parameter with Mach number.

$$\frac{Re}{p_t L} \text{ , psia}^{-1}\text{ft}^{-1}$$

10^2 10^1 10^0 10^{-1}

h_t, Btu/lb		
400		
600		
800		
1,000		
1,200		
1,400		
1,600		
1,800		
2,000		
3,000		
4,000		
6,000		
8,000		
10,000		
12,000		
16,000		
20,000		

M

M

$$\frac{Re}{p_t L} \text{ , psia}^{-1}\text{ft}^{-1}$$

10^5 10^4 10^3 10^2

(b) p_t = 10 atm

Chart 12.- Continued.

63

(c) p_t = 100 atm

Chart 12.- Continued.

(d) $p_t = 1000$ atm

Chart 12.- Concluded.

(a) p_t = 1 atm

(b) p_t = 10 atm

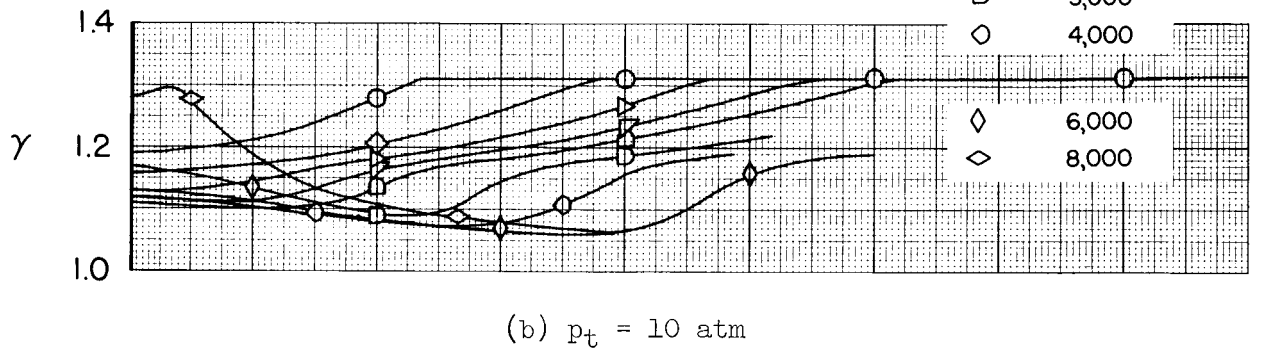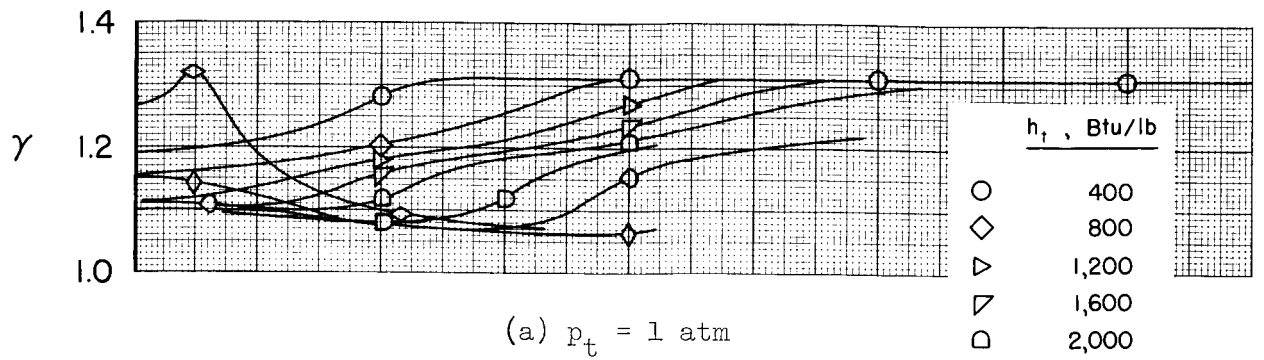(c) p_t = 100 atm
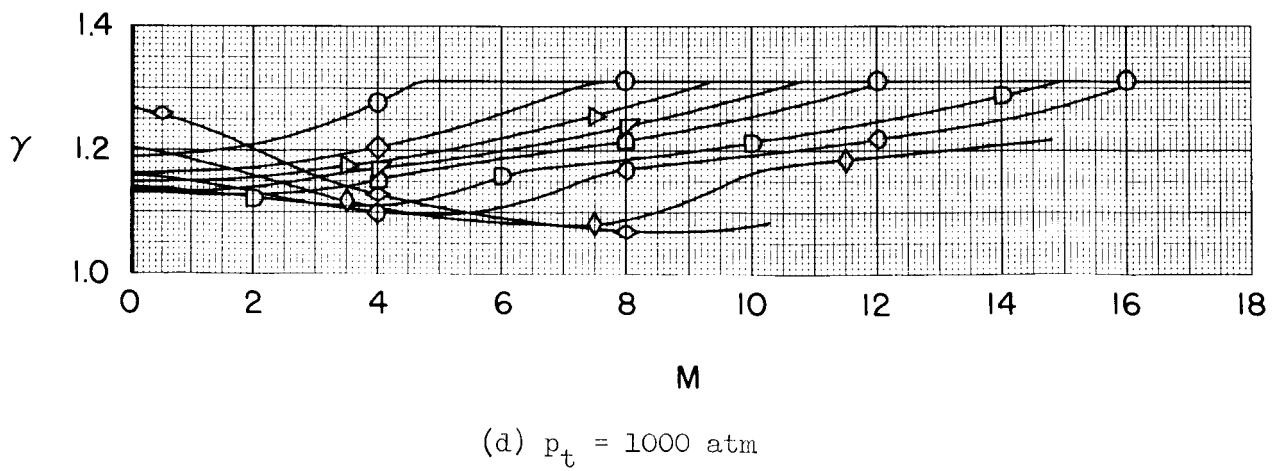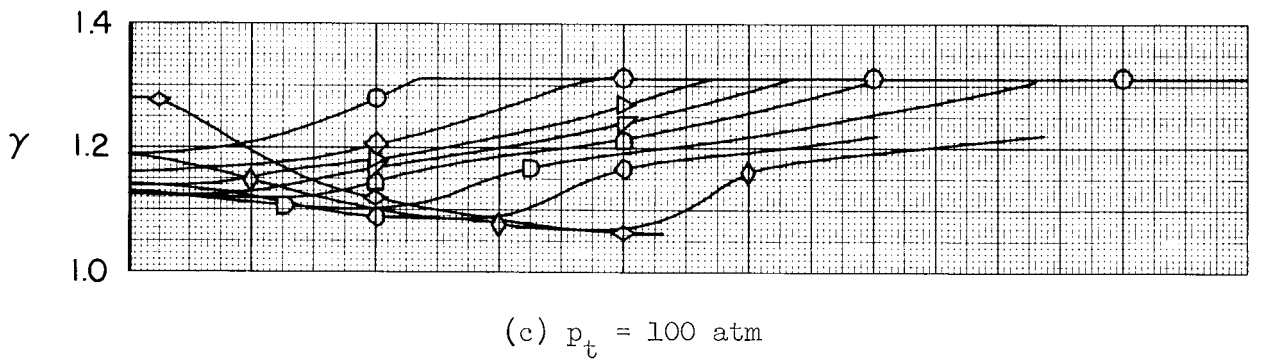
(d) p_t = 1000 atm

Chart 1.- Variation of isentropic exponent with Mach number.

Chart 14.- Isentropic exponent as a function of enthalpy for various pressures.

67

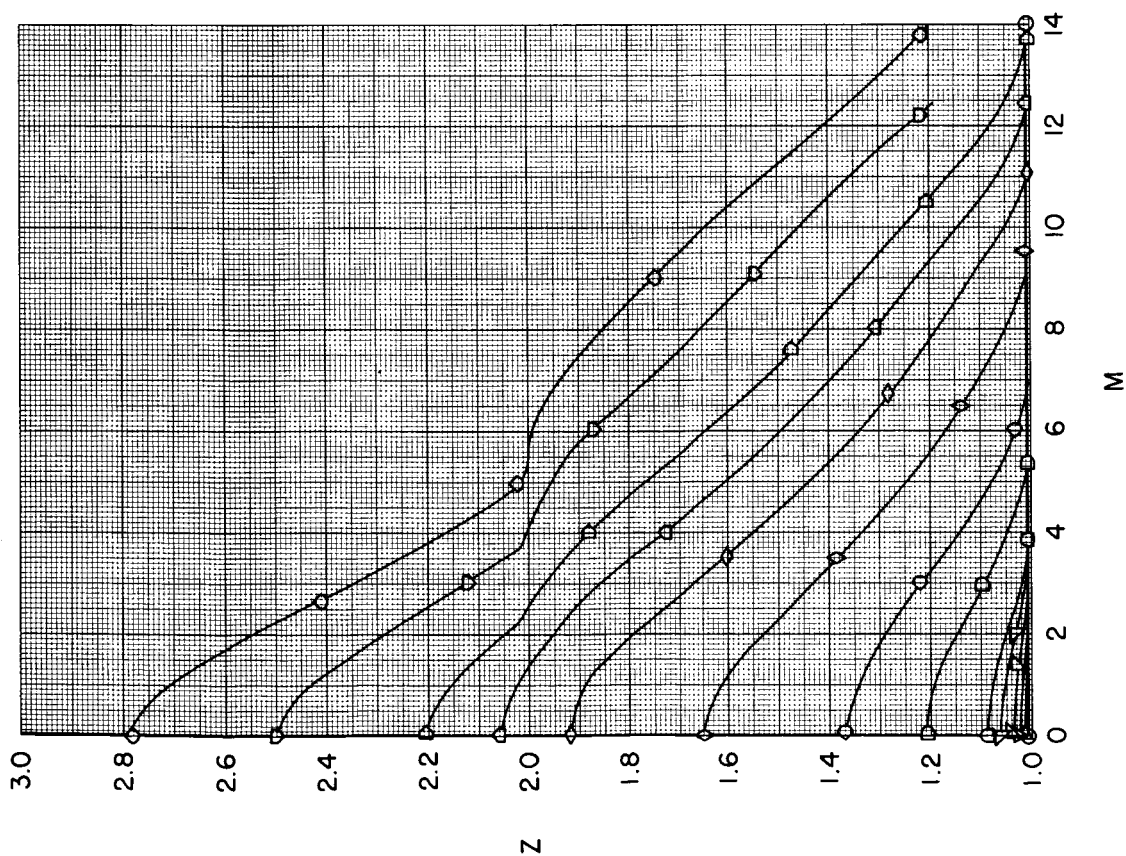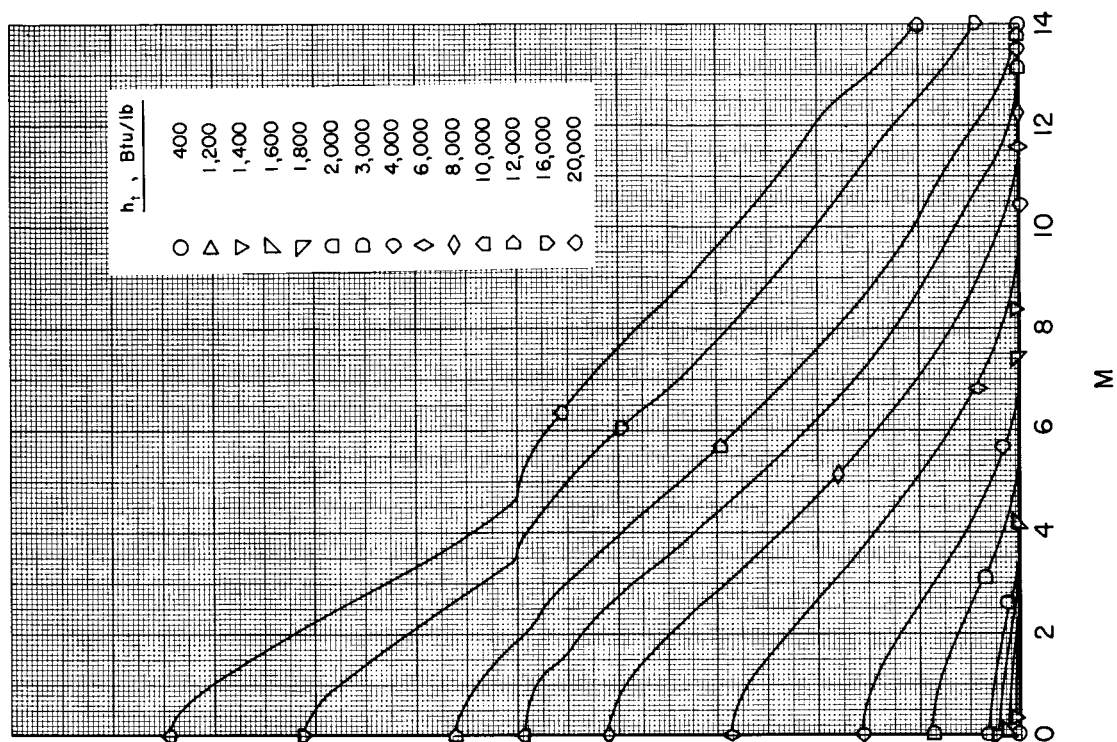| h_t, Btu/lb	
1,000	◁
1,200	△
1,400	▷
1,600	◸
1,800	◺
2,000	▢
3,000	◇
4,000	◈
6,000	◇
8,000	◁
10,000	◹
12,000	▷
16,000	◇
20,000	
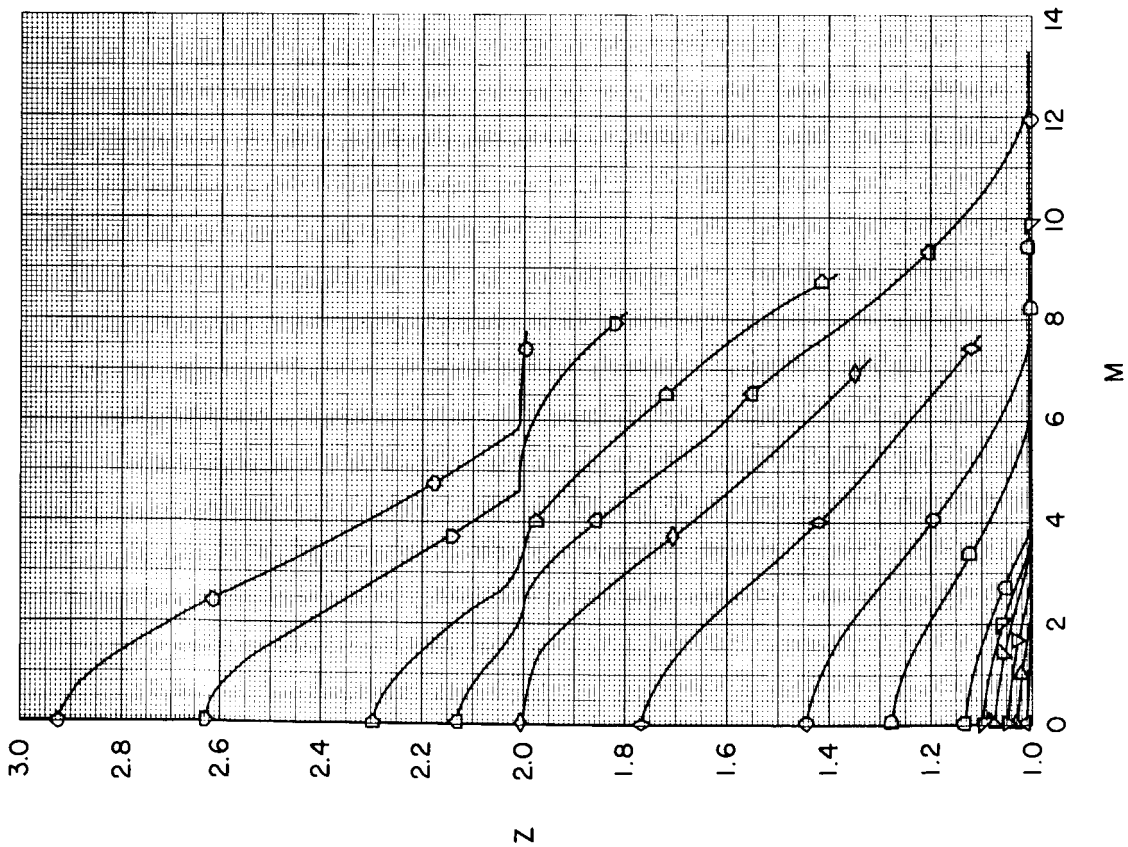
(a) $p_t = 1$ atm

(b) $p_t = 10$ atm

Chart 15.- Variation of molecular weight ratio with Mach number.

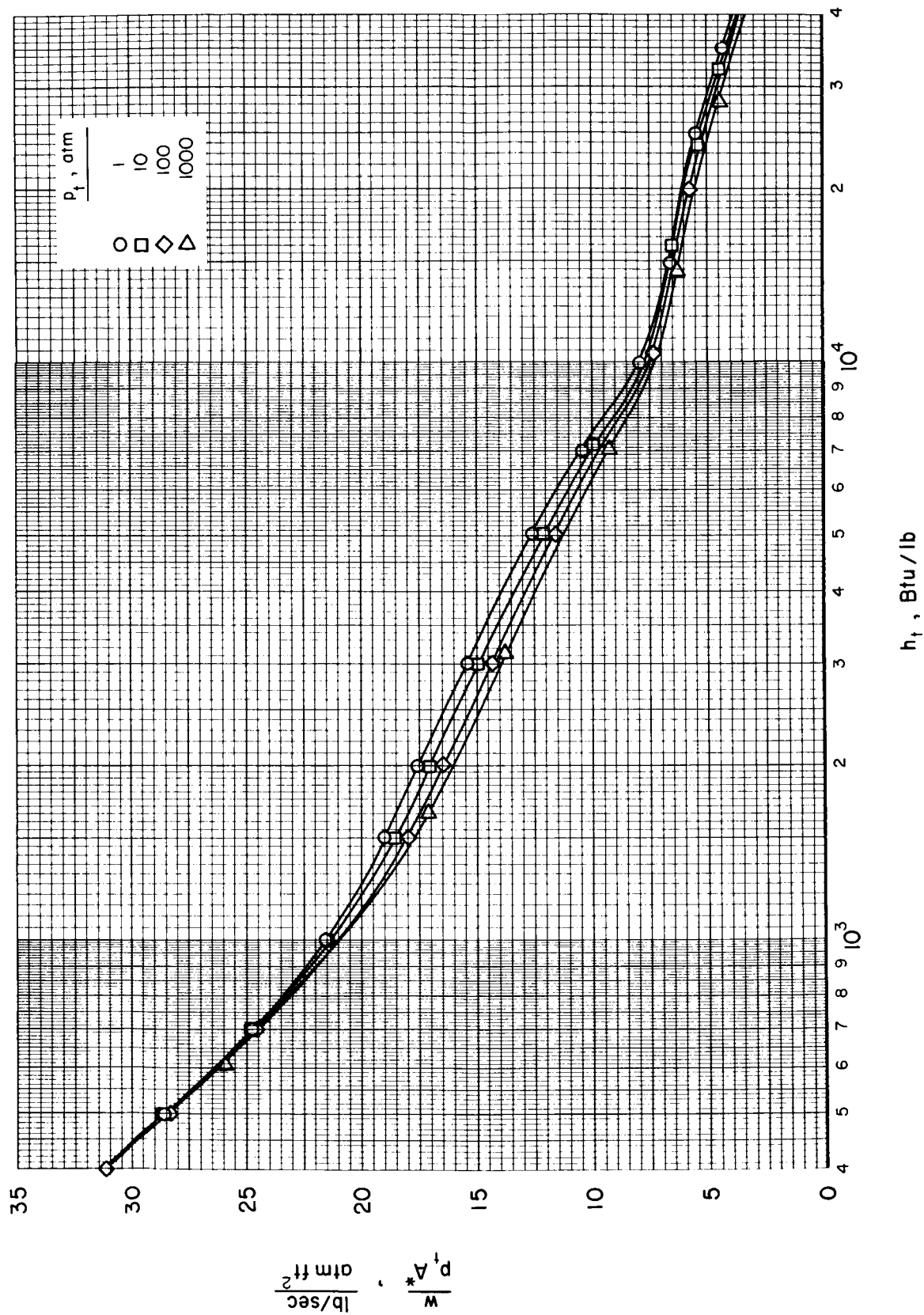(c) $p_t = 100$ atm

(d) $p_t = 1000$ atm

Chart 15.- Concluded.

Chart 16.— Variation of weight-flow parameter with total enthalpy.

h_t , Btu/lb

$\dfrac{w}{p_t A^*}$, $\dfrac{lb/sec}{atm\ ft^2}$

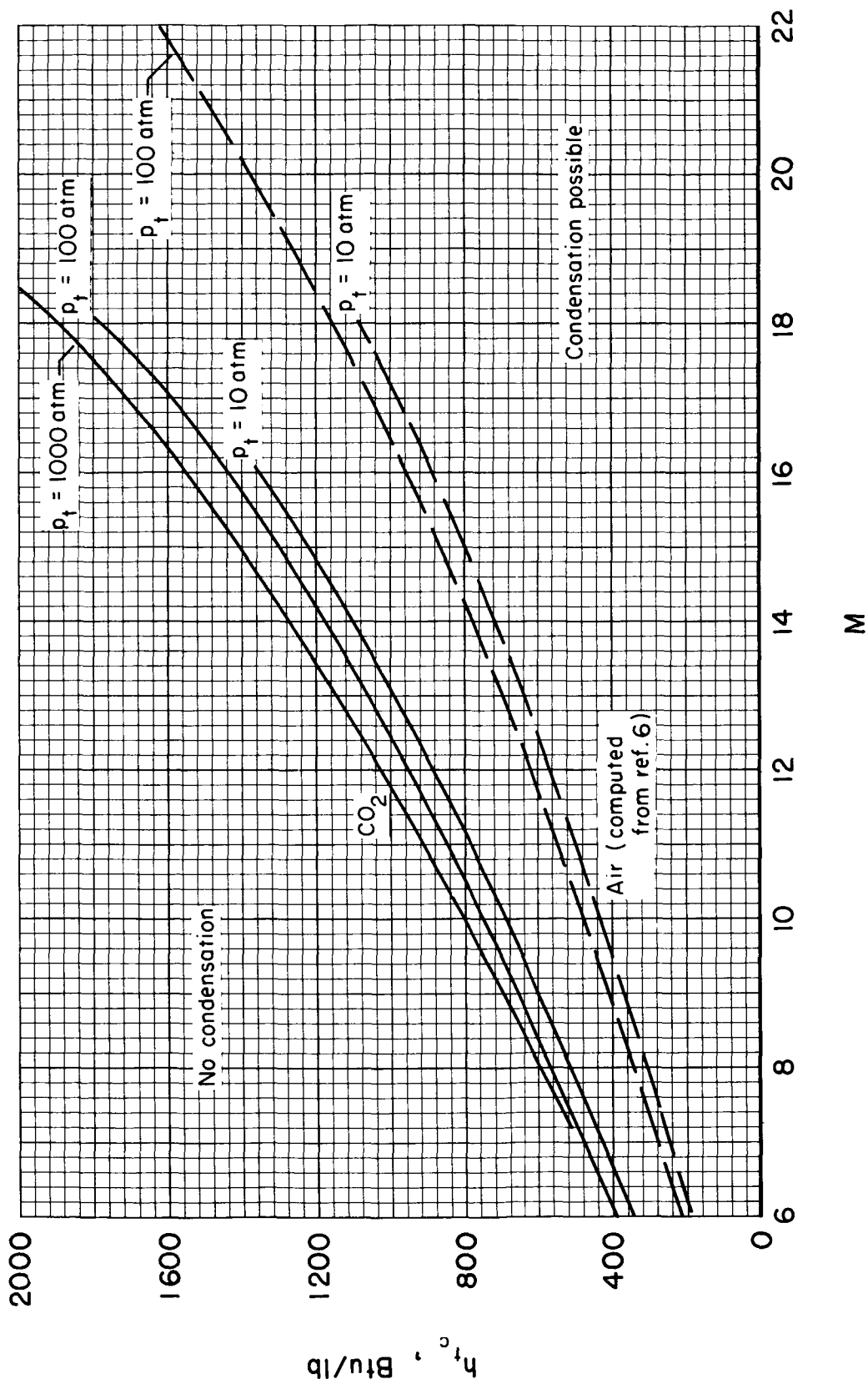| p_t , atm	
1	○
10	□
100	◇
1000	△

70

Chart 17.- Total enthalpy for condensation-free flow, based on saturated vapor pressures in figure 1.